

Ulm University Medical Centre
Institute of Orthopaedic Research and Biomechanics
Director: Prof. Dr. Anita Ignatius

Biomechanical Characterisation of a Potential Material for Meniscal Replacement

Cumulative dissertation to obtain the
doctoral degree of human biology (Dr. biol. hum.)
of the Medical Faculty of Ulm University

Daniela Warnecke,
born in Nienburg (Weser)

2019

Acting Dean: Prof. Dr. Thomas Wirth

1st Referee: apl. Prof. Dr. Lutz Dürselen

2nd Referee: Prof. Dr. Rainer Hanns Hermann Burgkart

Date of Defence: 26 July 2019

***In liebevoller Erinnerung an meinen Opi
& für meine Familie: Ihr seid die besten!***

Content

Abbreviations	V
Symbol.....	VI
Figures.....	VII
Tables	IX
1. Introduction	1
1.1. The knee joint.....	1
1.2. Clinical situation.....	6
1.3. Aim of the work	9
2. Biomechanical Characterisation of a Potential Material for Meniscal Repair	11
3. Friction Properties of a Silk Fibroin Scaffold in Comparison to the Physiology...	15
4. Friction analysis under simulated physiological loading and motion conditions	19
5. Conclusion.....	23
6. Abstract.....	25
7. Literature.....	27
8. Publications	33
8.1. Manuscript 1.....	33
8.2. Manuscript 2.....	45
8.3. Manuscript 3.....	53
Acknowledgements.....	63
Curriculum vitae.....	64

Abbreviations

Abbreviation	Description
AC	articular cartilage
ANOVA	analysis of variances
BW	bodyweight
CMI®	Collagen Meniscus Implant, Ivy Sports Medicine, Germany
DMA	dynamic mechanical analysis
DOF	degree of freedom
ECM	extracellular matrix
FC	femoral cartilage
OA	osteoarthritis
PBS	phosphate-buffered saline
PG	proteoglycan
PI	pars intermedia
S	scaffold
TC	tibial cartilage
μ-CT	micro computed tomography

Symbol

Symbol	Description	Unit
\emptyset	diameter	mm
δ	phase lag angle	°
ε_0	strain at the onset of the test	
$\varepsilon_{end}/\varepsilon_{eq}$	strain at the end of the testing duration, when equilibrium was reached	
E	linear elastic modulus	N/mm ² (= MPa)
E_{eq}	aggregate or equilibrium modulus	N/mm ² (= MPa)
E'	storage or elastic modulus	N/mm ² (= MPa)
E''	loss modulus	N/mm ² (= MPa)
F_F	friction force	N
F_N	axial, normal force	N
F_{max}	ultimate tensile force	N
h_0	initial sample height	mm
p	pressure	N/mm ² (= MPa)
s	stroke length	mm
$\tan(\delta)$	damping factor	
v	sliding velocity	mm/s
μ	friction coefficient	
μ_0	friction coefficient at the onset of the test	
μ_{end}/μ_{eq}	friction coefficient at the end of the testing duration, when equilibrium was reached	

Figures

Figure 1: The anatomical arrangement of the bony structures: femur, tibia, fibula and patella (not shown) and the surrounding soft tissue are responsible for the physiological function of the knee. Thereby, the two semi-lunar and wedge-shaped menisci with the three-layered morphology play an important role (detailed view.)...3

Figure 2: Macroscopic view of a cylindrical sample of the silk fibroin scaffold punched out of a scaffold's flat sheet manufactured by Orthox Ltd. (A). During μ -CT analysis the structural composition and architecture was additionally determined to complete the biomechanical characterisation of the scaffold (B). Modified figure from [51] with Creative Commons Attribution License 4.0 International (CC BY 4.0, <http://creativecommons.org/licenses/by/4.0/>). 14

Figure 3: Six cylindrical samples each from the medial meniscus (M), the tibial plateau (TC) of bovine knee joints or from flat sheets of the silk fibroin scaffold (S) were harvested (A) and tested against either a flat cartilage (FC) sample or against glass (G) using a customised pin-on-plate friction testing device (B). Modified figure from [34] with Creative Commons Attribution License 4.0 International (CC BY 4.0, <http://creativecommons.org/licenses/by/4.0/>). 16

Figure 4: Although the friction coefficient of the silk fibroin scaffold was significantly higher than the physiologically articulating surfaces within the knee joint: meniscus and cartilage, μ was still within the range of the requirements for materials for meniscal repair [21], when testing against the flat cartilage sample (A). Using glass as opposing surface always leads to significantly higher friction coefficients than using cartilage (B); * $p \leq 0.05$ using one-factor ANOVA with uncorrected Post-Hoc Fisher's LSD test (A) and two-factor ANOVA with repeated measures (B). Modified figure from [34] with Creative Commons Attribution License 4.0 International (CC BY 4.0, <http://creativecommons.org/licenses/by/4.0/>). 17

Figure 5: The dynamic friction testing device was developed to investigate the friction properties under defined testing conditions occurring during gait. It basically consists of a dynamic materials testing machine (ElectroForce® 5500, BOSE/TA Instruments, USA), which was equipped with a linear motor mounted on a customized aluminium frame (detailed view). Modified figure from [58] with Creative Commons Attribution License 4.0 International (CC BY 4.0, <http://creativecommons.org/licenses/by/4.0/>). 20

Figure 6: Comparison of the friction coefficients μ obtained for each material pairing: tibial cartilage (A), meniscus (B) and the silk fibroin scaffold (C) each against femoral cartilage within the three different friction test scenarios ($n = 8-10$, mean \pm standard deviation and raw data; \bigcirc FT-I, \ast FT-II, \bullet FT-III), $\ast p \leq 0.05$. Modified figure from [58] with Creative Commons Attribution License 4.0 International (CC BY 4.0, <http://creativecommons.org/licenses/by/4.0/>). 22

Tables

Table 1: Summarised overview of the basic requirements for meniscal replacement materials postulated by STONE and further elaborated by RONGEN ET AL. [21, 45].	8
Table 2: Tabular overview of the three friction test scenarios (FT-I, -II and -III) and the corresponding application of the testing parameters: normal load F_N and motion (motor position s in mm). Modified table from [58] with Creative Commons Attribution License 4.0 International (CC BY 4.0, http://creativecommons.org/licenses/by/4.0/)	21

1. Introduction

The two menisci play a crucial role within the knee joint. As they have to withstand high loads not only during sports but also during activities of daily life, lesions of the medial meniscus are second ranked within the most frequent internal knee injuries, requiring a surgical intervention in 80% of the cases [1]. In 2017, a total of 216627 surgical procedures were performed medicating either the articular cartilage or meniscus (statistisches Bundesamt, 2017) [2]. Depending on the localization and type of the tear, the meniscus is still frequently treated by resecting the injured tissue, although it has already been shown that total and also partial meniscectomy can lead to degeneration of the adjacent cartilage and osteoarthritis could be the consequence [3, 4]. Thus, there is an urgent need of alternative treatment strategies restoring and/or replacing the meniscus. However, only two research approaches for meniscal replacement got into clinical practice yet but without gaining widespread acceptance, as their biomechanical performance was insufficient and consequently, a successful long-term chondroprotection is still questionable.

1.1. The knee joint

The knee joint is anatomically and biomechanically the most complex synovial joint in the human musculoskeletal system. The anatomical arrangement of the bony structures femur, tibia, (fibula) and patella, and the surrounding soft tissue muscles, ligaments, articular cartilage and menisci are responsible for the physiological knee function (Figure 1). This arrangement allows movement over millions of load cycles during a whole life span, thereby accepting both, varying high loads and velocities [5]. Only during normal level walking, the double-peak loading regime of stance phase leads to a load transfer through the knee joint of up to three times body weight (BW) [5]. This inter alia requires efficient lubrication processes reducing friction between the articulating bony surfaces to keep the resultant wear to a minimum. Therefore, the ends of femur and tibia are covered with hyaline articular cartilage (AC) as a (bio-)bearing material [6, 7]. Additionally, to increase the contact area between the incongruent surfaces of femur and tibia and thus, reducing the contact pressure within the joint, the menisci, two semi-lunar and wedge-shaped fibrocartilaginous structures,

are located within the joint. Both cartilaginous tissues, articular cartilage and meniscus, mainly consist of water (70%-85%; fluid phase) and a solid phase, which is for each of the material a highly specialized extracellular matrix (ECM) [6]. While meniscus' ECM consists of 15%-25% collagen type I and only 1%-2% proteoglycan (PG) (based on the wet weight) the main collagen type in articular cartilage is collagen type II in almost the same amount. Additionally, a fivefold higher PG content is found in the AC's ECM [6, 8]. This special biphasic ultrastructure and the resultant viscoelasticity of both materials are responsible for and simultaneously provide their functionality [6, 8-14].

The menisci and their role within the knee joint

The main function of the menisci is to homogeneously distribute the contact loads over the tibiofemoral articulating surfaces. This crucial role is achieved by a synergy of the mentioned geometry and material properties but also by their anterior and posterior attachments to the tibia plateau. The axial loads, acting in the knee joint would lead to an extrusion of the wedge-shape menisci out of the joint space. However, as they are firmly attached to the tibial plateau, the axial compressive loads are transferred into circumferential tensile forces resisting the expansion and the loads are transferred to the meniscal insertions ligaments [9, 15]. The three-layered morphology of the menisci and the herein integrated special orientation of the collagen fibres directly relates to this function [8, 16]. In 1998, PETERSEN AND TILLMANN were the first researchers, who identified this structure using scanning electron microscopy [17]. They showed that the main portion of the collagen fibres is located within the central region, circumferentially orientated to withstand the mentioned tension forces. These collagen fibre bundles are additionally tied together by radial fibres, preventing longitudinal splitting of the meniscus. Directly above and below this main mid-layer, the collagen fibre bundles are lamellar showing a preferred radial direction but only in the external circumference of pars anterior and -posterior, whereas the tibial and femoral articulating surface is a superficial network of thin fibrils (Figure 1) [17].

Furthermore, the menisci are involved in joint stabilisation, nutrient distribution and joint lubrication [6, 9, 10, 18, 19]. Whether they also contribute to shock absorption in the knee could still not be fully confirmed or refuted, yet [20].

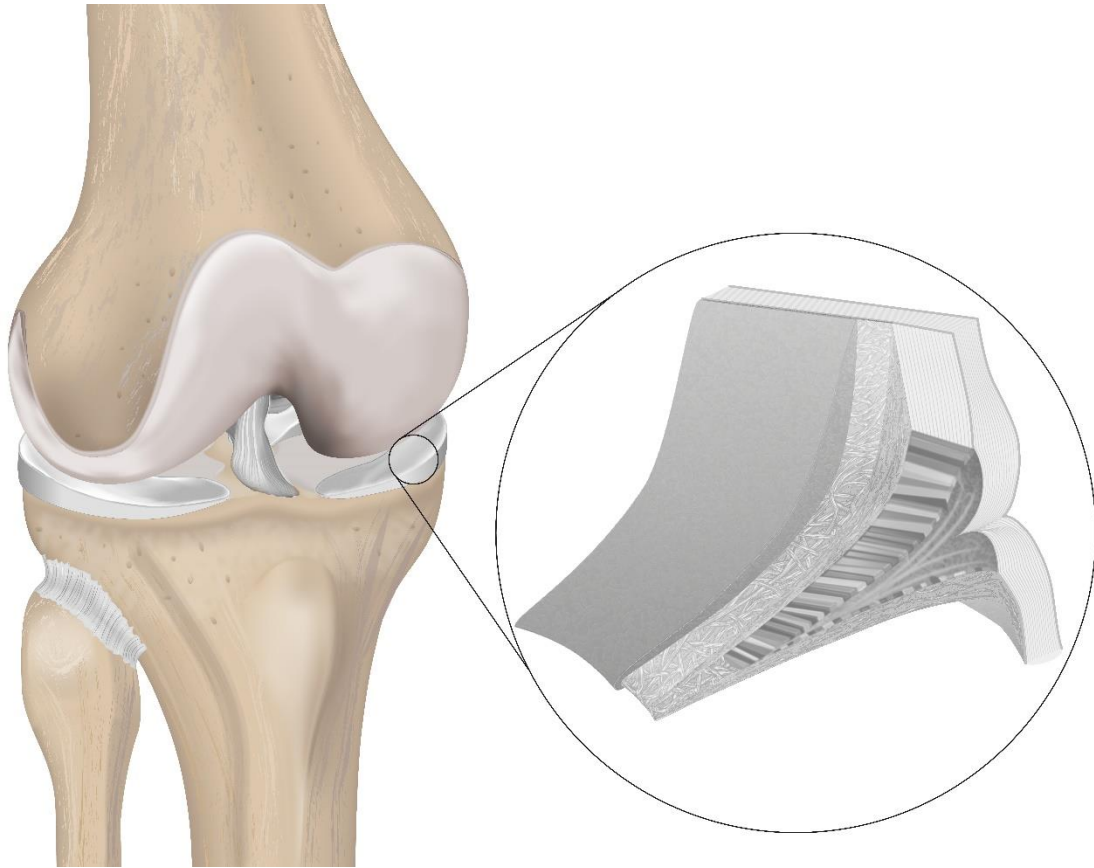


Figure 1: The anatomical arrangement of the bony structures: femur, tibia, fibula and patella (not shown) and the surrounding soft tissue are responsible for the physiological function of the knee. Thereby, the two semi-lunar and wedge-shaped menisci with the three-layered morphology play an important role (detailed view.)

Biomechanical material properties of the menisci

Over the last few years, several studies characterised the biomechanical properties of native meniscal tissue using standardised test methods, as tensile- and/or compression test. The obtained results were not only used to better understand the general function of this tissue but also to define requirements for the development of meniscal replacement materials [21].

Due to the mentioned inhomogeneous structural composition of the menisci, their biomechanical material properties differ between different regions of the meniscus, pars anterior, -intermedia and -posterior as well as between the different layers (anisotropy). Additionally, the side/compartments, from which the tested samples were harvested, medial or lateral meniscus and the testing procedure itself, play a role in the final evaluation of the biomechanical properties.

For example during tensile testing of standardised, dumbbell-shaped meniscal tissue samples, the main variations of the resulting elastic modulus were found in terms of the orientation of the collagen fibres [22-24]. Testing samples, which were harvested parallel to the circumferentially orientated collagen fibres, achieved a 10-fold higher elastic modulus in comparison to samples that were punched out parallel to the radial fibres. In detail, an elastic modulus up to 110 MPa was measured in circumferential direction, while in radial direction only approx. 10 MPa was reached. Since the main circumferentially orientated collagen fibres are located within the inner or central region, it is obvious that the tensile properties differ also within the three layers. Furthermore, TISSAKHT AND AHMED found elastic moduli of 120 MPa, 84 MPa and 130 MPa, for the proximal, middle and distal region of the lateral meniscus, respectively [22]. Further, these values were less for the medial meniscus [22, 23]. In addition, the central region seemed to be the less stiff section of both, lateral and medial meniscus (76 MPa and 68 MPa, respectively).

To determine the viscoelastic and, therefore time-dependent, compressive properties of meniscal tissue, there are two quasi-static testing configurations feasible: compression creep and -relaxation test. While during creep testing the applied load is kept constant, a relaxation test includes a constant applied strain over the testing duration. Out of these tests, several characteristic parameters, such as hydraulic permeability and aggregate/equilibrium modulus E_{eq} can be determined. Comparable to tensile testing, differences in the material properties depending on the location or compartment were observed [25-28]. CHIA AND HULL assessed the highest equilibrium modulus with approx. 130 kPa in the pars anterior when applying a physiological constant axial strain of 12%, while for the posterior part the lowest value of just 30 kPa was found [26]. A similar tendency was found within an unconfined compression relaxation test when applying 20% strain for 4000 s. However, lower values for the medial meniscus were reached (pars anterior: 70 kPa, pars intermedia: 35 kPa and pars posterior: 20 kPa) [27]. Moreover, there is a dynamical approach, characterising the viscoelastic properties of meniscal tissue with more detail. During this so called dynamic mechanical analysis DMA, sinusoidal loads are applied to the samples over a defined frequency range [29]. Due to the viscoelasticity of the meniscus, the deformation of the tissue lags behind the load. Using the specific phase lag angle δ , the damping factor $\tan(\delta)$ as well as the storage modulus E' and the amount of energy,

which is dissipated by the viscous mechanisms, the loss modulus E'' , can be determined [27, 29, 30]. Using this method, it could be shown that the anterior part of the meniscus has significantly higher damping properties ($\tan(\delta)$: 0.20 and 0.18 for 0.1 Hz and 10 Hz, respectively) than the mid body or pars posterior ($\tan(\delta)$: approx. 0.17-0.16 and $\tan(\delta)$: 0.15, respectively) [30]. However, in meniscus samples the viscous portion of the energy loss was generally smaller than the elastic portion, resulting in a lower loss modulus [27, 30]. For a physiological loading frequency of 1 Hz, the mid body of the medial meniscus showed an overall storage modulus E' of approx. 0.8 MPa and a loss modulus E'' of approx. 0.09 MPa [27, 30].

To complete not only the biomechanical characterisation of the native meniscus but also the list of requirements for a well-functioning replacement material, the friction properties are also of great importance. Friction in general is defined as the resistance of motion between two surfaces that are in contact. Using Coulomb's friction law, several studies investigated the frictional behaviour of both articular cartilage and meniscus using standardised test setups, like *pin-on-plate* or *pin-on-disc* configurations. Here, a remarkably low friction coefficient μ being partly less than 0.01 was demonstrated [12, 31-34]. However, as both tissues are biphasic materials, μ turned out to be multifactorial depending on different parameters and operating conditions, like time, lubricant, applied load/strain, rather than being just a material constant [31, 32, 34-36].

1.2. Clinical situation

Lesions of the medial meniscus are the second ranked injury within the knee joint, requiring a surgical intervention in 80% of these cases [1]. In 2014, more than 43'000 patients suffered from a meniscal tear [gbe-bund.de]. In general, meniscal tears can be classified according to their proximate cause – as a result of a traumatic injury or due to degenerative changes in the meniscus morphology. A traumatically induced lesion is mostly caused by sports activities, e.g. football, basketball or skiing, where the loaded and slightly flexed knee joint experiences considerable tibial rotation and varus or valgus moments. Here, the medial meniscus is more predisposed to injuries, as it is less flexible within the joint than the lateral meniscus. The pattern of the lesion is rather a vertical-longitudinal tear, which can also result in a bucket-handle tear [37]. Degenerated lesions of the meniscus however, are often horizontally or more complex, being located in several planes, like a flap tear.

In general, it is preferred to preserve the meniscus if clinically possible. However, depending on the localisation (vascular or avascular zone) and size of the lesion, it has to be treated surgically by resecting the injured meniscal tissue. Although, such partial meniscectomy is directly related to pain relief [38, 39], it was shown that this treatment strategy leads to degenerative changes to the adjacent articulating cartilage [3, 4, 38, 40-42]. As a part of the meniscal tissue is removed, the contact area is reduced and consequently the contact pressure is increased, resulting in an impaired load transmission within the knee joint and osteoarthritis can be the consequence [43]. Thus, there is an enhanced awareness developing new techniques and/or methods to preserve or replace meniscal tissue.

As the indications for meniscal repair by suturing technique are limited to tears located in the vascular region, replacement materials are alternative treatment strategies. Goal of such (partial) meniscal replacement is to restore the meniscal function to finally prevent degenerative changes of the surrounding articular cartilage. Therefore, different approaches are available, which in general can be divided into resorbable and non-resorbable strategies. Nevertheless, up to now only two alloplastic but regenerative scaffolds (CMI®, Collagen Meniscus Implant, Ivy Sports Medicine, Germany and Actifit®, Orteq Ltd., UK) for partial meniscal replacement are clinically available. Both porous scaffolds should promote the formation of new meniscus-like

tissue of comparable shape and functionality. However, none gained widespread adoption, as their ability to protect the underlying articular cartilage remains unclear [21]. One reason for that might be the significantly different mechanical/viscoelastic properties of both replacement materials in comparison to native human meniscal tissue [44]. To develop materials that successfully replace an injured meniscus, different requirements were postulated (Table 1) [21, 45]. Next to the fundamental material properties, like a comparable shape, biocompatibility, and especially important for tissue engineering approaches: (bio-)stability and biodegradability, it was stated that the biomechanical properties should mimic that of the native meniscus as close as possible. Thereby, the main function of the menisci – to transmit and distribute loads over the articulating surfaces of femur and tibia and thus reducing peak stresses – should be accomplished already in the initial phase after implantation. Additionally, the friction properties should be in the range of that for native meniscal tissue, whereby the friction coefficient μ should finally not exceed 0.05 [21, 45]. Furthermore, especially regarding resorbable scaffolds, the material should promote cell adhesion, differentiation, vascularisation and matrix deposition. Therefore, the “framework” should be a porous structure with total porosity > 70%, consisting of both large macro-pores with a diameter between 200 μm – 300 μm highly interconnected via micro-pores ($\varnothing = 10 \mu\text{m}$ – 50 μm) [21, 45].

Among different research approaches regarding non-resorbable materials for meniscal replacement [46-50], a silk fibroin scaffold (FibroFix™ Meniscus) for partial meniscal replacement was developed and manufactured by Orthox Ltd., UK. It is made from commercially obtained raw silk fibres from the silk worm (*Bombyx mori*, Silk Opportunities Ltd., Volketswil, Switzerland). After extracting the fibroin from the silk fibres, it was subsequently dissolved and the resulting solution is brought into a macro-porous internal structure [51]. Within a previous *in vivo* animal study, a first version of the silk fibroin scaffold showed an evidence of a chondroprotective effect as well as compression properties comparable to the native meniscal tissue after 6-month implantation [52, 53]. However, as the fixation and integration of the scaffold into the host meniscal tissue was insufficient, the material was subjected to an optimisation process and an orthogonal arranged silk fibre mesh was integrated into the porous matrix to improve anchoring of the fixation sutures. To bring this scaffold for

permanent meniscal repair successfully into clinics, it is indeed of major importance to previously characterise the biomechanical, material properties.

Table 1: Summarised overview of the basic requirements for meniscal replacement materials postulated by STONE and further elaborated by RONGEN ET AL. [21, 45].

Basic material requirements for meniscal substitutes:

Fundamental properties

- comparable shape and size ($\pm 10\%$) to native meniscus; most preferable: patient individual
- non-cytotoxic
- non-carcinogenic
- promote cell adhesion and -proliferation

(Initial) mechanical properties

“mimic the biomechanical properties of native meniscal tissue as close as possible”

- compressive modulus: 75 kPa – 150 kPa
- tensile modulus: 75 MPa – 150 MPa

Tribological properties

“mimic the biomechanical properties of native meniscal tissue as close as possible”

- friction coefficient $\mu \leq 0.05$

Structural composition

- porous structure
- large macro-pores (200 μm – 300 μm) interconnected with smaller micro-pores (10 μm – 50 μm)
- total porosity $\geq 70\%$
- high interconnectivity
- anisotropic architecture

Resorbable materials

- adequate degradation profile
- surface degradation profile (with decreasing size and mass in time but no change in molecular weight or mechanical properties) more preferable than bulk degradation profile
- duration: at least 12 months

1.3. Aim of the work

Although, it has been shown that even only partial meniscectomy is associated with degenerative changes of the adjacent articular cartilage and therefore osteoarthritis could be a consequence, it is still the gold standard therapy to treat different forms of an injured meniscus. Therefore, there is an increased need of new treatment strategies that successfully replace and restore the resected meniscus to finally prevent the formation of OA in the long-term. Over the last years, different research approaches were developed [21, 46-50, 54-57]. Since only two of them (CMI® and Actifit®) were brought into clinics but without the expected success, guidelines to successfully develop a replacement material were meanwhile postulated [21, 45]. Here, it was stated that the biomechanical properties of a potential replacement material should mimic that of the native meniscus as close as possible [21, 45].

Having these requirements in mind, the first experimental study of the work at hand was conducted to biomechanically evaluate the second generation of the mentioned silk fibroin scaffold for partial meniscal replacement [51]. Within an earlier animal study, it already displayed promising results regarding cartilage protection in comparison to a partial meniscectomy after six month of implantation. However, as its fixation to the meniscal host tissue was insufficient, the scaffold was subjected to an optimisation process and a fibre layer was integrated into the porous matrix. Using flat sheets manufactured of the optimised silk fibroin, which was materially and structurally identical to the corresponding meniscus implants (FibroFix™ Meniscus, ORTH REP M081), the aim of the study was to answer the question:

1. *Does the silk fibroin scaffold biomechanically meet the postulated requirements for meniscal replacement?*

One result of this study was that the silk fibroin scaffold showed mechanical competence, which is of course important for a replacement material to support and therefore, to distribute loads over the articulating surface [51]. However, it is obvious that additionally good friction and lubrication properties, which are comparable to that of the native meniscal tissue, are desirable for a well-functioning replacement material, as well. Therefore, a further friction study was designed to investigate the question:

2. *Does the silk fibroin scaffold exhibit friction properties comparable to that of the native menisci?*

Within the first friction study, constant testing parameters were used to evaluate the friction properties of the silk fibroin scaffold [34]. However, within the knee joint the loading and motion conditions vary considerably during physiological activities, like normal walking. Consequently, the following question arises:

3. *How is friction within the knee joint and especially of the artificial material for meniscal replacement affected by the varying testing conditions physiologically acting during gait?*

To answer this question, a second friction study was conceived to investigate the frictional behaviour of the silk fibroin scaffold in comparison to the physiologically articulating surfaces within the knee joint – meniscus and articular cartilage – under testing conditions characteristically occurring in the knee during walking [58].

2. Biomechanical Characterisation of a Potential Material for Meniscal Repair

WARNECKE D, STEIN S, HAFFNER-LUNTZER M, DE ROY L, SKAER N, WALKER R, KESSLER O, IGNATIUS A, DÜRSELEN L. Biomechanical, Structural and Biological Characterisation of a New Silk Fibroin Scaffold for Meniscal Repair. J Mech Behav Biomed Mater 86 (2018) 314-324. [51]

Meniscal injuries, especially irreparable lesions of the avascular, white-white region of the meniscus still require a partial or a total meniscectomy. As it has already been shown that removing meniscal tissue leads to an increased contact pressure and therefore, to cartilage degeneration, research mainly focused on meniscal preservation and/or replacement strategies. The menisci within the knee joint are of multifunctional nature, which is achieved by a synergy of their special geometry, unique material properties as well as their anterior and posterior attachments to the tibial plateau. Consequently, it is obvious that successfully replacing an injured meniscus and thus preventing early osteoarthritis, requires not only a simple “framework” but it also has to take up the versatile biomechanical functionality of native meniscus. Therefore, STONE once postulated basic requirements for meniscal replacement materials, which were almost 20 years later further elaborated by RONGEN ET AL. [21, 45]. Here, it was stated that especially the biomechanical properties like transmitting and distributing loads over the articulating surfaces and thus, reducing peak stresses, have to be fulfilled already in the initial phase after implantation [21]. Until now, only two research approaches were transferred into clinical use, which are, however, not widely accepted. Within preclinical *in vitro* studies, it was additionally shown that both artificial replacement concepts could not meet the requirements, displaying significantly different viscoelastic properties compared to human meniscal tissue [44]. A non-resorbable silk fibroin scaffold for partial meniscal replacement already showed compressive properties comparable to ovine meniscal tissue as well as evidence of a chondroprotective effect after 6-month implantation in a sheep model [52, 53]. However, due to an insufficient fixation and integration into the adjacent meniscal host tissue, the scaffold was exposed to an optimisation process including the integration of

a silk fibre mesh into the porous matrix. To answer the question “*Does the silk fibroin scaffold biomechanically meet the postulated requirements for meniscal replacement?*” the silk fibroin scaffold was characterised in terms of its biomechanical properties as well as its structural composition. Therefore, several quasi-static tests as well as a dynamic compression test were performed on scaffold samples with standardised geometry. These flat samples were materially and structural identical to meniscus shaped implants (Figure 2, A). The study comprised testing procedures including tensile, indentation, unconfined compression relaxation and creep as well as a dynamic mechanical analysis to characterise the viscous and elastic properties in detail.

During tensile testing, the ultimate tensile force F_{max} of $51.0 \text{ N} \pm 16.1 \text{ N}$ as well as the linear elastic modulus E with an average of $5.4 \text{ MPa} \pm 1.5 \text{ MPa}$ of dumbbell-shaped samples of the silk fibroin scaffold were assessed. To the best of our knowledge, the current study was the first one determining the tensile properties of a potential meniscal replacement material using samples of standardised geometry. Nevertheless, when comparing these results with meniscus tissue it is obvious that the obtained tensile elastic modulus was much lower. However, the silk fibroin scaffold is designed to address partial meniscal replacement, where the outer meniscal rim of the native tissue with the circumferential collagen fibres is still maintained. Therefore, the functionality transferring axial compressive loads into circumferential tensile loads could still be provided. Nevertheless, to improve the tensile properties of the scaffold, the arrangement of the integrated fibre mesh could be adapted to the circumferential arrangement of the native meniscus' collagen fibres.

As the silk fibroin scaffold should be used for partial meniscal replacement, it is consequently more exposed to compressive rather than tensile loads. Therefore, several quasi-static but also dynamic compression tests were performed. Among those, a cyclic indentation test according to SANDMANN ET AL. was included [44]. Here, five load cycles up to 7 N were applied to the scaffold, whereas a full load cycles additionally included a relaxation time of 60 s directly after the load application, followed by a load-release to 0.1 N and another 60 s recovery phase. This test setup was first conducted by SANDMANN ET AL. the only study evaluating the viscoelastic properties of the two clinically available meniscal implants CMI® and ActiFit® in comparison with meniscal tissue of different species [44]. The silk fibroin scaffold reached a fifth cycle stiffness of an average of 24.7 N/mm, which was significantly higher than in the first cycle (approx.

18 N/mm; paired Student's t-test, $p < 0.0001$ with a two-tailed p-value). Comparing these results with the results of SANDMANN's study, the scaffold tested in the current study was not only significantly stiffer than the two artificial materials CMI® and Actifit® but also in comparison to human meniscal tissue ($p < 0.05$, one-way analysis of variances (ANOVA) with Bonferroni's multiple comparison test). Nevertheless, the averaged fifth cycle stiffness displayed a value, which was more closely to that of human meniscal tissue than the other two scaffolds. Consequently, the silk fibroin scaffold showed an initial compressive competence as required by RONGEN ET AL. and STONE unlike the CMI® and Actifit® [21, 44, 45].

This increased stiffness compared to human meniscal tissue was also confirmed within both unconfined compression configurations – relaxation and creep. In each of the tests the equilibrium modulus was significantly different from human meniscal tissue, previously tested in comparable test setups. As the scaffold additionally showed a higher stiffness in comparison to the prior version [52], it is likely that the integration of the new fibre component during the optimisation process was responsible for this change in the material stiffness. However, this discrepancy regarding material properties could potentially prevent the permanent integration into the meniscal host tissue as a too stiff material may impede tissue ingrowth [21] and could damage the underlying articular cartilage [59].

During the dynamic mechanical analysis (DMA), the storage modulus E' of the scaffold material only slightly increased from approx. 1.2 MPa to 1.4 MPa with increasing testing frequency of 0.1 Hz to 10 Hz, respectively. A comparable tendency with values within the range of the silk fibroin scaffold were also found by PEREIRA ET AL., investigating the dynamic compressive properties of fresh frozen human menisci [30]. Nevertheless, the DMA showed that the scaffold had a slightly higher capability to dissipate energy than human meniscal tissue, also indicated by a higher loss modulus. Consequently, the scaffold's elastic properties were more present than its viscous character.

To complete the material characterisation of the silk fibroin scaffold, the structural composition as well as the architecture were also determined using micro computed tomography (μ -CT) (Figure 2, B). The μ -CT analysis revealed a mean total porosity of $\sim 80\%$ with a mean pore size of approx. 216 μm . Both results meet the basic requirements for meniscal replacement materials [21]. However, adjusting these

parameters with respect to the distribution of pore sizes and wall thickness could be an opportunity to reduce the material's stiffness resembling especially the compressive properties of human menisci. Nevertheless, it will always be a big challenge mimicking the characteristic anisotropy and inhomogeneity of the native meniscal tissue using an artificial material. This is even more complicated in case of partial meniscal replacement, as the required high mechanical competence already before implantation combined with a high flexibility allowing for adaption to the complex movement of the femoral condyle as well as the meniscal host tissue, ensuring successful implant integration.

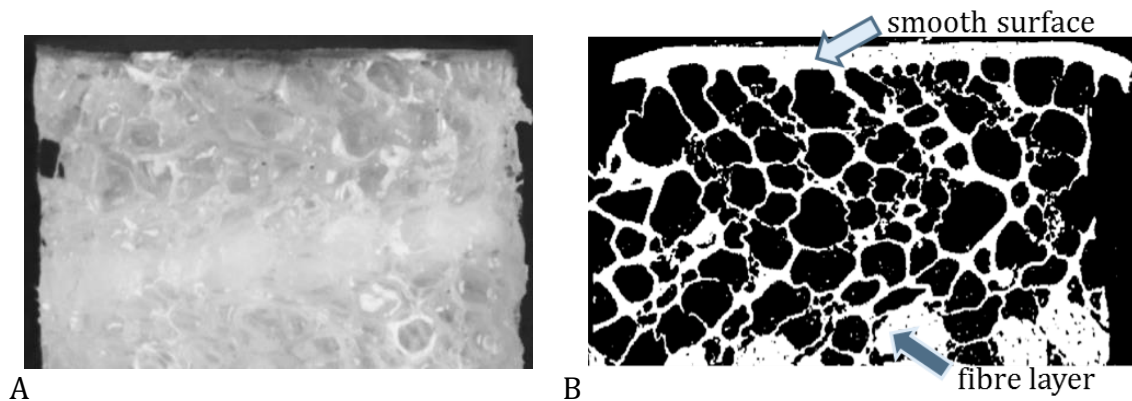


Figure 2: Macroscopic view of a cylindrical sample of the silk fibroin scaffold punched out of a scaffold's flat sheet manufactured by Orthox Ltd. (A). During μ -CT analysis the structural composition and architecture was additionally determined to complete the biomechanical characterisation of the scaffold (B). Modified figure from [51] with Creative Commons Attribution License 4.0 International (CC BY 4.0, <http://creativecommons.org/licenses/by/4.0/>).

3. Friction Properties of a Silk Fibroin Scaffold in Comparison to the Physiology

WARNECKE D, SCHILD NB, KLOSE S, JOOS H, BRENNER RE, KESSLER O, SKAER N, WALKER R, FREUTEL M, IGNATIUS A, DÜRSELEN L. Friction properties of a new silk fibroin scaffold for meniscal replacement. *Tribol Int* 109 (2017) 586-92. [34]

In a healthy knee joint, the menisci protect the articular cartilage by reducing the contact pressure [9, 18]. Consequently, if an injured meniscus is even partially resected, the resultant reduced contact area leads to an increased contact pressure [3, 4, 40]. Furthermore, meniscal resection additionally increases the friction within the joint [33] and McCANN ET AL. identified the formation of cartilage fibrillation and signs of wear instantaneously after removing meniscal tissue [33]. Therefore, new approaches for meniscal replacement should not only consider mimicking the biomechanical properties of the native meniscus but also the remarkably low friction properties as close as possible [21, 45]. Consequently, the frictional behaviour is of major importance to maintain the chondroprotective function of meniscal implants, as high friction coefficients might lead to cartilage wear.

Several studies investigating the friction properties of articular cartilage and meniscal tissue have already shown that the friction coefficient of these tissues is rather a multifactorial parameter than just a material property as it depends on a variety of testing parameters [6, 7, 31, 35, 36, 60]. The opposing surface for instance has a major effect on the friction coefficient. In most cartilage friction studies, glass was typically used as it provides a counter surface of reproducible smooth properties [12, 31, 61, 62]. Nevertheless, the resulting friction coefficient might be debatable as the characteristic biphasic material properties of cartilaginous tissues are missing.

The aim of the current study was to evaluate the friction properties of the mentioned silk fibroin scaffold. Based on the promising results of the prior *in vivo* study and of a study by PARKES ET AL., where a silk fibroin hydrogel for cartilage repair showed a cartilage-like friction response [63], we attributed (1) the silk fibroin scaffold to have friction properties comparable to the physiologically articulating surfaces in the knee joint – meniscus and articular cartilage. Additionally, in terms of glass as a

homogeneous and even opposing surface, we further hypothesised (2) that its use leads to higher friction coefficients not only for AC but also for meniscus and its possible replacement material. Therefore, cylindrical samples (*pin*, $\varnothing = 6$ mm) were retrieved from the medial meniscus (M) and the tibial plateau (TC) of 6 bovine knee joints as well as from flat sheets of the silk fibroin scaffold (S, $n = 6$) (Figure 3). Afterwards, they were tested against the *plate*: a flat cartilage sample harvested from each of the medial femoral condyles and a smooth glass slide (VWR* Plain Micro Slides, VWR International GmbH, Germany), respectively. For standardised testing, a *pin-on-plate* friction-testing device was designed applying a constant load ($F_N = 14,6$ N) to the *pin* resulting in a moderate physiological contact pressure in quadrupeds of 0.5 MPa [64] while the *plate* slid cyclically against it (stroke length $s = \pm 15$ mm, sliding velocity: $v = 1$ mm/s) for 250 cycles. Bovine synovial fluid was used as a lubricant. For friction analysis, the friction coefficient was determined at the beginning of the experiment (μ_0) as well as at the end of the testing duration, when equilibrium was reached (μ_{eq}). Additionally, the strains of the cylindrical samples were evaluated at both time points (ε_0 and ε_{eq} , respectively) by dividing the deformation recorded by a laser distance sensor by the initial samples height h_0 .

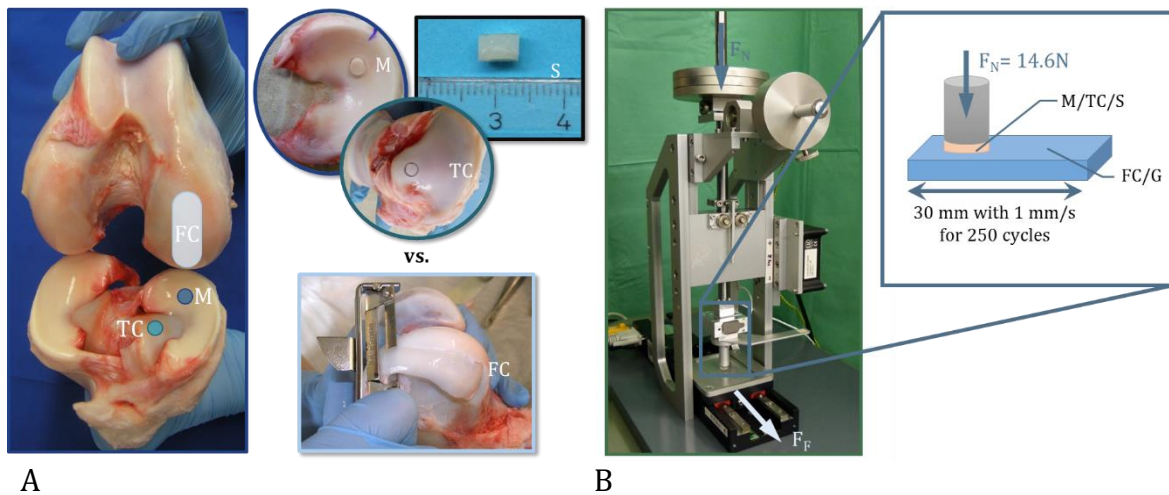


Figure 3: Six cylindrical samples each from the medial meniscus (M), the tibial plateau (TC) of bovine knee joints or from flat sheets of the silk fibroin scaffold (S) were harvested (A) and tested against either a flat cartilage (FC) sample or against glass (G) using a customised pin-on-plate friction testing device (B). Modified figure from [34] with Creative Commons Attribution License 4.0 International (CC BY 4.0, <http://creativecommons.org/licenses/by/4.0/>).

The current study is the first one evaluating the friction properties of a silk fibroin scaffold as a possible new material for partial meniscal replacement. The scaffold reached a friction coefficient, when testing against articular cartilage, of 0.056 ± 0.012 , which was significantly higher than both meniscus and tibial cartilage each against cartilage ($\mu_{eq} = 0.021 \pm 0.006$ and $\mu_{eq} = 0.014 \pm 0.007$, respectively) (Figure 4, A). Consequently, the first postulated hypothesis was refused. Nevertheless, the friction coefficient after >2h of testing was still within the range of the basic requirements for meniscal replacement materials, further elaborated by RONGEN ET AL. [21]. However, testing against glass, which was typically done in most previous friction studies [12, 31, 61, 62], led to significantly higher friction coefficients for all three cylindrical samples (M: $\mu_{eq} = 0.100 \pm 0.058$, TC: $\mu_{eq} = 0.215 \pm 0.065$ and S: $\mu_{eq} = 0.446 \pm 0.047$) than testing against articular cartilage, thereby confirming the second hypothesis (Figure 4, B). Thus, it is obvious that the use of glass as an opposing surface might be useful to perform comparative studies on different biomaterials but did not reveal physiological relevant friction coefficients for joints. This additionally should be taken into account especially when testing new implant materials regarding their long-term chondroprotective function. As these results still fit quite well to the mentioned previous studies [12, 31, 61, 62], it emphasises the validity of the friction testing device and therefore of the results of the current study.

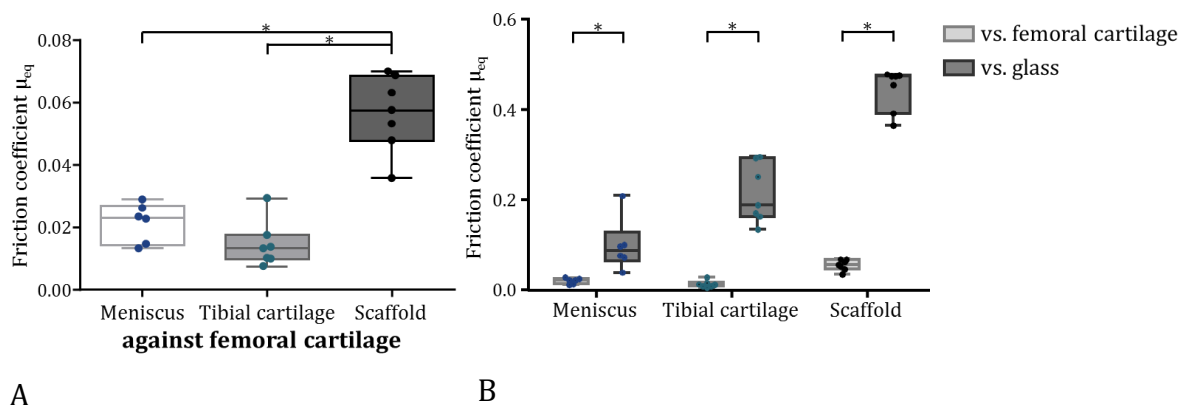


Figure 4: Although the friction coefficient of the silk fibroin scaffold was significantly higher than the physiologically articulating surfaces within the knee joint: *meniscus* and *cartilage*, μ was still within the range of the requirements for materials for meniscal repair [21], when testing against the flat cartilage sample (A). Using glass as opposing surface always leads to significantly higher friction coefficients than using cartilage (B); $*p \leq 0.05$ using one-factor ANOVA with uncorrected Post-Hoc Fisher's LSD test (A) and two-factor ANOVA with repeated measures (B). Modified figure from [34] with Creative Commons Attribution License 4.0 International (CC BY 4.0, <http://creativecommons.org/licenses/by/4.0/>).

Additionally, all cylindrical samples showed an increase in their strain values over time until an equilibrium was reached. This was true for both opposing surfaces demonstrating a typical behaviour for biphasic materials in an unconfined creep configuration. When a biphasic material like articular cartilage or meniscus is loaded over a period of time, the applied load is only initially supported by the fluid phase. During the creep process a continuous load transfer from the fluid to the solid phase occurs, whereas after equilibrium was reached the applied load is completely carried by the solid phase [6]. Assuming that the tissue that bears the load is also responsible for the friction, it becomes clear that the friction coefficient for all cylindrical samples only increases with time when testing against glass, whereas using cartilage as opposing surface, μ stayed at a constant low level. This is most likely attributable to the lack of pressurisation of the interstitial fluid in non-biological materials [61]. Therefore, testing against glass leads to a decrease of the fluid load support from almost 100% at the onset to almost 0% when equilibrium was reached [12, 13, 32, 61, 65]. While using cartilage, the fluid load support remained at a high level of > 80% and consequently it was always the fluid phase that supported the applied load [65]. As the *plate* slid cyclically against the loaded *pin*, the cartilage was just alternately loaded. This enables the different regions of the cartilage to recover before the pin is going to load this region again, leading to a constant low friction coefficient.

Regarding the second research question if "*the silk fibroin scaffold exhibits friction properties comparable to that of the native menisci*", the current study showed that even if the friction coefficient of the scaffold is significantly higher in comparison to native meniscal tissue, it is still within the range of the basic requirements for meniscal substitutes [21]. Whether this enables also an *in vivo* long-term chondroprotective function of the scaffold has to be proven within an additional animal study.

4. Friction analysis under simulated physiological loading and motion conditions

WARNECKE D, MEßEMER M, DE ROY L, STEIN S, GENTELINI C, WALKER R, SKAER N, IGNATIUS A, DÜRSELEN L. Articular cartilage and meniscus reveal higher friction in swing phase than in stance phase under dynamic gait conditions. *Sci Rep* 9 (2019) 5785. [58]

Within the knee joint, the (axial) loading and motion conditions vary considerably during activities of daily life [5]. During one walking-gait cycle, which can be divided into a stance- (60%) and a swing phase (40%), the tibiofemoral contact forces rise up to 2-3 times body weight during stance phase while during the low-loaded swing phase the velocities are highest [5, 7, 66-68]. Nevertheless, most previous friction studies investigated the friction properties of articular cartilage and meniscus under constant axial loading conditions and sliding velocities and therefore, neglected these variations. Out of these, several tribological theories were postulated based on the three lubrication modes: boundary-, mixed- and fluid lubrication to describe the extremely low but complex friction properties of both cartilaginous tissues [7, 60, 69-73]. Consequently, the question arises *how these dynamic conditions affect the friction within the knee joint and especially of the mentioned silk fibroin scaffold as potential meniscal replacement material*. To answer this question a new dynamic friction testing device was developed in a *pin-on-plate* configuration. Its centrepiece was a dynamic materials testing machine (ElectroForce® 5500, BOSE/TA Instruments, USA), which was equipped with a linear motor (VT-75, PI miCos, Germany) mounted on a customized aluminium frame (Figure 5). Using the mentioned testing device it was possible to investigate the friction properties under defined but more physiological testing conditions, as the dynamic normal forces, which are typically acting in the knee joint during gait, were applied to cylindrical samples (*pin*) of the silk fibroin scaffold, meniscus or articular cartilage. Synchronously, a flat cartilage sample (*plate*) slid against it with varying velocities derived from stance- and swing phase of a human gait cycle.

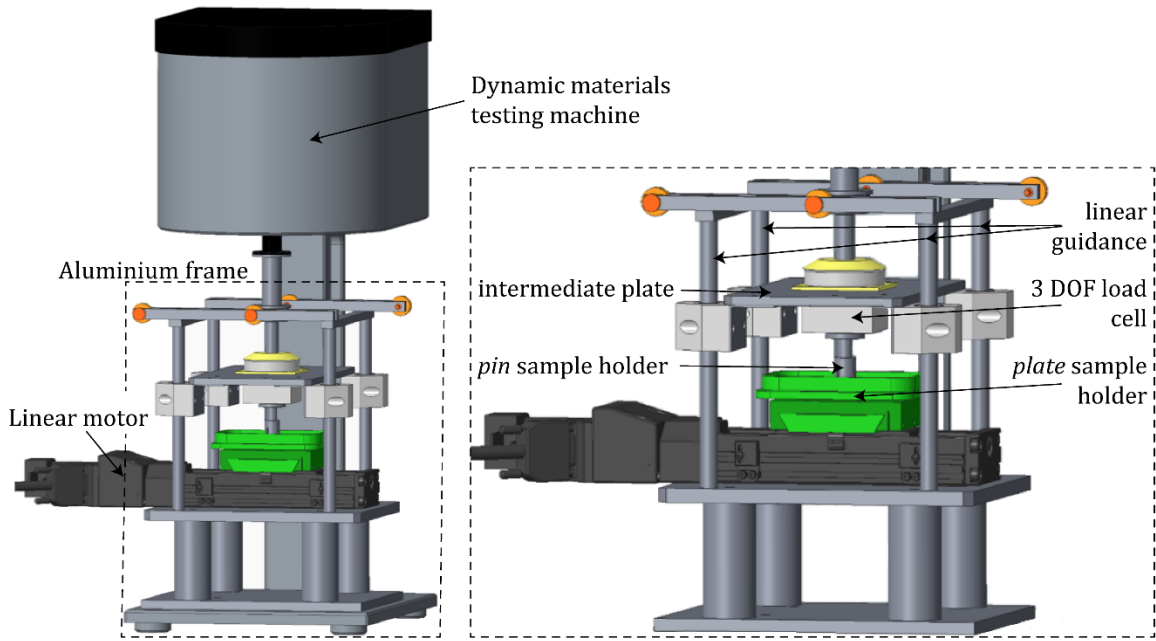
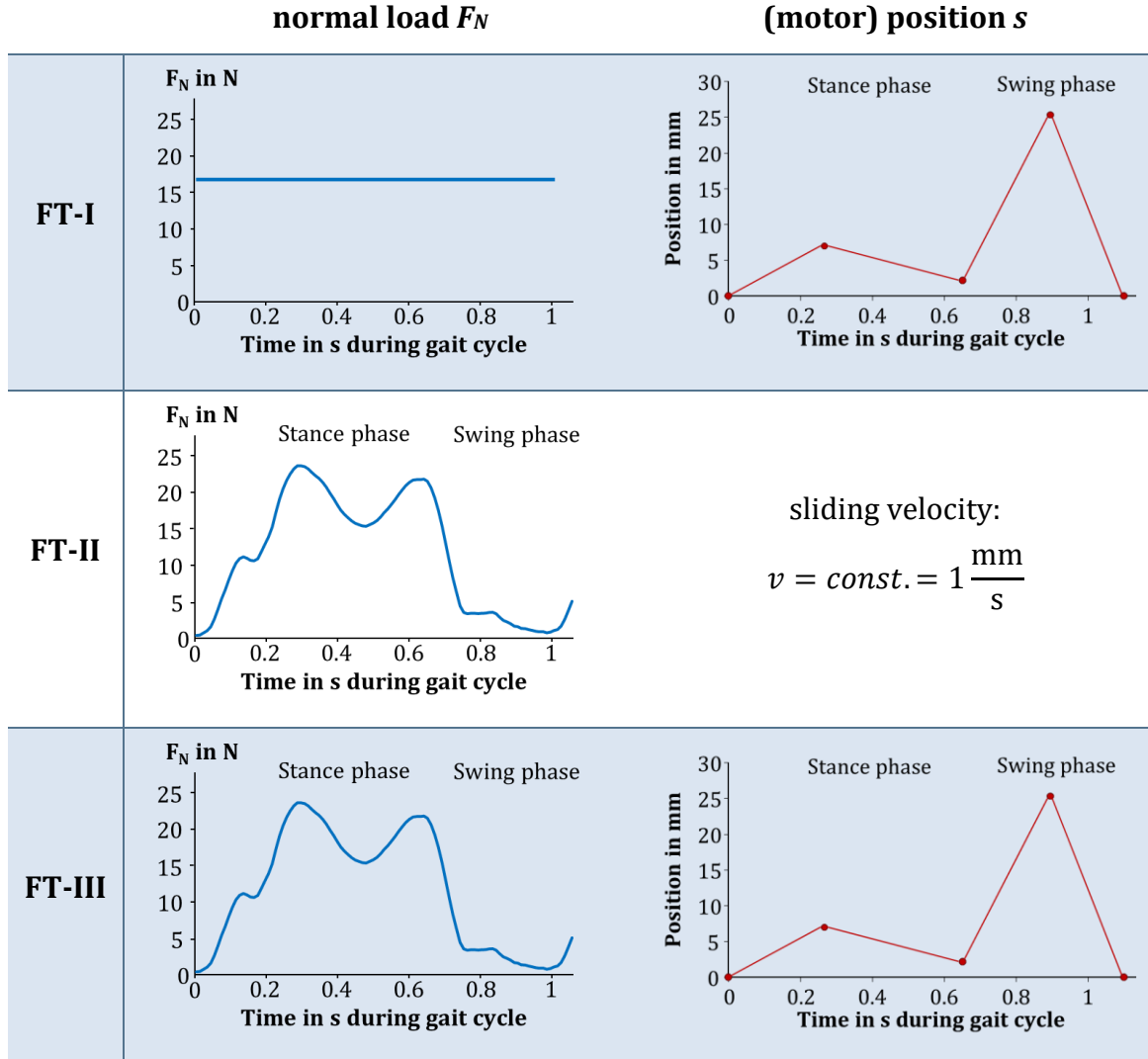


Figure 5: The dynamic friction testing device was developed to investigate the friction properties under defined testing conditions occurring during gait. It basically consists of a dynamic materials testing machine (ElectroForce® 5500, BOSE/TA Instruments, USA), which was equipped with a linear motor mounted on a customized aluminium frame (detailed view). Modified figure from [58] with Creative Commons Attribution License 4.0 International (CC BY 4.0, <http://creativecommons.org/licenses/by/4.0/>).

As this was the first study synchronously varying axial load as well as sliding velocity, the study comprised three test scenarios: **Friction Test-I**; **-II** and **-III**. Thereby in **FT-I** and **-II** only one testing parameter was modified, normal load F_N or velocity v : **FT-I**: $F_N = \text{const.}$, v according to a gait cycle; **FT-II**: F_N according to a gait cycle, $v = \text{const.} = 1\text{mm/s}$, whereas in **FT-III** both loading and motion conditions (F_N and s , respectively) varied according to a gait cycle (Table 2).

Both native forms of cartilaginous tissues showed higher friction coefficients during the low-loaded swing phase than during stance phase when testing under the most physiological testing conditions (**FT-III**, meniscus: $\mu(\text{stance phase}) \cong 0.015$, $\mu(\text{swing phase}) \cong 0.03$ and cartilage: $\mu(\text{stance phase}) \cong 0.02$, $\mu(\text{swing phase}) \cong 0.03$; Figure 6, A and B). This is in line with the literature, where KRISHNAN ET AL. showed an increased friction coefficient when testing articular cartilage against glass during low-loaded phases [74]. A reason for that might be the simultaneously detectable negative values of the fluid load support, leading to the assumption that suction might occur when the load changes to a lower level [74].

Table 2: Tabular overview of the three friction test scenarios (FT-I, -II and -III) and the corresponding application of the testing parameters: normal load F_N and motion (motor position s in mm). Modified table from [58] with Creative Commons Attribution License 4.0 International (CC BY 4.0, <http://creativecommons.org/licenses/by/4.0/>).



Testing the silk fibroin scaffold, this phenomenon could also be observed during **FT-II**, when only varying the normal load, but resulting in higher friction coefficients (FT-II averaged stance phase: $\mu = 0.069 \pm 0.011$ and swing phase: $\mu = 0.107 \pm 0.021$) in comparison to **FT-I** and **-III** (0.038 ± 0.009 and 0.047 ± 0.020 , respectively; Figure 6, C). Nevertheless, the scaffold revealed friction coefficients comparable to that of the first friction study and consequently met again the basic requirements for a meniscal replacement material in terms of the friction coefficient even when testing under the most physiological testing conditions (**FT-III**) [21, 34].

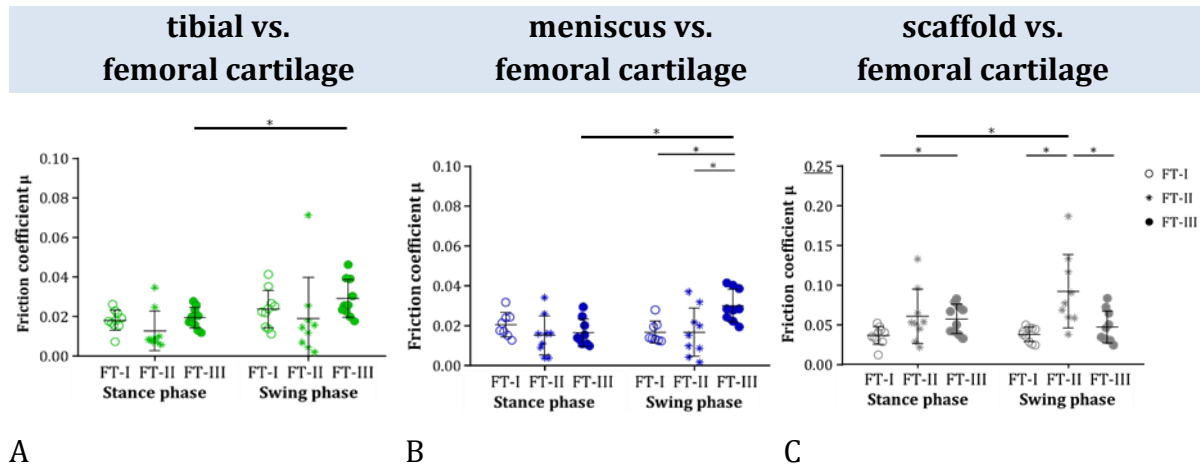


Figure 6: Comparison of the friction coefficients μ obtained for each material pairing: tibial cartilage (A), meniscus (B) and the silk fibroin scaffold (C) each against femoral cartilage within the three different friction test scenarios ($n = 8-10$, mean \pm standard deviation and raw data; \circ FT-I, $*$ FT-II, \bullet FT-III), $*p \leq 0.05$. Modified figure from [58] with Creative Commons Attribution License 4.0 International (CC BY 4.0, <http://creativecommons.org/licenses/by/4.0/>).

Next to the soaking effect and the resultant rise in the friction, it is also known that a consistent fluid film is formed during swing phase that additionally can be maintained throughout the entire gait cycle [7, 66]. This fluid film in connection with the different loads and velocities during a gait cycle, lead to the assumption that the already postulated lubrication modes, especially hydro- and elasto-hydrodynamic lubrication synergistically contribute to the remarkably low friction properties of the physiologically articulating surfaces in the knee joint [7, 75]. Although, friction testing under static testing conditions and defined lubrication regimes might be important, the current study showed that testing under physiological testing conditions revealed higher friction coefficients, especially during the low-loaded swing phase. Consequently, this leads to the assumption that static friction tests can underestimate friction coefficients rather than reflecting the complex *in vivo* behaviour, which especially might be important for potential replacement materials.

5. Conclusion

The menisci play a decisive role within the knee joint, as they protect the underlying articular cartilage by reducing the contact pressure. This function is accomplished by a synergy of the characteristic geometry and special viscoelastic and anisotropic material properties. Nevertheless, (partial) meniscal resection is still the gold standard therapy for meniscal lesions in the avascular region, even if it is already known that this can finally precipitate the formation of osteoarthritis. Therefore, over the last years research has focused on alternative treatment strategies to repair and/or restore the meniscal tissue. However, only two artificial devices for partial meniscal replacement were brought into clinics so far but without widespread acceptance among the surgeons. A reason for that might be that their long-term chondroprotective function could not be fully proven, yet. Significant differences in their biomechanical properties in comparison to native meniscal tissue might be the reason. As a guideline for the development of adequate materials for meniscal repair, basic requirements have already been postulated providing fundamental material properties, like biocompatibility, as well as key data for the biomechanical competence and friction properties. Based on these specifications, a redesign of a non-resorbable silk fibroin scaffold for partial meniscal replacement was characterised within three experimental *in vitro* studies with regard to the biomechanical as well as structural (1) and its friction properties (2), always in comparison with meniscal tissue. Finally, the investigation of the scaffold's friction properties was enlarged by using simulated physiological testing conditions (3) as they typically occur within the knee joint during gait.

The present work depicts the first comprehensive material characterisation of a prospective meniscus replacement material. Thereby, not only quasi-static but also dynamic and therefore, more physiological testing procedures were chosen to investigate the silk fibroin scaffold for its crucial role within the knee joint. The resultant material properties were then compared to the basic requirements for meniscal replacement materials as well as to native meniscal tissue. Although the examined scaffold material showed properties partially within the range of the basic requirements for meniscal replacement materials, the data however, were always exceeding the remarkable meniscus material properties. Consequently, further material improvements especially regarding its compressibility are necessary to

promote tissue regeneration and simultaneously prevent potential cartilage destruction underneath the scaffold *in vivo*. Furthermore, the reduction in compressive stiffness may also improve the friction properties, since the silk fibroin scaffold can assimilate the movements of femur and tibia within the knee joint more closely. Even if the scaffold is currently not yet suitable for clinical use, the findings of the work at hand are important to initiate optimisation procedures to achieve the main goal of replicating the remarkable material properties of native meniscal tissue as closely as possible. Imitating its characteristic inhomogeneity and anisotropy as well as the high stiffness and flexibility at the same time, additionally impede a successful meniscal replacement. Furthermore, it was constituted that developing an adequate material, especially for partial meniscal replacement, would always be a big challenge as there would always be a mismatch in the material's stiffness between the artificial material and the meniscal host tissue.

6. Abstract

Among different research approaches to replace an injured meniscus, a silk fibroin scaffold for partial meniscal replacement has been introduced showing promising results in terms of biocompatibility and chondroprotection experimentally *in vivo*. Basic requirements for meniscal replacement have previously been postulated, stating that a replacement material should resemble the biomechanical properties of the native meniscus as close as possible. Based on these specifications, the present study biomechanically characterised a materially optimised version of the mentioned silk fibroin scaffold.

A first *in vitro* study comprised the comprehensive evaluation of the biomechanical material properties as well as the structural composition of the scaffold to address the question: “*Does the silk fibroin scaffold biomechanically meet the postulated requirements for meniscal replacement?*” Comparing the obtained results to the material properties of the postulated requirements as well as of native meniscal tissue, it could be shown that the silk fibroin scaffold displayed an adequate mechanical competence, which is important to distribute loads over the articulating surfaces already in the initial phase after implantation. However, the achieved compressive stiffness was in excess of native meniscal tissue, which may impede tissue ingrowth and can additionally cause damage of the underlying cartilage *in vivo*. A new fibre mesh, which was integrated into the porous matrix during the material optimisation process in order to enhance surgical fixation *in vivo*, could have led to this increased stiffness. However, this new fibre component could not provide tensile strength comparable to that of the native meniscus. Especially for larger meniscal defects, the scaffold could be improved by modifying this fibre component to better mimic the circumferentially orientated collagen fibres of native meniscal tissue. Adjusting the additionally obtained structural parameters, like distribution of the pore-walls as well as their thickness, could be an option to reduce the material’s compressive stiffness, thereby imitating native meniscal tissue more closely.

To prevent wear, an adequate replacement material should exhibit next to its competent behaviour under compression and tension, friction properties comparable to meniscal tissue. Therefore, the question arises “*Does the silk fibroin scaffold exhibit friction properties comparable to that of the native menisci?*” Within a friction study, the

scaffold revealed significantly higher friction coefficients in comparison to that of meniscal tissue but still within the range of the postulated basic requirements when tested against articular cartilage. Additionally, it could also be shown that glass, which is typically used as opposing surface in cartilage friction studies, always led to significantly higher friction coefficients. This emphasizes the importance of choosing an appropriate material as opposing surfaces to obtain relevant friction coefficients for joints. This in particular applies to friction analyses of future meniscal implants in order to assess whether they ensure long-term chondroprotective function from a tribological point of view.

During activities of daily live, e.g. normal walking, the axial loads as well as the velocities of the femoral and tibial surface vary considerably within the knee joint. Consequently, it is questionable if static friction studies as they are typically performed, also within the prior friction study, reflect the conditions occurring *in vivo*. Hence, the question arises, if *friction within the knee joint and especially of the artificial material for meniscal repair is affected by the varying conditions physiologically acting during gait*. Therefore, the subsequent study investigated the friction behaviour of the silk fibroin scaffold as well as of the articulating surfaces within the knee joint under testing conditions characteristically occurring during gait. Using a new dynamic friction testing device, both cartilaginous tissues, meniscus and articular cartilage, revealed statistically higher friction coefficients during the simulated low-loaded swing phase than during the high-loaded stance phase. This suggests that static testing methods can rather underestimate friction coefficients. Consequently, the second friction study additionally emphasises the relevance of testing under physiological loading and motion conditions.

In summary, although the characterised silk fibroin scaffold partly meets the basic requirements for meniscal replacement materials, further improvement are necessary to mimic the remarkable material properties of the native meniscus more closely, thereby enhancing its chondroprotective function *in vivo*.

7. Literature

- [1] Majewski, M., Susanne, H., Klaus, S., Epidemiology of athletic knee injuries: A 10-year study. *Knee*. 13: 184-8, 2006.
- [2] Bundesamt, S., Die 20 häufigsten Operationen insgesamt (OPS-Schlüssel 5). Vollstationäre behandelte Patientinnen und Patienten in Krankenhäuser 2017, Statistisches Bundesamt, 2017.
- [3] Fairbank, T. J., Knee joint changes after meniscectomy. *J Bone Joint Surg Br*. 30B: 664-70, 1948.
- [4] Seitz, A. M., Lubomierski, A., Friemert, B., Ignatius, A., Dürselen, L., Effect of partial meniscectomy at the medial posterior horn on tibiofemoral contact mechanics and meniscal hoop strains in human knees. *J Orthop Res*. 30: 934-42, 2012.
- [5] ISO, B., 14243-1, Implants for surgery–Wear of total knee joint prostheses– Part 1: Loading and displacement parameters for wear-testing machines with load control and corresponding environmental conditions for test, 2009.
- [6] Mow, V. C., Huiskes, R., Structure and function of articular cartilage and meniscus, Third Edition. In: *Basic Orthopaedic Biomechanics & Mechano-Biology* (ed. Mow, V. C., Huiskes, R.), 182-257; Lippincott Williams & Wilkins, 2005.
- [7] Neu, C. P., Komvopoulos, K., Reddi, A. H., The interface of functional biotribology and regenerative medicine in synovial joints. *Tissue Eng Part B Rev*. 14: 235-47, 2008.
- [8] McDermott, I. D., Masouros, S. D., Bull, A. M., Amis, A. A., Anatomy, In: *The Meniscus* (ed. Beaufils, P., Verdonk, R.), 11-18; Springer, 2010.
- [9] Masouros, S. D., McDermott, I. D., Amis, A. A., Bull, A. M., Biomechanics of the meniscus-meniscal ligament construct of the knee. *Knee Surg Sports Traumatol Arthrosc*. 16: 1121-32, 2008.
- [10] Masouros, S. D., McDermott, I. D., Bull, A. M., Amis, A. A., Biomechanics, In: *The Meniscus* (ed. Beaufils, P., Verdonk, P.), 29-37; Springer, 2010.
- [11] Ateshian, G. A., Wang, H., A theoretical solution for the frictionless rolling contact of cylindrical biphasic articular cartilage layers. *J Biomech*. 28: 1341-55, 1995.
- [12] Caligaris, M., Ateshian, G. A., Effects of sustained interstitial fluid pressurization under migrating contact area, and boundary lubrication by synovial fluid, on cartilage friction. *Osteoarthr Cartil*. 16: 1220-7, 2008.

- [13] Soltz, M. A., Ateshian, G. A., Experimental verification and theoretical prediction of cartilage interstitial fluid pressurization at an impermeable contact interface in confined compression. *J Biomech.* 31: 927-34, 1998.
- [14] McCann, L., et al., Tribological testing of articular cartilage of the medial compartment of the knee using a friction simulator. *Tribol Int.* 41: 1126-1133, 2008.
- [15] Amis, A. A., Gupta, C. M., Bull, A. M., Edwards, A., Anatomy of the posterior cruciate ligament and the meniscomfemoral ligaments. *Knee Surg Sports Traumatol Arthrosc.* 14: 257-63, 2006.
- [16] Petersen, W., Tillmann, B., Funktionelle Anatomie der Menisken des Kniegelenks Kollagentextur und Biomechanik. *Arthroskopie.* 11: 133-135, 1998.
- [17] Petersen, W., Tillmann, B., Collagenous fibril texture of the human knee joint menisci. *Anat Embryol (Berl).* 197: 317-24, 1998.
- [18] Brindle, T., Nyland, J., Johnson, D. L., The meniscus: review of basic principles with application to surgery and rehabilitation. *J Athl Train.* 36: 160-9, 2001.
- [19] Danzig, L. A., et al., Increased transsynovial transport with continuous passive motion. *J Orthop Res.* 5: 409-13, 1987.
- [20] Andrews, S., Shrive, N., Ronsky, J., The shocking truth about meniscus. *J Biomech.* 44: 2737-40, 2011.
- [21] Rongen, J. J., van Tienen, T. G., van Bochove, B., Grijpma, D. W., Buma, P., Biomaterials in search of a meniscus substitute. *Biomaterials.* 35: 3527-40, 2014.
- [22] Tissakht, M., Ahmed, A. M., Tensile stress-strain characteristics of the human meniscal material. *J Biomech.* 28: 411-22, 1995.
- [23] Lechner, K., Hull, M. L., Howell, S. M., Is the circumferential tensile modulus within a human medial meniscus affected by the test sample location and cross-sectional area? *J Orthop Res.* 18: 945-51, 2000.
- [24] Fithian, D. C., Kelly, M. A., Mow, V. C., Material properties and structure-function relationships in the menisci. *Clin Orthop Relat Res.* 19-31, 1990.
- [25] Sweigart, M. A., et al., Intraspecies and Interspecies Comparison of the Compressive Properties of the Medial Meniscus. *Ann Biomed Eng.* 32: 1569-79, 2004.
- [26] Chia, H. N., Hull, M. L., Compressive moduli of the human medial meniscus in the axial and radial directions at equilibrium and at a physiological strain rate. *J Orthop Res.* 26: 951-6, 2008.

- [27] Bursac, P., Arnoczky, S., York, A., Dynamic compressive behavior of human meniscus correlates with its extra-cellular matrix composition. *Biorheology*. 46: 227-37, 2009.
- [28] Seitz, A. M., Galbusera, F., Kraus, C., Ignatius, A., Duerksen, L., Ph.D., Stress-relaxation response of human menisci under confined compression conditions. *J Mech Behav Biomed Mater*. 26: 68-80, 2013.
- [29] Menard, K. P., Dynamic Mechanical Analysis: A Practical Introduction, CRC Press LLC, Florida, 1999.
- [30] Pereira, H., et al., Biomechanical and cellular segmental characterization of human meniscus: building the basis for Tissue Engineering therapies. *Osteoarthr Cartil*. 22: 1271-81, 2014.
- [31] Gleghorn, J. P., Bonassar, L. J., Lubrication mode analysis of articular cartilage using Stribeck surfaces. *J Biomech*. 41: 1910-8, 2008.
- [32] Ateshian, G. A., The role of interstitial fluid pressurization in articular cartilage lubrication. *J Biomech*. 42: 1163-76, 2009.
- [33] McCann, L., Ingham, E., Jin, Z., Fisher, J., Influence of the meniscus on friction and degradation of cartilage in the natural knee joint. *Osteoarthr Cartil*. 17: 995-1000, 2009.
- [34] Warnecke, D., et al., Friction properties of a new silk fibroin scaffold for meniscal replacement. *Tribol Int*. 109: 586-92, 2017.
- [35] Forster, H., Fisher, J., The influence of loading time and lubricant on the friction of articular cartilage. *Proc Inst Mech Eng H*. 210: 109-19, 1996.
- [36] Forster, H., Fisher, J., The influence of continuous sliding and subsequent surface wear on the friction of articular cartilage. *Proc Inst Mech Eng H*. 213: 329-45, 1999.
- [37] The Meniscus, Springer, Heidelberg, 2010.
- [38] Hede, A., Larsen, E., Sandberg, H., Partial versus total meniscectomy. A prospective, randomised study with long-term follow-up. *J Bone Joint Surg Br*. 74: 118-21, 1992.
- [39] Schimmer, R. C., Brulhart, K. B., Duff, C., Glinz, W., Arthroscopic partial meniscectomy: A 12-year follow-up and two-step evaluation of the long-term course. *Arthroscopy*. 14: 136-42, 1998.
- [40] Baratz, M. E., Fu, F. H., Mengato, R., Meniscal tears: The effect of meniscectomy and of repair on intraarticular contact areas and stress in the human knee. A preliminary report. *Am J Sports Med*. 14: 270-5, 1986.

- [41] Roos, H., et al., Knee osteoarthritis after meniscectomy: prevalence of radiographic changes after twenty-one years, compared with matched controls. *Arthritis Rheum.* 41: 687-93, 1998.
- [42] Englund, M., Lohmander, L. S., Risk factors for symptomatic knee osteoarthritis fifteen to twenty-two years after meniscectomy. *Arthritis Rheum.* 50: 2811-9, 2004.
- [43] Fukubayashi, T., Kurosawa, H., The contact area and pressure distribution pattern of the knee. A study of normal and osteoarthrotic knee joints. *Acta Orthop Scand.* 51: 871-9, 1980.
- [44] Sandmann, G. H., et al., Biomechanical comparison of menisci from different species and artificial constructs. *BMC Musculoskelet Disord.* 14: 324, 2013.
- [45] Stone, K. R., Rodkey, W. G., Webber, R. J., McKinney, L., Steadman, J. R., Future directions. Collagen-based prostheses for meniscal regeneration. *Clin Orthop Relat Res.* 129-35, 1990.
- [46] Balint, E., Gatt, C. J., Jr., Dunn, M. G., Design and mechanical evaluation of a novel fiber-reinforced scaffold for meniscus replacement. *J Biomed Mater Res A.* 100: 195-202, 2012.
- [47] Merriam, A. R., Patel, J. M., Culp, B. M., Gatt, C. J., Jr., Dunn, M. G., Successful total meniscus reconstruction using a novel fiber-reinforced scaffold: A 16- and 32-week study in an ovine model. *Am J Sports Med.* 43: 2528-37, 2015.
- [48] Patel, J. M., Merriam, A. R., Kohn, J., Gatt, C. J., Jr., Dunn, M. G., Negative outcomes of poly(l-lactic acid) fiber-reinforced scaffolds in an ovine total meniscus replacement model. *Tissue Eng Part A.* 22: 1116-25, 2016.
- [49] Elsner, J. J., et al., Design of a free-floating polycarbonate-urethane meniscal implant using finite element modeling and experimental validation. *J Biomech Eng.* 132: 095001, 2010.
- [50] Shemesh, M., et al., Viscoelastic properties of a synthetic meniscus implant. *J Mech Behav Biomed Mater.* 29: 42-55, 2014.
- [51] Warnecke, D., et al., Biomechanical, structural and biological characterisation of a new silk fibroin scaffold for meniscal repair. *J Mech Behav Biomed Mater.* 86: 314-24, 2018.
- [52] Gruchenberg, K., et al., In vivo performance of a novel silk fibroin scaffold for partial meniscal replacement in a sheep model. *Knee Surg Sports Traumatol Arthrosc.* 23: 2218-29, 2015.

- [53] Gruchenberg, K., et al., Correction to: In vivo performance of a novel silk fibroin scaffold for partial meniscal replacement in a sheep model. *Knee Surg Sports Traumatol Arthrosc.* 2018.
- [54] Rodkey, W. G., Steadman, J. R., Li, S. T., A clinical study of collagen meniscus implants to restore the injured meniscus. *Clin Orthop Relat Res.* 365S: 281-92, 1999.
- [55] Buma, P., Ramrattan, N. N., van Tienen, T. G., Veth, R. P., Tissue engineering of the meniscus. *Biomaterials.* 25: 1523-32, 2004.
- [56] Verdonk, P., et al., Successful treatment of painful irreparable partial meniscal defects with a polyurethane scaffold: two-year safety and clinical outcomes. *Am J Sports Med.* 40: 844-53, 2012.
- [57] Verdonk, P. C., et al., Transplantation of viable meniscal allograft. Survivorship analysis and clinical outcome of one hundred cases. *J Bone Joint Surg Am.* 87: 715-24, 2005.
- [58] Warnecke, D., et al., Articular cartilage and meniscus reveal higher friction in swing phase than in stance phase under dynamic gait conditions. *Sci Rep.* 9: 5785, 2019.
- [59] Maher, S. A., et al., Evaluation of a porous polyurethane scaffold in a partial meniscal defect ovine model. *Arthroscopy.* 26: 1510-9, 2010.
- [60] Jahn, S., Seror, J., Klein, J., Lubrication of Articular Cartilage. *Annu Rev Biomed Eng.* 18: 235-58, 2016.
- [61] Krishnan, R., Kopacz, M., Ateshian, G. A., Experimental verification of the role of interstitial fluid pressurization in cartilage lubrication. *J Orthop Res.* 22: 565-70, 2004.
- [62] Galley, N. K., et al., Frictional properties of the meniscus improve after scaffold-augmented repair of partial meniscectomy: a pilot study. *Clin Orthop Relat Res.* 469: 2817-23, 2011.
- [63] Parkes, M., Myanr, C., Dini, D., Cann, P., Tribology-optimised silk protein hydrogels for articular cartilage repair. *Tribol Int.* 89: 9-18, 2015.
- [64] Taylor, W. R., et al., Tibio-femoral joint contact forces in sheep. *J Biomech.* 39: 791-8, 2006.
- [65] Shi, L., Sikavitsas, V. I., Striolo, A., Experimental friction coefficients for bovine cartilage measured with a pin-on-disk tribometer: testing configuration and lubricant effects. *Ann Biomed Eng.* 39: 132-46, 2011.
- [66] Unsworth, A., Tribology of human and artificial joints. *Proc Inst Mech Eng H.* 205: 163-72, 1991.

- [67] Taylor, W. R., Heller, M. O., Bergmann, G., Duda, G. N., Tibio-femoral loading during human gait and stair climbing. *J Orthop Res.* 22: 625-32, 2004.
- [68] Heinlein, B., et al., ESB Clinical Biomechanics Award 2008: Complete data of total knee replacement loading for level walking and stair climbing measured in vivo with a follow-up of 6-10 months. *Clin Biomech (Bristol, Avon).* 24: 315-26, 2009.
- [69] Ateshian, G. A., Mow, V. C., Friction, lubrication, and wear of articular cartilage and diarthrodial joints, Third Edition. In: *Basic Orthopaedic Biomechanics & Mechano-Biology* (ed. Mow, V. C., Huiskes, R.), 447-493; Lippincott Williams & Wilkins, 2005.
- [70] McCutchen, C. W., The frictional properties of animal joints. *Wear.* 5: 1-17, 1962.
- [71] Walker, P. S., Dowson, D., Longfield, M. D., Wright, V., "Boosted lubrication" in synovial joints by fluid entrapment and enrichment. *Ann Rheum Dis.* 27: 512-20, 1968.
- [72] Medley, J. B., Dowson, D., Wright, V., Transient elastohydrodynamic lubrication models for the human ankle joint. *Eng Med.* 13: 137-51, 1984.
- [73] Hou, J. S., Mow, V. C., Lai, W. M., Holmes, M. H., An analysis of the squeeze-film lubrication mechanism for articular cartilage. *J Biomech.* 25: 247-59, 1992.
- [74] Krishnan, R., Mariner, E. N., Ateshian, G. A., Effect of dynamic loading on the frictional response of bovine articular cartilage. *J Biomech.* 38: 1665-73, 2005.
- [75] Thier, S., Tonak, M., Influence of Synovial Fluid on Lubrication of Articular Cartilage in Vitro. *Z Orthop Unfallchir.* 156: 205-213, 2018.

8. Publications

8.1. Manuscript 1

WARNECKE D, STEIN S, HAFFNER-LUNTZER M, DE ROY L, SKAER N, WALKER R, KESSLER O, IGNATIUS A, DÜRSELEN L. Biomechanical, structural and biological characterisation of a new silk fibroin scaffold for meniscal repair. J Mech Behav Biomed Mater 2018; 86: 314 - 24. DOI: 10.1016/j.jmbbm.2018.06.041.

Open access

Creative Commons Attribution License 4.0 International (CC BY 4.0,
<http://creativecommons.org/licenses/by/4.0/>)

DW carried out all mechanical evaluation as well as the structural characterisation of the scaffold. Additionally, DW performed the evaluations, including the statistical analyses. DW also drafted the manuscript.



Biomechanical, structural and biological characterisation of a new silk fibroin scaffold for meniscal repair

Daniela Warnecke^{a,*,1}, Svenja Stein^{a,1}, Melanie Haffner-Luntzer^a, Luisa de Roy^a, Nick Skaer^b, Robert Walker^b, Oliver Kessler^{c,d}, Anita Ignatius^a, Lutz Dürselen^a

^a Institute of Orthopaedic Research and Biomechanics, Centre for Trauma Research Ulm, Ulm University Medical Centre, Helmholtzstr. 14, 89081 Ulm, Germany

^b Orthox Ltd., Abingdon, UK

^c Centre of Orthopaedics and Sports, Zurich, Switzerland

^d University Medical Centre, Clinic for Orthopaedic Surgery, Magdeburg, Germany

ARTICLE INFO

Keywords:

Meniscus replacement

Silk scaffold

Biomechanical tests

μ-CT

ABSTRACT

Meniscal injury is typically treated surgically via partial meniscectomy, which has been shown to cause cartilage degeneration in the long-term. Consequently, research has focused on meniscal prevention and replacement. However, none of the materials or implants developed for meniscal replacement have yet achieved widespread acceptance or demonstrated conclusive chondroprotective efficacy.

A redesigned silk fibroin scaffold, which already displayed promising results regarding biocompatibility and cartilage protection in a previous study, was characterised in terms of its biomechanical, structural and biological functionality to serve as a potential material for permanent partial meniscal replacement. Therefore, different quasi-static but also dynamic compression tests were performed. However, the determined compressive stiffness (0.56 ± 0.31 MPa and 0.30 ± 0.12 MPa in relaxation and creep configuration, respectively) was higher in comparison to the native meniscal tissue, which could potentially disturb permanent integration into the host tissue. Nevertheless, μ-CT analysis met the postulated requirements for partial meniscal replacement materials in terms of the microstructural parameters, like mean pore size (215.6 ± 10.9 μm) and total porosity ($80.1 \pm 4.3\%$). Additionally, the biocompatibility was reconfirmed during cell culture experiments. The current study provides comprehensive mechanical and biological data for the characterisation of this potential replacement material. Although some further optimisation of the silk fibroin scaffold may be advantageous, the silk fibroin scaffold showed sufficient biomechanical competence to support loads already in the early post-operative phase.

1. Introduction

The menisci are two crescent-shaped fibrocartilaginous structures, located between the femur and tibia in the knee joint. Their crucial role in load bearing and distribution of contact load over the articular surfaces, achieved by a synergy of their geometry, unique material properties and the anterior and posterior attachments to the tibia plateau, is well established. Furthermore, the menisci are involved in joint stabilisation and lubrication (Bullough et al., 1970; Masouros et al., 2010; Brindle et al., 2001; Mow and Huiskes, 2005).

During everyday activities, high loads occur in the knee joint, with resultant forces of 2–3.5 times body weight (Kutzner et al., 2010). Thereby, up to 81% of the axial forces are transferred through the

menisci (Pena et al., 2005). Being subjected to these high mechanical stresses, the menisci are particularly prone to injury. In total, 37% of all sports-related injuries are knee-joint related. Lesions of the medial meniscus are the second most frequent internal knee injury (24%), requiring surgical intervention in approximately 80% of the cases (Majewski et al., 2006). The most commonly performed procedure to treat a torn meniscus is partial meniscectomy, initially combining the advantage of rapid pain relief and restoration of joint function (Hede et al., 1992; Schimmer et al., 1998). Nevertheless, meniscectomy can cause degeneration of the articular cartilage in the long-term (Hede et al., 1992; Baratz et al., 1986; Seitz et al., 2012; Fairbank, 1948; Roos et al., 1998; Englund and Lohmander, 2004). This is due to the fact that a decreased contact area after meniscal resection leads to increased

* Corresponding author.

E-mail address: daniela.warnecke@uni-ulm.de (D. Warnecke).

¹ These authors contributed equally.

stress on the articular surface (Fukubayashi and Kurosawa, 1980), which becomes greater with increased removal of meniscal tissue (Baratz et al., 1986; Lee et al., 2006; Ahmed and Burke, 1983).

Consequently, there has been an increased awareness of meniscus preservation or replacement techniques in recent years. Between 2005 and 2011, the number of repairs performed increased by 11.4% for isolated meniscus tears (Abrams et al., 2013). However, irreparable lesions in the avascular region of the meniscus require partial or even total meniscectomy. In these cases, natural (e.g. allografts) or synthetic meniscal substitutes are options to restore meniscal function. To successfully replace an injured meniscus, Stone et al. once postulated basic requirements for meniscal replacement materials (Stone, 1996; Stone et al., 1997), which were later further elaborated by Rongen et al. (2014). The authors stated that the biomechanical properties of a substitute should mimic that of native meniscal tissue as close as possible. Thereby, transmitting and distributing loads over the articulating surfaces and reducing peak stresses also already in the initial phase after implantation (Stone, 1996; Stone et al., 1997; Rongen et al., 2014). Additionally, the friction coefficient should not exceed 0.05 to prevent early cartilage abrasion. Furthermore, a meniscal scaffold is thought to serve as a “framework”, encouraging cell adhesion and differentiation, vascularisation and matrix deposition. Therefore, macropores (200–300 μm), interconnected via micropores (10–50 μm) and a high total porosity ($\geq 70\%$) are demanded (Rongen et al., 2014). This is particularly true for a partial replacement device, for which a connection to the remaining host tissue is essential. Many studies have evaluated the suitability of different artificial materials for meniscal replacement, but none have clinically demonstrated the capacity to protect the articular cartilage (Rongen et al., 2014; Rodkey et al., 1999; Buma et al., 2004; Kohn et al., 1992; Walsh et al., 1999; Bruns et al., 1998; Gastel et al., 2001; Peters and Wirth, 2003; Verdonk et al., 2005; Milachowski et al., 1990; Noyes and Barber-Westin, 2005). Nevertheless, two alloplastic scaffolds for partial meniscal replacement are clinically available (CMI®, Collagen Meniscus Implant, Ivy Sports Medicine, Gräfelfing, Germany and Actifit®, Orteq Ltd., London, UK) but have not gained widespread clinical adoption and their ability to protect the articular cartilage in the long-term remains unclear (Rongen et al., 2014). Sandmann et al. (2013) additionally had shown that the mechanical/viscoelastic properties of both replacement materials were significantly different to that of human menisci. Consequently, there is still a need for an adequate replacement material. Further approaches, but primarily for total meniscal replacement, are in preclinical development (e.g. Meniscofix™, Novopedics Inc. (Balint et al., 2012; Merriam et al., 2015; Patel et al., 2016) or NuSurface®, Active Implants Ltd. (Elsner et al., 2010; Shemesh et al., 2014; Zur et al., 2011)). Another non-resorbable scaffold based on silk fibroin (FibroFix™, Orthox Ltd., Abingdon, UK), designed for partial meniscal replacement, was previously tested by us in a sheep model and displayed superior results in comparison to partial meniscectomy after six months of implantation with compressive properties in the range of meniscal tissue and evidence of a chondroprotective effect (Gruchenberg et al., 2015). However, fixation and integration into the adjacent meniscal tissue was insufficient. Therefore, the material was subjected to an optimisation process and a silk fibre mesh was integrated into the porous matrix to improve anchoring of the fixation sutures. Recently, we investigated the frictional properties of this second generation of silk fibroin scaffolds (Warnecke et al., 2017). The scaffold, in comparison to the physiologically articulating surfaces of the meniscus and articular cartilage, displayed slightly higher friction coefficients than the native meniscus (Warnecke et al., 2017), but still remaining within the range of the mentioned requirements (Stone, 1996; Stone et al., 1997; Rongen et al., 2014).

Having these requirements in mind, the aim of the present study was to characterise the biomechanical, structural and biological properties of the second generation of silk fibroin scaffolds for partial meniscal replacement.

2. Material and methods

2.1. Study design

To characterise the biomechanical and structural properties, as well as the biocompatibility of the silk fibroin scaffold (FibroFix™ Meniscus, Orthox Ltd.), several tests were performed on specimens of standardised geometry. Silk fibroin flat sheet scaffolds were delivered by Orthox Ltd., which were materially and structurally identical to the meniscus implants (FibroFix™ Meniscus, ORTH REP M081), differing only in the final shape.

The study comprised testing procedures, including tensile, indentation, unconfined compression creep and relaxation tests, to determine the viscoelastic material parameters of the scaffold. Here, the ultimate tensile force F_{max} in N, the linear elastic modulus E in MPa, the residual force F_{res} in N and the equilibrium moduli E_{eq} in MPa in compression creep and the relaxation configuration were determined. Additionally, a dynamic mechanical analysis (DMA) was included to characterise the viscous (damping factor $\tan(\delta)$) and loss modulus E'' in MPa) and elastic properties (storage or elastic modulus E' in MPa) in greater detail.

The microstructure and morphology of the silk fibroin scaffold were assessed by micro-computed tomography ($\mu\text{-CT}$). Thereby, total porosity and pore size were evaluated. Finally, biocompatibility was determined by MTT and BrdU tests for cell metabolism and proliferation, respectively.

2.2. Material

Silk fibroin scaffolds were manufactured from commercially obtained *Bombyx mori* silk fibroin fibres (Silk Opportunities Ltd, Volketswil, Switzerland). Raw fibres were degummed according to Gulrajani et al. (1996) and dissolved in lithium bromide before transferring the resulting solution to semi-permeable moulding vessels. These contained organised fibroin fibre layers comprising braided fibroin threads of approximately 0.4 mm gauge arranged in orthogonal meshes to improve anchoring of sutures used in vivo for fixation of the scaffold to the host tissue. To ensure preservation of these mesh elements, moulding vessels were rapidly dialysed against excess ultrapure water, before perfusion with a dilute acidic solution to initiate transition of fibroin to the β -pleated-sheet conformation. A macroporous internal structure was introduced through a freeze-thaw cycle. Afterwards, the scaffolds were dehydrated to maximise β -pleated-sheet content in the fibroin and increase fibroin crystallinity, before washing in ultrapure water and final transfer to phosphate-buffered saline (PBS).

2.3. Mechanical tests

2.3.1. Test setup

All biomechanical tests were performed at room temperature (20–22 °C). Care was taken to keep specimens moist in PBS during sample preparation as well as during testing using custom-made testing chambers filled with PBS for indentation-, unconfined compression creep and –relaxation tests.

2.3.1.1. Quasi-static testing. The quasi-static tests were performed using standard materials testing machines (Z 010 or BXE-EZ001.A50-000, Zwick & Roell, Zwick GmbH & Co. KG, Ulm, Germany) associated with the Zwick® test software TextXpertII for testing and data acquisition.

Tensile test to failure: The tensile properties of the silk fibroin scaffold were determined in a tensile test to failure, performed according to Villegas et al. (2007). Dumbbell-shaped specimens ($n = 9$, approximately 25 mm \times 10 mm \times 5 mm) were cut from each silk fibroin flat sheet using a custom-made punch and mounted in the materials testing machine equipped with a 500-N load cell (KAF-W, A.S.T GmbH, Blaustein, Germany, accuracy $\leq 0.24\%$) (Fig. 1). Here, special

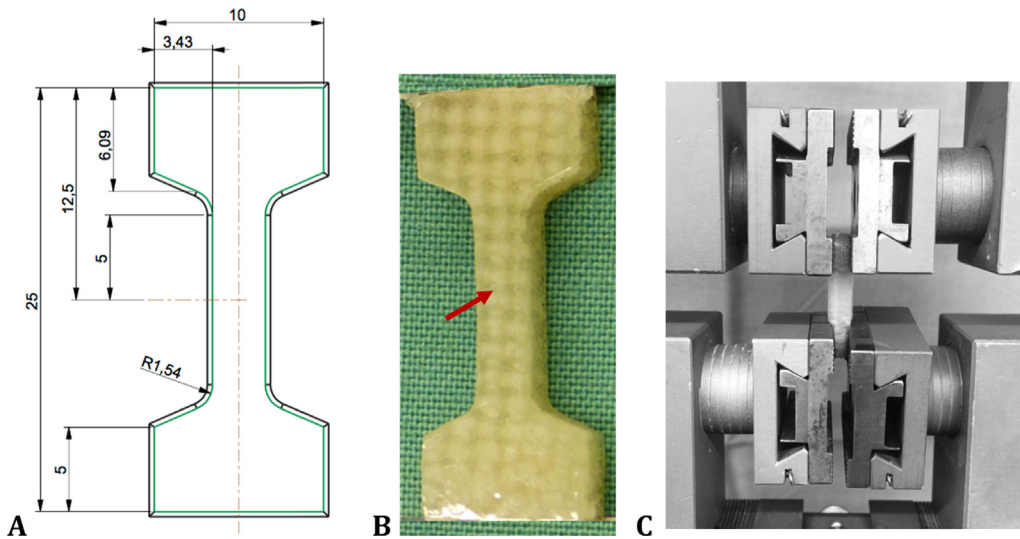


Fig. 1. Dimensions of a custom-made punch (A) to obtain dumbbell-shaped samples from a flat sheet of the silk fibroin scaffold (B). Here, special care was taken that at least one longitudinal fibre bundle was within the tapering of the sample (red arrow, B). Afterwards, it was clamped within a standard materials testing machine (Z 010, Zwick & Roell, Ulm, Germany) using standard clamps for testing the tensile properties (C). (For interpretation of the references to color in this figure legend, the reader is referred to the web version of this article.)

care was taken that one whole fibre bundle was within the tapering of the specimen's shape (Fig. 1, red arrow B). Standard clamps were used for fixation. Initially, to ensure the same testing conditions at the beginning of each test, the specimens were preconditioned for 10 cycles ranging over 0–3% strain at a constant velocity of 10 mm/min. Then the tensile test was conducted at a strain rate of 2%/s until failure. During testing, the time, load and displacement were recorded and the F_{max} , displacement at maximum force s_{max} in mm and the linear elastic modulus E were assessed. Here, the linear elastic modulus was defined as the slope in the linear region of the stress-strain diagram using linear regression.

Indentation test: To compare the biomechanical properties of the silk fibroin scaffold with literature data, an experimental test setup was used as previously published by Sandmann et al. (2013), the first and only research group, who evaluated the pre-implantation biomechanical properties of the two clinically available meniscal replacement devices CMI® (Ivy Sports Medicine) and Actifit® (Orteq Ltd.).

Cylindrical samples ($n = 9$) were cut from silk fibroin flat sheets indicated above (initial height h_0 : 5.12 ± 0.26 mm) using an 8-mm biopsy punch. The specimens were mounted in the materials testing machine, centred on a steel plate within a custom-made testing chamber filled with PBS. Furthermore, the setup for the indentation test included a calibrated 50-N load cell (KAP-S, A.S.T. GmbH, Blaustein, Germany, accuracy $\leq 0.28\%$) and a laser distance sensor (optoNCDT 2200-20, Micro-Epsilon, Ortenburg, Germany) to determine scaffold deformation. After applying an initial preload of 0.5 N, the cylindrical silk fibroin specimens were exposed to 5 load cycles using a steel-ball indenter ($\varnothing = 5$ mm). One cycle comprised a loading phase up to 7 N at 5 mm/min with a subsequent relaxation time of 60 s, followed by a load-release to 0.1 N at a constant velocity of 1 mm/min and finally deformation was held constant for another 60 s (recovery phase).

The stiffness k (N/mm) in cycles 1 and 5 was determined from the linear region of the force-displacement diagram between 2 N and 5 N (Fig. 2A). The F_{res} , which was defined as the force remaining after the relaxation time at the end of the loading phase, was evaluated as a measure for the viscoelastic behaviour (Fig. 2B). Finally, the relative compression of the specimens in % was assessed by relating the recorded displacement of the indenter to the initial sample height.

Unconfined compression relaxation test: Unconfined compression tests were performed with a modified testing protocol according to Chia and Hull (2008), who determined the compressive properties of human menisci in axial and radial direction. Accordingly, cylindrical silk fibroin samples ($n = 9$) were obtained using a 5-mm biopsy punch. Within the materials testing machine, which was equipped with a 50-N load cell (KAP-S, A.S.T. GmbH, accuracy: $\leq 0.28\%$), the cylindrical

samples were mounted in a custom-made testing chamber filled with PBS and cyclically preconditioned to 12% strain for 10 cycles. Subsequently, a stress-relaxation test at 12% strain, controlled via a laser distance sensor (optoNCT 2200-2, Micro-Epsilon), was executed over a testing period of 60 min to ensure that an equilibrium state was reached. For evaluation, the E_{eq} was determined, which was defined by the quotient of the recorded stress at equilibrium $\sigma_{t \rightarrow \infty}$ averaged over the last 10 min of testing time and the applied constant strain ϵ_i (1).

$$E_{eq} = \frac{\sigma_{t \rightarrow \infty}}{\epsilon_i}; \epsilon_i = 0.12 \quad (1)$$

Unconfined compression creep test: To test the compressive behaviour of the silk fibroin scaffold under more physiological-like conditions, an unconfined compression test under creep conditions was performed. Here, the test setup was in accordance to Joshi et al. (1995), who quantified the differences in compressive properties of menisci of various species using the linear biphasic theory. Cylindrical samples of 5 mm in diameter, placed within a special testing chamber filled with PBS, were first preloaded to 0.02 N at a velocity of 1.6 mm/min for 15 min in the materials testing machine equipped with a 20-N load cell (Xforce P, Zwick GmbH & Co. KG, accuracy: $\leq 0.26\%$) and a laser distance sensor (optoNCDT 2200-20, Micro-Epsilon). Subsequently, the samples were loaded to 0.1 N at a velocity of 31% h_0 /min. This force was held constant for 60 min and the E_{eq} was determined (1).

2.3.1.2. DMA. The dynamic loading measurements were performed using an ElectroForce® 5500 dynamic materials testing machine (BOSE/TA ElectroForce Systems Group, New Castle, USA) equipped with a 200-N load cell (BOSE/TA ElectroForce Systems Group, accuracy: $\leq 1\%$) in an unconfined compression test setup. Additional cylindrical samples harvested using a 6-mm biopsy punch ($n = 6$; initial height $h_0 = 5.47$ mm ± 0.12 mm) were mounted in the dynamic materials testing machine and preloaded to 0.2 N to ensure surface contact between the samples and the compression plates. Afterwards, a dynamic, sinusoidal strain with constant amplitude of approximately 60 μ m was applied, passing through 5 cycles over a frequency spectrum of 0.1–10 Hz. The testing protocol used in the current study was based on Yan et al., who tested the material properties of silk fibroin scaffolds with different initial silk concentrations (Yan et al., 2012).

The standard software for the ElectroForce® 5500 WinTest7® continuously recorded the time, applied displacement and resulting force at a sampling rate of 100 Hz during testing. For a detailed characterisation of the silk fibroin scaffold, the loss factor $\tan(\delta)$, the storage modulus E' and the loss modulus E'' were evaluated from the first three recorded cycles of each frequency run.

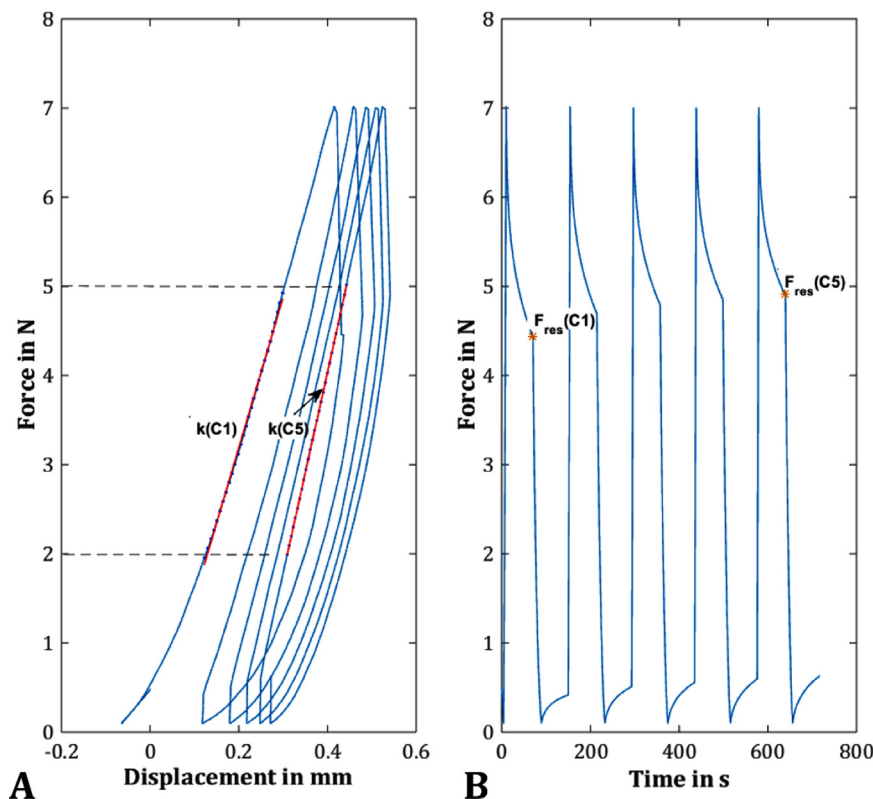


Fig. 2. Representative curve of an indentation test, which comprised 5 load cycles up to 7 N with a subsequent relaxation time of 60 s, followed by a load-release to 0.1 N and another recovery phase. The stiffness in cycles 1 and 5 ($k(C1)$ and $k(C5)$, respectively) were determined from the linear region of the force-displacement diagram between 2 N and 5 N (A). As a measure for the viscoelastic behaviour, the residual force ($F_{res}(C1)$ and $F_{res}(C5)$) were defined as the force remaining after the relaxation time at the end of the loading phase in cycle 1 and 5 (orange *, B). (For interpretation of the references to color in this figure legend, the reader is referred to the web version of this article.)

2.4. Structural analysis: μ -CT

For structural analysis of the scaffold, μ -CT scans were executed with cylindrical samples punched out of 5-mm silk fibroin flat sheets, which had also been used for biomechanical testing. Because of the sample hydration, they first had to be dried. To preserve the geometrical dimensions and structure, a critical point drying method was chosen (E3100 Critical Point Dryer, LOT-QuantumDesign GmbH, Darmstadt, Germany). Prior to this, the samples were dehydrated through an ascending alcohol series (70%, 98% and 100%, each for 12 h).

Subsequently, the dried scaffolds were scanned (Skyscan[®] 1172, Bruker microCT, Kontich, Belgium) with an approximate 8- μ m image pixel size. The X-ray source was set at 40 kV and 250 μ A. Projections were acquired over a rotation range of 180° with rotation steps of 0.36°. The reconstruction and analysis were performed using the standardised Skyscan[®] software NRecon[®] and CTAn[®], respectively. All slices were converted to binary images with a threshold of 40–255 (grey values). To assess the microstructure of the silk fibroin scaffold, parameters like the total porosity, the mean pore size as well as the pore size distribution were evaluated.

2.5. Cell-culture experiments

2.5.1. Scaffold preparation

Meniscus-shaped silk fibroin scaffolds were disinfected with 95% ethanol, washed three times with sterile PBS and pre-incubated for 24 h in standard culture medium (DMEM/Ham's F12, Gibco, ThermoFisher Scientific, Waltham, USA) containing 10% foetal calf serum (FCS) (PAA Laboratories, Cölbe, Germany), 1% penicillin/streptomycin (Gibco, ThermoFisher Scientific) 1% L-glutamine (Biochrom, Merck KGaA, Darmstadt, Germany), 10 μ g/ml transferrin and 3×10^8 M selenite (both Sigma-Aldrich, Taufkirchen, Germany).

2.5.2. Cell cultivation

Chondrogenic murine ATDC5 cells, which were purchased from Sigma-Aldrich, and human mesenchymal stem cells (MSCs) isolated from bone-marrow aspirates as described previously (Mietsch et al., 2013) were used for the experiments. Briefly, the fresh human bone-marrow aspirates were obtained after informed consent and approval from the local ethical committee. Afterwards, the MSCs were isolated by density gradient centrifugation and plastic adherence. These types of cells were chosen since we assume that these cell types would have the closest contact to the scaffold material in vivo.

2.5.3. Assessment of biocompatibility

Biocompatibility of the material was assessed by measuring cell metabolism and proliferation of both cells types separately cultured together with the scaffold material. Scaffolds were cut into square pieces (0.15 \times 0.15 cm), which were placed in 96-well plates. A total of 200 μ l culture medium containing 10,000 MSCs was added. The cells were cultivated for 1, 3, 14 or 21 days and cell metabolism was determined by the MTT test as described previously ($n = 3$ per time point) (Sarem et al., 2013). In a second experiment cell-proliferation was measured by a BrdU test according to the manufacturer's protocol ($n = 6$ per time point) using chondrogenic cells. For this, 200 μ l culture medium containing 1000 ATDC5 cells was added to the scaffolds and cultivated for 7 or 14 days.

2.6. Statistics

Because the evaluated data were normally distributed (normal probability plot, Shapiro-Wilk test (Shapiro and Wilk, 1965)), the data were averaged and presented as means \pm standard deviation. All further statistical analyses were performed using GraphPad Prism[®] software (GraphPad Software Inc., La Jolla, USA).

- 1) The effect of cyclic indentation on the silk fibroin scaffold stiffness, residual force and compression were evaluated using paired

Student's *t*-test.

To compare these results with the existing data of Actifit®, CMI® and human menisci obtained by Sandmann et al., additional one-way analysis of variances (ANOVA) with Bonferroni's multiple comparison tests were performed.

- 2) To determine any changes in the elastic/storage modulus E' , in the loss factor $\tan(\delta)$ and in the loss modulus E'' depending on the frequency, one-way ANOVA with Tukey's multiple comparison tests were performed.
- 3) Within the biocompatibility test, changes in the cell metabolism and proliferation rate were analysed via one-way ANOVA and Student's *t*-test, respectively.

The statistical significance level was set to $p < 0.05$.

Due to the lack of comparability of the obtained data and the material analysis character of the study, all further obtained results were analysed descriptively.

3. Results and discussion

3.1. Biomechanical tests

3.1.1. Tensile test to failure

Within this study, the tensile properties of a potential material for partial meniscal replacement were investigated for the first time using dumbbell-shaped samples (Fig. 3). They reached an ultimate tensile force of 51.0 ± 16.0 N at a maximum displacement of 4.7 ± 0.9 mm. Based on a rectangular cross-sectional area (length \times width: 3.0 ± 0.1 mm \times 5.1 ± 0.3 mm), the ultimate tensile force led to a maximum tensile strength of 3.28 ± 1.01 MPa. The mean elastic modulus, which was defined as the slope of the linear region of the stress-strain diagram, was 5.4 ± 1.4 MPa.

In general, there is a lack of information regarding the biomechanical characterisation of potential materials for (partial) meniscal replacement in the literature. Consequently, a comparison of the tensile properties of the silk fibroin scaffold with other materials was not

possible. Therefore, data for the tensile properties of human menisci were consulted. Since the material properties of the meniscus are anisotropic, there are differences in the elastic modulus depending on the orientation of the collagen fibres (Tissakht and Ahmed, 1995; Lechner et al., 2000). Tissakht and Ahmed (1995), who determined the tensile characteristics of human menisci in two directions, found an almost 10-fold higher elastic modulus in the circumferential than in the radial direction (radial: lateral meniscus 11.6 MPa, medial meniscus 9.9 MPa; circumferential: lateral meniscus 111.7 MPa, medial meniscus 83 MPa). Comparing the properties of the scaffold with the literature, it is clear that the elastic modulus of the silk fibroin test samples was lower than that of native meniscus. However, the silk fibroin scaffold tested in the current study is designed to address partial meniscal replacement, in which the outer region of the meniscus and, therefore, the native circumferential collagen fibres are still maintained. Therefore, the functionality of transferring axial load into circumferential tensile stress is still provided in this scenario (Masouros et al., 2010; Beaupre et al., 1986). Furthermore, within the inner two-thirds, the menisci are predominantly exposed to compressive loads (Beaupre et al., 1986; McDermott et al., 2010), which leads to the assumption that the compressive properties of a potential material for partial meniscal replacement might be more important than its tensile properties. The integrated single layer of fibre mesh, which was implemented to enhance the fixation to the remaining host meniscus rather than to take up circumferential loads was arranged in an orthogonal array in the scaffolds. Therefore, it is possible that the scaffold may be improved by adopting a higher density of fibres with orientation that better mimics the circumferential arrangement of the collagen fibres found in the native meniscus especially for larger partial or for total meniscal replacements.

3.1.2. Indentation test

The indentation stiffness of the silk fibroin scaffold increased significantly between cycles 1–5 by approximately 38% from 17.9 ± 2.7 N/mm to 24.7 ± 3.7 N/mm (Fig. 4A1; $p < 0.0001$, two-tailed *p*-value). The residual force as a parameter for the viscosity also

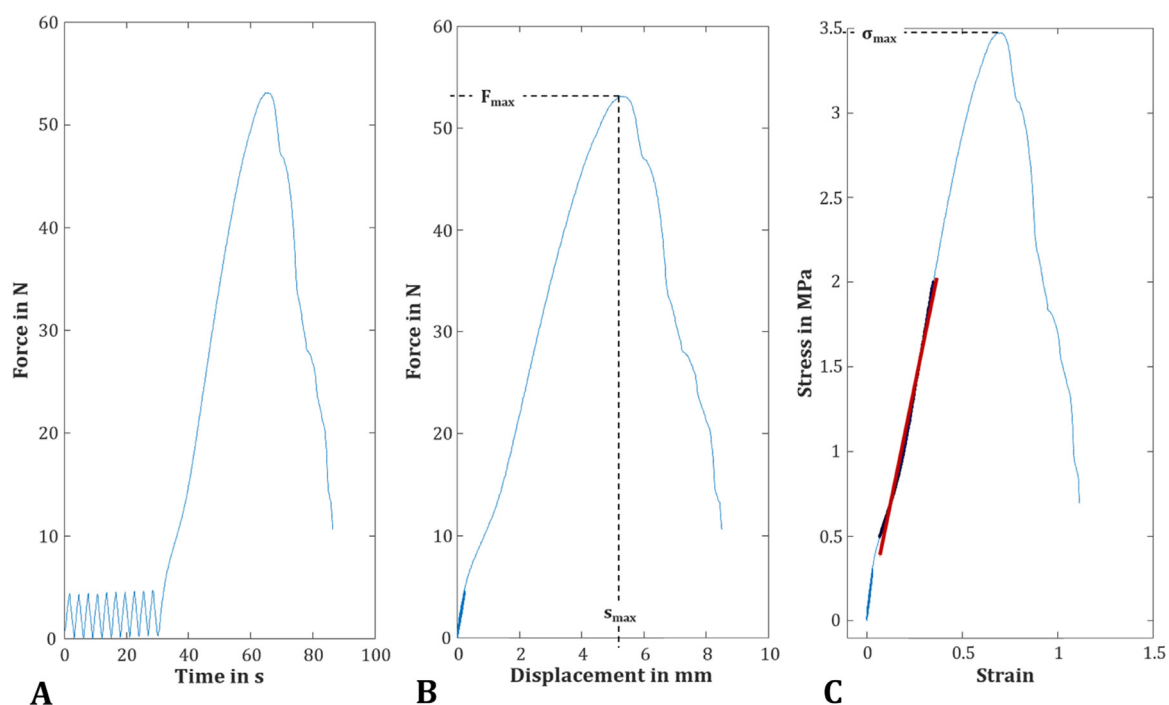


Fig. 3. After 10-cycle preconditioning (A), the dumbbell-shaped samples of the silk fibroin scaffold were tested until failure at constant strain rate of 2%/s to determine the parameters F_{max} , s_{max} (B) the ultimate tensile strength σ_{max} and the linear elastic modulus E out of the linear region of the stress-strain diagram (C; here: a representative curve).

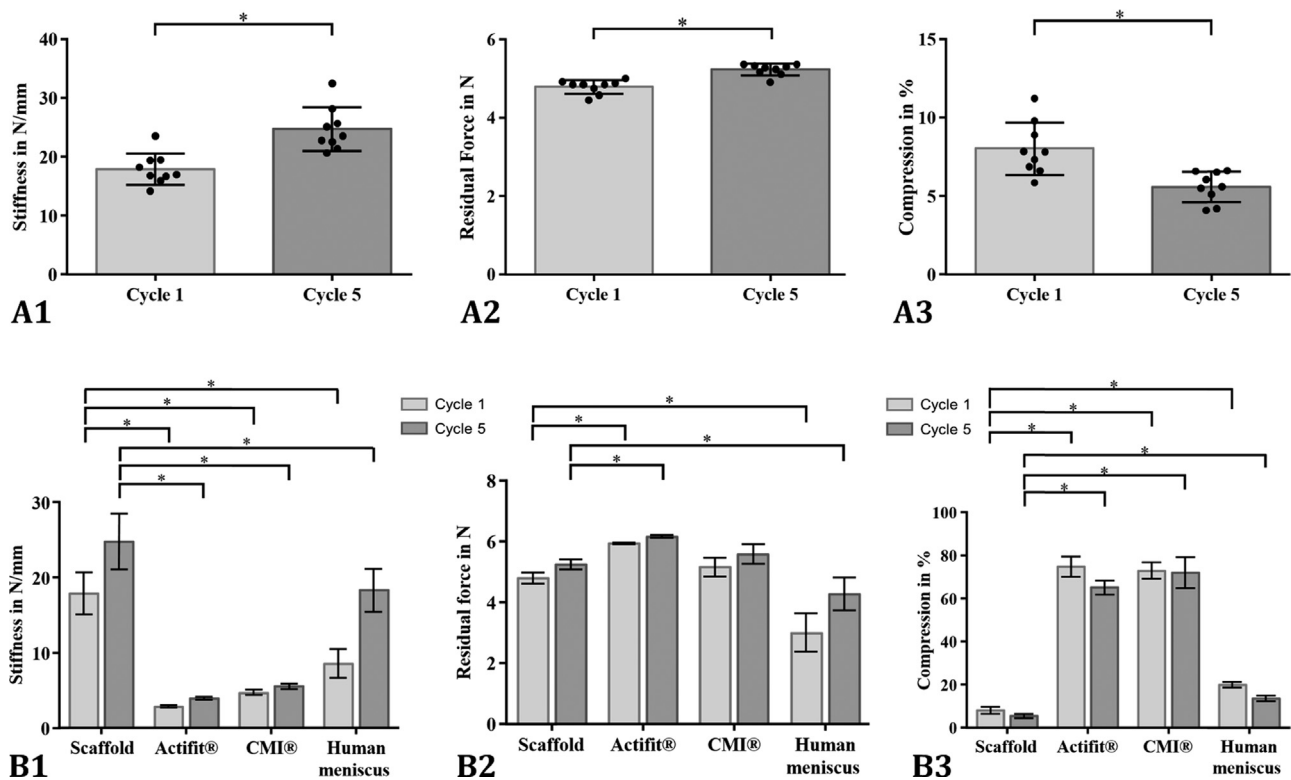


Fig. 4. Mean and standard deviation of the silk fibroin scaffold's stiffness k in N/mm, residual force in N and their increase throughout the testing duration and the resultant compression rate at a 7 N load in the indentation test (cycle 1 vs. cycle 5, A 1–3, * $p < 0.05$). For a better comparison of these three parameters with the existing data of Sandmann et al. (2013), additional statistical analysis was performed (B1–3, * $p < 0.05$).

significantly increased from 4.8 ± 0.2 N in cycle 1– 5.2 ± 0.1 N in cycle 5 (Fig. 4A2; $p < 0.0001$, two-tailed p -value). Consequently, the compression significantly decreased during test cycles 1–5 from $8.0 \pm 1.7\%$ to $5.6 \pm 1.0\%$ (Fig. 4A3; $p = 0.002$, two-tailed p -value within a paired t -test).

Attempting to find suitable test setups to compare the biomechanical properties of the silk fibroin scaffold with other meniscus replacement materials was difficult, because most investigators only reported histological analysis or gross examination via magnetic resonance imaging within in vivo studies (Stone et al., 1997; Maher et al., 2010; Verdonk et al., 2011). Therefore, we chose the test setup for a cyclic indentation test performed by Sandmann et al. (2013), the only research group investigating the biomechanical properties of the two clinically available implants CMI® and Actifit® in comparison with meniscus tissue of different species. They found significant differences in the viscoelastic properties and stiffness of both artificial materials in comparison to the native meniscal tissue (Fig. 4B1 and B2). It is clear that the silk fibroin scaffold was significantly stiffer in the first and fifth cycles not only compared to the two other artificial materials but also to human meniscal tissue (Fig. 4B1) but displayed fifth cycle average values that more closely approached meniscal tissue than either CMI® and Actifit®. Similar differences were found in the compressive strain of the materials at a 7 N load (Fig. 4B3) with the silk fibroin scaffold, however, demonstrating average values that were closer to those of human meniscal tissue than the other two scaffolds. The F_{res} of the scaffold, defined by Sandmann et al. as a measure for the viscoelastic behaviour, was statistically significantly different in comparison to Actifit® but also to human meniscal tissue also for both cycles 1 and 5 (Fig. 4B2). Consequently, the silk fibroin scaffold displayed initial compressive competence as required by Rongen et al. (2014) and Stone et al. (1997) unlike the CMI® and Actifit®. Sandmann et al. (2013) speculated that the low stiffness of these two implants might increase after implantation because of matrix deposition by ingrowing cells

within the artificial materials, which was confirmed by Tienen et al. (2006) for a prior material version of the Actifit® implant. Here, the increased stiffness was detected within an unconfined compression test after 3 and 6 months of implantation compared to the preoperative conditions. Nevertheless, the mechanical properties were still significantly different from native meniscal tissue. After 24 months, no further improvement of the mechanical properties occurred (Tienen et al., 2006). Rather, some scaffolds were totally destroyed, leading to considerable cartilage degeneration, contradicting the speculation by Sandman et al. (Welsing et al., 2008; Hannink et al., 2011).

3.1.3. Unconfined compression relaxation and creep tests

Based on the test setup of Chia and Hull (2008), we performed an unconfined compression relaxation test at a physiological strain level of 12% (Fig. 5). The resultant equilibrium modulus, representing the elastic properties of a viscoelastic material, was 560 ± 310 kPa.

This was stiffer than the compressive modulus at equilibrium of human medial menisci determined by Chia and Hull via a nonlinear least-squares regression using Fung's two-parameter exponential model. They assessed the highest equilibrium modulus to be approximately 138 kPa in the anterior region of the meniscus in the axial direction. However, such low values might partially be attributable to the extremely small sample dimensions of the tested 2 mm cubes. Samples of this dimension possibly do not reflect the properties of the largely inhomogeneous meniscal tissue correctly.

Gruchenberg et al. (2015, 2018) investigated a previous version of the silk fibroin scaffold in a sheep model, evaluating the equilibrium modulus preoperatively and 3 and 6 months post implantation and compared it with ovine meniscal tissue. They performed inter alia a stress-relaxation test at 20% strain and found a significantly higher equilibrium modulus for meniscal tissue (approximately 750 kPa) than for the scaffold (approximately 420 kPa) (Gruchenberg et al., 2015, 2018). In addition to the lower stiffness, the results of Gruchenberg

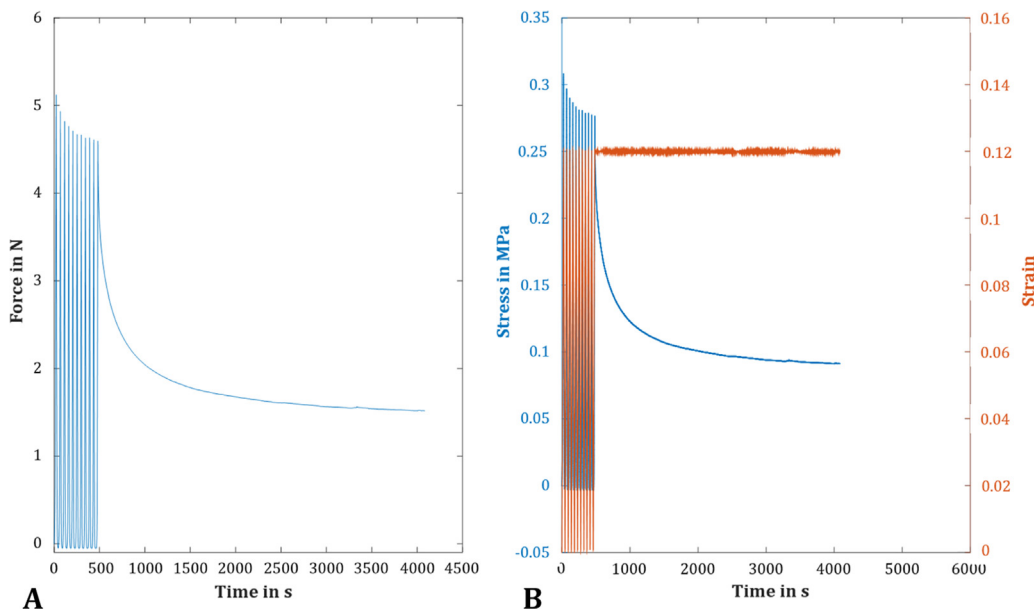


Fig. 5. A representative curve of the decreasing force when performing an unconfined compression relaxation test at a physiological strain level of 12%, which was held constant for 1 h (A). The resultant stress (B, blue) was averaged over the last 10 min and divided by the applied strain (red) to determine the equilibrium modulus E_{eq} . (For interpretation of the references to color in this figure legend, the reader is referred to the web version of this article.)

et al. (2015, 2018) showed an insufficient fixation of the scaffold with the remaining meniscal tissue. Therefore, a new fibre layer was integrated within the porous matrix to enhance the surgical fixation. However, the authors postulate that the increased stiffness of the silk fibroin scaffold tested in the current study compared to the previous version may be due to this new fibre layer.

To observe the material's behaviour under more physiological conditions, unconfined compression creep tests were also performed. Here, we adapted our test setup to that of Joshi et al. (1995), who quantified the compressive biomechanical properties of menisci of various species. The silk fibroin scaffold displayed a typical viscoelastic creep response, with a mean deformation of approximately 2.2% (0.15 ± 0.05 mm, Fig. 6) after 1 h. The equilibrium modulus was 0.30 ± 0.12 MPa. Joshi et al. determined an aggregate modulus H_A in MPa, which reflects the stiffness of the extracellular matrix, using the linear biphasic model. They found an aggregate modulus of approximately 0.2 MPa for human menisci (Joshi et al., 1995). The highest modulus was found for porcine meniscal tissue (approximately 0.27 MPa), which was, however, not significantly different to human menisci but even less than that of the silk fibroin scaffold.

Merriam et al. (2015) and Patel et al. (2016) investigated a fibre-reinforced scaffold with two different material compositions (p(DTD DD) vs. PLLA, respectively) for total meniscal replacement in a sheep

model. For mechanical characterisation of the scaffolds, they performed inter alia an unconfined compression creep test preoperatively and 16 and 32 weeks after implantation. They also used Mow's biphasic theory to evaluate the aggregate modulus of their collagen scaffold (p(DTD DD) fibres) and its modification (PLLA fibres), respectively (Merriam et al., 2015; Patel et al., 2016). They found that their scaffolds preoperatively reached an aggregate modulus of only 25% of the native meniscus (approximately 0.2 MPa versus 0.8 MPa for native ovine meniscal tissue), which, however, doubled after 16 weeks of implantation time. Despite the still existing discrepancy of the values between the p(DTD DD) fibre implant and the ovine meniscal tissue, the authors looked forward to a successful implant for total meniscal replacement due to the greater protection of the articular cartilage compared to a meniscectomy (Merriam et al., 2015).

The testing protocol according to Joshi et al. provided small loads of only 0.1 N, which may represent a limitation also of the current study. However, these low load magnitudes are necessary to ensure the assumption of the infinitesimal linearity of the linear biphasic model used by Joshi et al. (1995) as well as by Merriam et al. (2015) and Patel et al. (2016). Nevertheless, to the best of the authors' knowledge, the indicated studies are the only ones testing (different) menisci and also a potential meniscal replacement material under compression creep conditions.

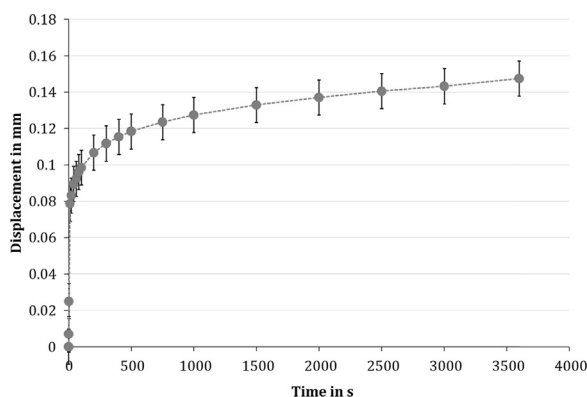


Fig. 6. The unconfined compression creep tests of the silk fibroin scaffold revealed a typical viscoelastic creep response of the material with a mean deformation of approximately 2.2% (here: the averaged creep curve for all tested samples, $n = 9$).

3.1.4. Dynamic mechanical analysis

With increasing frequency, the storage modulus E' of the silk fibroin scaffold did not increase significantly. Only a slight tendency of a continuous increase in E' from 1.20 ± 0.97 MPa at 0.1 Hz to 1.43 ± 1.17 MPa at 10 Hz could be identified (Fig. 7A1). This leads to the assumption that the energy, which is stored within the scaffold due to the elastic part of the material did not increase significantly with increasing loading frequency. The damping factor $\tan(\delta)$, which was calculated from the phase lag angle δ between the applied strain and the resultant material stress response, did not depend on the testing frequency (0.1 Hz: $\tan(\delta) = 0.18 \pm 0.06$ and 10 Hz: $\tan(\delta) = 0.19 \pm 0.04$; one-way ANOVA; Fig. 7A2), as well. Consequently, the damping properties are uninfluenced by the testing frequency, as well.

Comparing the obtained data with Yan et al. (2012), who investigated the dynamic compressive properties of silk fibroin scaffolds prepared with four different initial silk concentrations, with the scaffold tested in the current study, we found the material tested in this study to be two- to three-fold stiffer. However, the damping properties were

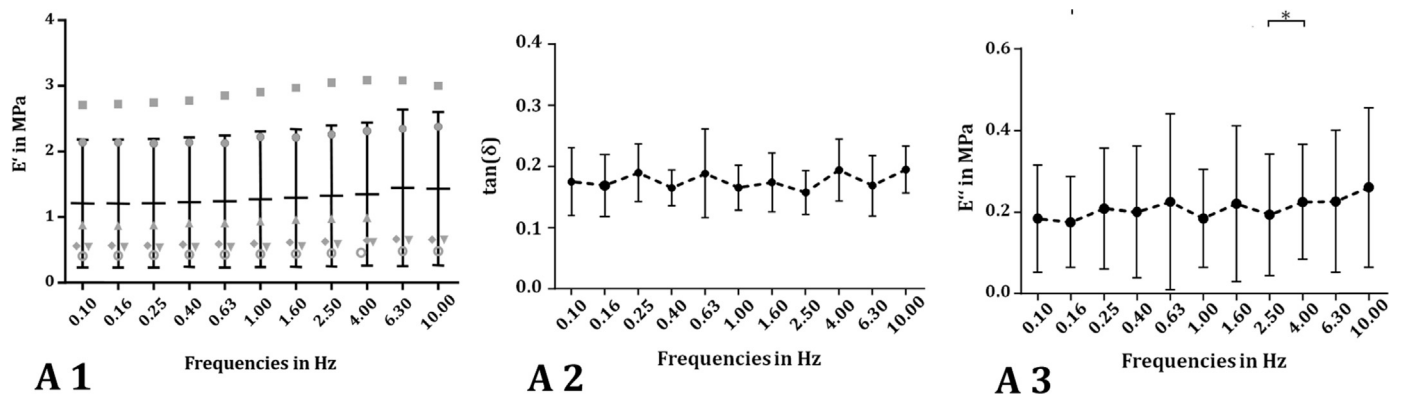


Fig. 7. Within the dynamic mechanical analysis (DMA), a sinusoidal stress σ (or strain ϵ) is applied over a frequency spectrum and the material's response strain ϵ (or stress σ) is recorded. Because of the viscoelastic properties of the material, the response lags behind the applied stress (strain) with a phase-lag angle δ . For detailed characterisation of the silk fibroin scaffold, the dynamic elastic or storage modulus E' in MPa (A 1), the loss factor $\tan(\delta)$ (A 2) and the so-called loss modulus E'' in MPa, as a parameter for the amount of energy dissipated by the viscous mechanisms (A 3), were evaluated.

quite similar to Yan's scaffold, particularly at a silk concentration of 12 or 16 wt%, whereas the dissolved fibroin concentration of the scaffold tested in the current study was 20%. [Pereira et al. \(2014\)](#) also determined the dynamic compressive properties of fresh human menisci, performing a DMA. They similarly found a tendency for an increased E' with increasing frequency for medial and lateral menisci. However, the E' was slightly different for both sides and also varied between the anterior, mid body and posterior regions. The mid body of the medial meniscus was stiffest and displayed elastic moduli between 0.83 MPa and 0.93 MPa for 0.1 Hz and 10 Hz, respectively, which was in the range of the silk fibroin scaffold tested in the current study ([Pereira et al., 2014](#)).

Additionally, we evaluated the loss modulus E'' as a parameter for the energy, which is dissipated by the viscous mechanisms within the material. Here, it was clear that E'' was also uninfluenced by the varied frequencies, comparable to the loss factor $\tan(\delta)$, whereby E'' ranged from 0.18 ± 0.13 MPa to 0.26 ± 0.19 MPa at 0.1–10 Hz, respectively ([Fig. 7A3](#)).

Comparing these data with human meniscal tissue, the silk fibroin scaffold tested in the current study had a slightly higher capability to dissipate energy than in the studies of [Pereira et al. \(2014\)](#) and [Bursac et al. \(2009\)](#), as indicated by the higher loss modulus. Therefore, the elastic properties of the silk fibroin scaffold were more pronounced than its viscous character. Consequently, the amount of energy dissipated by the viscous mechanisms was minor compared to the energy stored within the material because of the elastic components.

3.2. Structural analysis: μ -CT

The structural composition and architecture of the silk fibroin scaffold was determined by μ -CT analysis ([Fig. 8](#)). Here, a mean volume of 24.2 ± 6.87 mm³ of each sample was analysed. The variations in the analysed volume arose from the location of the integrated fibre layer ([Fig. 8](#)), which was excluded from the analysis to prevent any misinterpretations of the ultrastructure of the scaffold. μ -CT analysis revealed a total porosity of $80.13 \pm 4.32\%$ (open porosity: of $80.12 \pm 4.32\%$), with a mean pore size of 215.6 ± 10.9 μ m. In general, the pore size distribution was Gaussian, but slightly shifted to the left. However, it ranged over 8–663 μ m, with more than 65% of the pores being 100–300 μ m in diameter ([Fig. 8](#)). A mean pore wall thickness of 53.6 ± 9.6 μ m was observed, with almost 30% of the pore walls measuring 24–40 μ m ([Fig. 8](#)).

Microstructural parameters, including pore size and total porosity, are crucial for replacement materials, because they can affect not only the integration but also the regeneration of new meniscal tissue. Therefore, [Rongen et al.](#) included these parameters in their

requirements for meniscal replacement materials. They suggest having both large macropores (200–300 μ m) in turn connected by smaller micropores (10–50 μ m), resulting in a high interconnectivity. Additionally, one should aim for a high total porosity of $> 70\%$ ([Rongen et al., 2014](#)). Comparing the obtained values in the present study with these requirements, it is clear that the silk fibroin scaffold fits well with these guidelines for structural composition of meniscal replacement materials.

3.3. In vitro biocompatibility test

The MTT and BrdU tests demonstrated undisturbed cell viability and increasing proliferation over time in the presence of the scaffold material, indicating a sufficient biocompatibility of the material, with no toxic side effects on co-cultured cells ([Fig. 9A and B](#)). Therefore, we conclude that the scaffold material does not have a general negative effect on cell proliferation and metabolic activity.

Because of its unique material properties, silk has been used decades long in biomedical applications. Combined high mechanical strength and favourable elasticity make silk a suitable suture material ([Altman et al., 2003](#)). Silk extracted from the silkworm cocoon (*Bombyx mori*) mainly consists of two fibroin proteins, which are encased with a sericin coat. Thereby, sericin serves as a “glue” to hold the two core fibres together ([Altman et al., 2003](#)). The immunogenicity of silk-based biomaterials arises from the sericin coating of the fibroin proteins, because isolated fibroin proteins did not activate the immune system ([Panilaitis et al., 2003](#)). Therefore, the biocompatibility of isolated fibroin has been demonstrated in various in vitro and in vivo studies ([Santini et al., 1999](#); [Meinel et al., 2005](#); [Cassinelli et al., 2006](#); [Seo et al., 2009](#)). During the manufacturing process of the silk fibroin scaffold used in the current study, fibroin was extracted and processed into a porous matrix. Biocompatibility of the first generation of this scaffolds was previously confirmed in an in vivo study using a partial meniscal replacement model ([Gruchenberg et al., 2015](#)). Furthermore, there was insufficient fixation stability resulted in less integration of the scaffold into the remaining meniscal tissue, leading to displacement of the material during the experimental period in a third of all cases. Therefore, this study revealed the need to improve scaffold fixation to the meniscal rim ([Gruchenberg et al., 2015](#)) and a fibre mesh was accordingly inserted into the porous matrix. The current study showed that the material properties in terms of biocompatibility did not change during this process, therefore the second generation of this material can be used in an in vivo setting in the future.

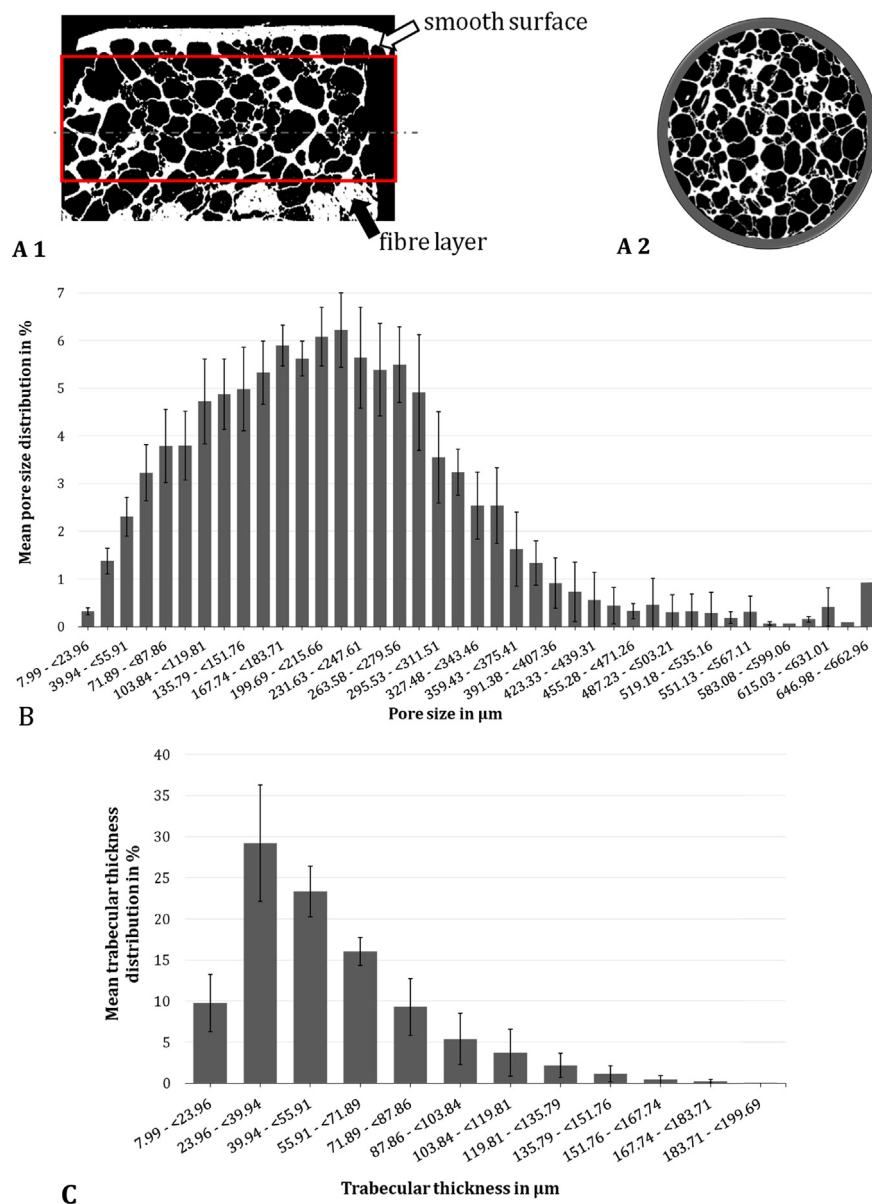


Fig. 8. Exemplary sagittal (A 1) and transversal (A 2) μ -CT images of a critical point dried silk fibroin scaffold. From μ -CT analysis, the mean and standard deviation of the pore size distribution (B) and the distribution of the trabecular thickness (C) were evaluated ($n = 5$).

4. Conclusion

Within the current study, we characterised the mechanical and structural properties as well as the biocompatibility of a second generation, new, silk fibroin scaffold as a potential material for permanent partial meniscal replacement (Table 1).

Many approaches have been published to restore rather than resect the injured meniscus (Rongen et al., 2014; Rodkey et al., 1999; Buma et al., 2004; Kohn et al., 1992; Walsh et al., 1999; Bruns et al., 1998; Gastel et al., 2001; Peters and Wirth, 2003; Verdonk et al., 2005; Milachowski et al., 1990; Noyes and Barber-Westin, 2005). Only two artificial substitutes (CMI[®] and Actifit[®]) are used clinically, but these are still not widely accepted by medical professionals. Additionally, their pre-operatively mechanical properties do not approach those of human meniscal tissue as Sandmann et al. showed significant differences in the viscoelastic properties of both artificial replacement concepts in comparison to human menisci. Long-term biomechanical data of these implants are not available in the literature.

Rongen et al. (2014) further elaborated the basic requirements for

meniscal replacement materials first postulated by Stone et al. (1997). It is important for a replacement material to support mechanical loads already in the initial phase following implantation and that it should mimic the native meniscus as closely as possible (Stone et al., 1997; Rongen et al., 2014). Considering these requirements, the silk fibroin scaffold for partial meniscal replacement tested in the current study displayed a sufficient compressive competence although slightly in excess of the native human meniscus. The material showed an increased stiffness in comparison to the first scaffold generation, which is likely to be associated with a fibre component integrated in the scaffold to enhance fixation strength to the meniscal host tissue. These new fibres did not provide comparable tensile strength to native meniscus but, because the inner region of the meniscus, which is the target for a partial meniscal replacement, is more exposed to compressive rather than to high tensile loads (Masouros et al., 2010; Beaupre et al., 1986; McDermott et al., 2010). Nevertheless, it is expected that the scaffold could be improved, especially for larger replacement defects, by adopting a higher density of fibres with orientation, which better mimics the circumferential orientation of the collagen fibres of native meniscal tissue.

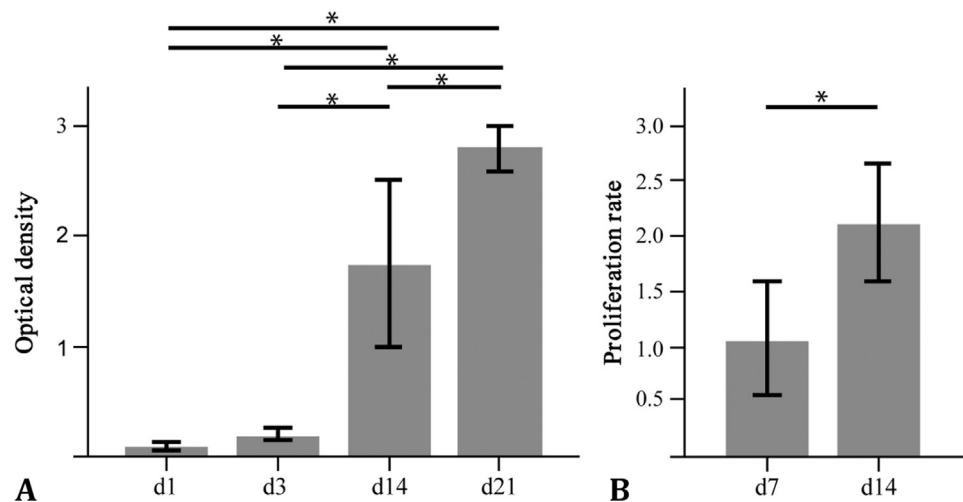


Fig. 9. Assessment of the biocompatibility (A, B) of the silk scaffold. Therefore, ATDC5 cells and human MSCs were co-cultured with the silk fibroin scaffold and the cell metabolism of MSCs was assessed by the MTT test (C), whereas the cell-proliferation rate of ATDC5 cells was assessed by the BrdU test (D). (n = 3–6) *p < 0.05.

Table 1

Summary of all biomechanical measurements and evaluated data achieved during tensile-, indentation-, unconfined compression relaxation and creep tests and during dynamic mechanical analysis (DMA).

Tensile test	Ultimate tensile force	51.0 ± 16.1 N
	F _{max}	
	Ultimate tensile strength	3.28 ± 1.01 MPa
	Elastic Modulus E	5.37 ± 1.45 MPa
	Displacement at ultimate force s _{max}	4.75 ± 0.92 mm
Indentation test	Stiffness k	
	Cycle 1	17.9 ± 2.69 N/mm
	Cycle 5	24.7 ± 3.73 N/mm
	Residual force F _{res}	
	Cycle 1	4.79 ± 0.17 N
	Cycle 5	5.23 ± 0.15 N
	Compression	
Unconfined compression	Cycle 1	8.03 ± 1.68%
	Cycle 5	5.58 ± 0.97%
	Relaxation (Equilibrium modulus E _{eq})	0.56 ± 0.31 MPa
	Creep (Equilibrium modulus E _{eq})	0.30 ± 0.12 MPa
	Frequency range	0.1–10 Hz
DMA	Storage/elastic modulus E'	1.20 ± 0.97 MPa–1.43 ± 1.17 MPa
	Loss factor tan(δ)	0.18 ± 0.06–0.19 ± 0.04
	Loss modulus E''	0.18 ± 0.13 MPa–0.26 ± 0.19 MPa

Although the silk fibroin scaffold presented mechanical competence, which is important to distribute loads over the articulating surfaces and therefore, reducing peak stresses already in the initial phase after implantation, a too stiff construct may impede tissue ingrowth and additionally damage the underlying articular cartilage (Rongen et al., 2014). Maher et al. (2010) also indicate that the transition zone between implant and meniscal host tissue is always a critical region as the mismatch in stiffness could inhibit the success of partial meniscal replacement materials. Therefore, adjusting the structural parameters, like pore size distribution and pore wall thickness, may present an opportunity to reduce the material's stiffness to more closely simulate the biomechanical/compressive properties of menisci, even if they were in the range of the requirements postulated by Rongen et al. (2014). Initial mechanical competence is important and desirable for load transmission and therefore, chondroprotection even in the early post-operative phase. However, addressing this mechanical capability over the full range of meniscal tissue loading is important in developing a stable implant-tissue interface. Given the characteristic anisotropy and

inhomogeneity of meniscal tissue, this will always be a major challenge to replicate. Nevertheless, we conclude that varying the ratio and orientation of the stiffer fibres in the silk fibroin scaffolds tested in the current study to a more compressible porous hydrogel matrix may offer a route to better emulating the full range of native meniscus properties.

Acknowledgements

This work was supported by the Wellcome Trust [100917/z/13/z] and the German Armed Forces [E/U2AD/ED001/EF551]. FibroFix™ is being developed with funding from the NIHR Invention for Innovation (i4i) Programme [II-LS-1010-10009].

We acknowledge the support of the Department of Systematic Botany and Ecology, Ulm University for letting us use their critical point drying facilities.

Disclosures

Authors Nick Skaer and Robert Walker are employees of Orthox Ltd. (Abingdon, UK). Oliver Kessler is a consultant of Orthox Ltd. (Abingdon, UK). All other authors have no conflict of interest.

References

- Abrams, G.D., Frank, R.M., Gupta, A.K., Harris, J.D., McCormick, F.M., Cole, B.J., 2013. Trends in meniscus repair and meniscectomy in the united states, 2005–2011. *Am. J. Sports Med.* 41 (10), 2333–2339.
- Ahmed, A.M., Burke, D.L., 1983. In-vitro measurement of static pressure distribution in synovial joints-part I: tibial surface of the knee. *J. Biomech. Eng.* 105 (3), 216–225.
- Altman, G.H., Diaz, F., Jakuba, C., Calabro, T., Horan, R.L., Chen, J., Lu, H., Richmond, J., Kaplan, D.L., 2003. Silk-based biomaterials. *Biomaterials* 24 (3), 401–416.
- Balint, E., Gatt Jr., C.J., Dunn, M.G., 2012. Design and mechanical evaluation of a novel fiber-reinforced scaffold for meniscus replacement. *J. Biomed. Mater. Res. A* 100 (1), 195–202.
- Baratz, M.E., Fu, F.H., Mengato, R., 1986. Meniscal tears: the effect of meniscectomy and of repair on intraarticular contact areas and stress in the human knee. A preliminary report. *Am. J. Sports Med.* 14 (4), 270–275.
- Beaupre, A., Choukroun, R., Guidouin, R., Garneau, R., Gerardin, H., Cardou, A., 1986. Knee menisci. Correlation between microstructure and biomechanics. *Clin. Orthop. Relat. Res.* 208, 72–75.
- Brindle, T., Nyland, J., Johnson, D.L., 2001. The meniscus: review of basic principles with application to surgery and rehabilitation. *J. Athl. Train.* 36 (2), 160–169.
- Bruns, J., Kahrs, J., Kampen, J., Behrens, P., Plitz, W., 1998. Autologous perichondral tissue for meniscal replacement. *J. Bone Jt. Surg. Br.* 80 (5), 918–923.
- Bullough, P.G., Munuera, L., Murphy, J., Weinstein, A.M., 1970. The strength of the menisci of the knee as it relates to their fine structure. *J. Bone Jt. Surg. Br.* 52 (3), 564–567.
- Buma, P., Ramrattan, N.N., van Tienen, T.G., Veth, R.P., 2004. Tissue Engineering of the meniscus. *Biomaterials* 25 (9), 1523–1532.
- Bursac, P., Arnoczky, S., York, A., 2009. Dynamic compressive behavior of human

- meniscus correlates with its extra-cellular matrix composition. *Biorheology* 46 (3), 227–237.
- Cassinelli, C., Cascardo, G., Morra, M., Draghi, L., Motta, A., Catapano, G., 2006. Physical-chemical and biological characterization of silk fibroin-coated porous membranes for medical applications. *Int. J. Artif. Organs* 29 (9), 881–892.
- Chia, H.N., Hull, M.L., 2008. Compressive moduli of the human medial meniscus in the axial and radial directions at equilibrium and at a physiological strain rate. *J. Orthop. Res.* 26 (7), 951–956.
- Elsner, J.J., Portnoy, S., Zur, G., Guilak, F., Shterling, A., Linder-Ganz, E., 2010. Design of a free-floating polycarbonate-urethane meniscal implant using finite element modeling and experimental validation. *J. Biomech. Eng.* 132 (9), 095001.
- Englund, M., Lohmander, L.S., 2004. Risk factors for symptomatic knee osteoarthritis fifteen to twenty-two years after meniscectomy. *Arthritis Rheum.* 50 (9), 2811–2819.
- Fairbank, T.J., 1948. Knee joint changes after meniscectomy. *J. Bone Jt. Surg. Br.* 30B (4), 664–670.
- Fukubayashi, T., Kurosawa, H., 1980. The contact area and pressure distribution pattern of the knee. A study of normal and osteoarthrotic knee joints. *Acta Orthop. Scand.* 51 (6), 871–879.
- Gastel, J.A., Muirhead, W.R., Lifrak, J.T., Fadale, P.D., Hulstyn, M.J., Labrador, D.P., 2001. Meniscal tissue regeneration using a collagenous biomaterial derived from porcine small intestine submucosa. *Arthroscopy* 17 (2), 151–159.
- Gruchenberg, K., Ignatius, A., Friemert, B., von Lubken, F., Skaer, N., Gellynck, K., Kessler, O., Durselen, L., 2015. In vivo performance of a novel silk fibroin scaffold for partial meniscal replacement in a sheep model. *Knee Surg. Sports Traumatol. Arthrosc.* 23 (8), 2218–2229.
- Gruchenberg, K., Ignatius, A., Friemert, B., von Lubken, F., Skaer, N., Gellynck, K., Kessler, O., Durselen, L., 2018. Correction to: in vivo performance of a novel silk fibroin scaffold for partial meniscal replacement in a sheep model. *Knee Surg. Sports Traumatol. Arthrosc.*
- Gulrajani, M.L., Gupta, S.V., Gupta, A., Suri, M., 1996. Degumming of silk with different protease enzymes. *Indian J. Fibre Text.* 21 (4), 270–275.
- Hannink, G., van Tienen, T.G., Schouten, A.J., Buma, P., 2011. Changes in articular cartilage after meniscectomy and meniscus replacement using a biodegradable porous polymer implant. *Knee Surg. Sports Traumatol. Arthrosc.* 19 (3), 441–451.
- Hede, A., Larsen, E., Sandberg, H., 1992. Partial versus total meniscectomy. A prospective, randomised study with long-term follow-up. *J. Bone Jt. Surg. Br.* 74 (1), 118–121.
- Joshi, M.D., Suh, J.K., Marui, T., Woo, S.L., 1995. Interspecies variation of compressive biomechanical properties of the meniscus. *J. Biomed. Mater. Res. A* 29 (7), 823–828.
- Kohn, D., Wirth, C.J., Reiss, G., Plitz, W., Maschek, H., Erhardt, W., Wulker, N., 1992. Medial meniscus replacement by a tendon autograft. Experiments in sheep. *J. Bone Jt. Surg. Br.* 74 (6), 910–917.
- Kutzner, I., Heinlein, B., Graichen, F., Bender, A., Rohlmann, A., Halder, A., Beier, A., Bergmann, G., 2010. Loading of the knee joint during activities of daily living measured in vivo in five subjects. *J. Biomech.* 43 (11), 2164–2173.
- Lechner, K., Hull, M.L., Howell, S.M., 2000. Is the circumferential tensile modulus within a human medial meniscus affected by the test sample location and cross-sectional area? *J. Orthop. Res.* 18 (6), 945–951.
- Lee, S.J., Aadalen, K.J., Malaviya, P., Lorenz, E.P., Hayden, J.K., Farr, J., Kang, R.W., Cole, B.J., 2006. Tibiofemoral contact mechanics after serial medial meniscectomies in the human cadaveric knee. *Am. J. Sports Med.* 34 (8), 1334–1344.
- Maher, S.A., Rodeo, S.A., Doty, S.B., Brophy, R., Potter, H., Foo, L.F., Rosenblatt, L., Deng, X.H., Turner, A.S., Wright, T.M., Warren, R.F., 2010. Evaluation of a porous polyurethane scaffold in a partial meniscal defect ovine model. *Arthroscopy* 26 (11), 1510–1519.
- Majewski, M., Susanne, H., Klaus, S., 2006. Epidemiology of athletic knee injuries: a 10-year study. *Knee* 13 (3), 184–188.
- Masouros, S.D., McDermott, I.D., Bull, A.M., Amis, A.A., 2010. Biomechanics. In: Beaufils, P., Verdonk, P. (Eds.), *The Meniscus*. Springer-Verlag, Heidelberg, New York, pp. 29–37.
- McDermott, I.D., Masouros, S.D., Bull, A.M., Amis, A.A., 2010. Anatomy. In: Beaufils, P., Verdonk, P. (Eds.), *The Meniscus*. Springer-Verlag, Heidelberg, New York, pp. 11–18.
- Meinel, L., Hofmann, S., Karageorgiou, V., Kirker-Head, C., McCool, J., Gronowicz, G., Zichner, L., Langer, R., Vunjak-Novakovic, G., Kaplan, D.L., 2005. The inflammatory responses to silk films in vitro and in vivo. *Biomaterials* 26 (2), 147–155.
- Merriam, A.R., Patel, J.M., Culp, B.M., Gatt Jr., C.J., Dunn, M.G., 2015. Successful total meniscus reconstruction using a novel fiber-reinforced scaffold: a 16- and 32-week study in an ovine model. *Am. J. Sports Med.*
- Mietsch, A., Neidlinger-Wilke, C., Schrezenmeier, H., Mauer, U.M., Friemert, B., Wilke, H.J., Ignatius, A., 2013. Evaluation of platelet-rich plasma and hydrostatic pressure regarding cell differentiation in nucleus pulposus tissue engineering. *J. Tissue Eng. Regen. Med.* 7 (3), 244–252.
- Milachowski, K.A., Kohn, D., Wirth, C.J., 1990. Meniscus replacement using Hoffa's infrapatellar fat bodies—initial clinical results. *Unfallchirurgie* 16 (4), 190–195.
- Mow, V.C., Huiskes, R., 2005. Structure and function of articular cartilage and meniscus. In: Mow, V.C., Huiskes, R. (Eds.), *Basic Orthopaedic Biomechanics & Mechanobiology*. Lippincott Williams & Wilkins, Philadelphia, pp. 182–257.
- Noyes, F.R., Barber-Westin, S.D., 2005. Meniscus transplantation: indications, techniques, clinical outcomes. *Instr. Course Lect.* 54, 341–353.
- Panilaitis, B., Altman, G.H., Chen, J., Jin, H.J., Karageorgiou, V., Kaplan, D.L., 2003. Macrophage responses to silk. *Biomaterials* 24 (18), 3079–3085.
- Patel, J.M., Merriam, A.R., Kohn, J., Gatt Jr., C.J., Dunn, M.G., 2016. Negative outcomes of poly(L-lactic acid) fiber-reinforced scaffolds in an ovine total meniscus replacement model. *Tissue Eng. Part A* 22 (17–18), 1116–1125.
- Pena, E., Calvo, B., Martinez, M.A., Palanca, D., Doblare, M., 2005. Finite element analysis of the effect of meniscal tears and meniscectomies on human knee biomechanics. *Clin. Biomech.* 20 (5), 498–507.
- Pereira, H., Caridade, S.G., Frias, A.M., Silva-Correia, J., Pereira, D.R., Cengiz, I.F., Mano, J.F., Oliveira, J.M., Espregueira-Mendes, J., Reis, R.L., 2014. Biomechanical and cellular segmental characterization of human meniscus: building the basis for tissue engineering therapies. *Osteoarthritis Cartil.* 22 (9), 1271–1281.
- Peters, G., Wirth, C.J., 2003. The current state of meniscal allograft transplantation and replacement. *Knee* 10 (1), 19–31.
- Rodkey, W.G., Steadman, J.R., Li, S.T., 1999. A clinical study of collagen meniscus implants to restore the injured meniscus. *Clin. Orthop. Relat. Res. Suppl* 367, S281–S292.
- Rongen, J.J., van Tienen, T.G., van Bochove, B., Grijpma, D.W., Buma, P., 2014. Biomaterials in search of a meniscus substitute. *Biomaterials* 35 (11), 3527–3540.
- Roos, H., Lauren, M., Adalberth, T., Roos, E.M., Jonsson, K., Lohmander, L.S., 1998. Knee osteoarthritis after meniscectomy: prevalence of radiographic changes after twenty-one years, compared with matched controls. *Arthritis Rheum.* 41 (4), 687–693.
- Sandmann, G.H., Adamczyk, C., Grande Garcia, E., Doebele, S., Buettner, A., Milz, S., Imhoff, A.B., Vogt, S., Burkart, R., Tischer, T., 2013. Biomechanical comparison of menisci from different species and artificial constructs. *BMC Musculoskelet. Disord.* 14, 324.
- Santin, M., Motta, A., Freddi, G., Cannas, M., 1999. In vitro evaluation of the inflammatory potential of the silk fibroin. *J. Biomed. Mater. Res.* 46 (3), 382–389.
- Sarem, M., Moztafzadeh, F., Mozafari, M., Shastri, V.P., 2013. Optimization strategies on the structural modeling of gelatin/chitosan scaffolds to mimic human meniscus tissue. *Mater. Sci. Eng. C. Mater. Biol. Appl.* 33 (8), 4777–4785.
- Schimmer, R.C., Brulhart, K.B., Duff, C., Glinz, W., 1998. Arthroscopic partial meniscectomy: a 12-year follow-up and two-step evaluation of the long-term course. *Arthroscopy* 14 (2), 136–142.
- Seitz, A.M., Lubomierski, A., Friemert, B., Ignatius, A., Durselen, L., 2012. Effect of partial meniscectomy at the medial posterior horn on tibiofemoral contact mechanics and meniscal hoop strains in human knees. *J. Orthop. Res.* 30 (6), 934–942.
- Seo, Y.K., Yoon, H.H., Song, K.Y., Kwon, S.Y., Lee, H.S., Park, Y.S., Park, J.K., 2009. Increase in cell migration and angiogenesis in a composite silk scaffold for tissue-engineered ligaments. *J. Orthop. Res.* 27 (4), 495–503.
- Shapiro, S.S., Wilk, M.B., 1965. An analysis of variance test for normality (complete samples). *Biometrika* 52 (3/4), 591–611.
- Shemesh, M., Asher, R., Zylberberg, E., Guilak, F., Linder-Ganz, E., Elsner, J.J., 2014. Viscoelastic properties of a synthetic meniscus implant. *J. Mech. Behav. Biomed. Mater.* 29, 42–55.
- Stone, K.R., 1996. Meniscus replacement. *Clin. Sports Med.* 15 (3), 557–571.
- Stone, K.R., Steadman, J.R., Rodkey, W.G., Li, S.T., 1997. Regeneration of meniscal cartilage with use of a collagen scaffold. Analysis of preliminary data. *J. Bone Jt. Surg. Am.* 79 (12), 1770–1777.
- Tienen, T.G., Heijkants, R.G., de Groot, J.H., Schouten, A.J., Pennings, A.J., Veth, R.P., Buma, P., 2006. Meniscal replacement in dogs. Tissue regeneration in two different materials with similar properties. *J. Biomed. Mater. Res. B Appl. Biomater.* 76 (2), 389–396.
- Tissakht, M., Ahmed, A.M., 1995. Tensile stress-strain characteristics of the human meniscal material. *J. Biomech.* 28 (4), 411–422.
- Verdonk, P.C., Demurie, A., Almqvist, K.F., Vey, E.M., Verbruggen, G., Verdonk, R., 2005. Transplantation of viable meniscal allograft. Survivorship analysis and clinical outcome of one hundred cases. *J. Bone Jt. Surg. Am.* 87 (4), 715–724.
- Verdonk, R., Verdonk, P., Huysse, W., Forsyth, R., Heinrichs, E.L., 2011. Tissue ingrowth after implantation of a novel, biodegradable polyurethane scaffold for treatment of partial meniscal lesions. *Am. J. Sports Med.* 39 (4), 774–782.
- Villegas, D.F., Maces, J.A., Magee, S.D., Donahue, T.L., 2007. Failure properties and strain distribution analysis of meniscal attachments. *J. Biomech.* 40 (12), 2655–2662.
- Walsh, C.J., Goodman, D., Caplan, A.I., Goldberg, V.M., 1999. Meniscus regeneration in a rabbit partial meniscectomy model. *Tissue Eng.* 5 (4), 327–337.
- Warnecke, D., Schild, N.B., Klose, S., Joos, H., Brenner, R.E., Kessler, O., Skaer, N., Walker, R., Freutel, M., Ignatius, A., Durselen, L., 2017. Friction properties of a new silk fibroin scaffold for meniscal replacement. *Tribol. Int.* 109, 586–592.
- Welsing, R.T.C., van Tienen, T.G., Ramrattan, N., Heijkants, R., Schouten, A.J., Veth, R.F.H., Buma, P., 2008. Effect on tissue differentiation and articular cartilage degradation of a polymer meniscus implant – a 2-year follow-up study in dogs. *Am. J. Sports Med.* 36 (10), 1978–1989.
- Yan, L.P., Oliveira, J.M., Oliveira, A.L., Caridade, S.G., Mano, J.F., Reis, R.L., 2012. Macro/microporous silk fibroin scaffolds with potential for articular cartilage and meniscus tissue engineering applications. *Acta Biomater.* 8 (1), 289–301.
- Zur, G., Linder-Ganz, E., Elsner, J.J., Shani, J., Brenner, O., Agar, G., Hershsman, E.B., Arnoczky, S.P., Guilak, F., Shterling, A., 2011. Chondroprotective effects of a polycarbonate-urethane meniscal implant: histopathological results in a sheep model. *Knee Surg. Sports Traumatol. Arthrosc.* 19 (2), 255–263.

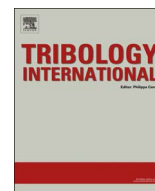
8.2. Manuscript 2

WARNECKE D, SCHILD NB, KLOSE S, JOOS H, BRENNER RE, KESSLER O, SKAER N, WALKER R, FREUTEL M, IGNATIUS A, DÜRSELEN L. Friction properties of a new silk fibroin scaffold for meniscal replacement. *Tribol Int* 2017; 109: 586 - 92. DOI: 10.1016/j.triboint.2017.01.038

Open access

Creative Commons Attribution License 4.0 International (CC BY 4.0,
<http://creativecommons.org/licenses/by/4.0/>)

DW carried out all mechanical tests and evaluations as well as the statistical analyses. Additionally, DW drafted the manuscript.



Friction properties of a new silk fibroin scaffold for meniscal replacement

Daniela Warnecke^{a,*}, N.B. Schild^a, S. Klose^a, H. Joos^b, R.E. Brenner^b, O. Kessler^{c,d}, N. Skaer^e, R. Walker^e, M. Freutel^a, A. Ignatius^a, L. Dürselen^a

^a Institute of Orthopaedic Research and Biomechanics, Centre for Trauma Research Ulm, Ulm University Medical Centre, Germany

^b Division for Biochemistry of Joint and Connective Tissue Diseases, Department of Orthopaedics, Ulm University Medical Centre, Germany

^c Centre of Orthopaedics and Sports, Zurich, Switzerland

^d University Medical Centre, Clinic for Orthopaedic Surgery, Magdeburg, Germany

^e Orthox Ltd. Abingdon, UK

ARTICLE INFO

Keywords:

Friction

Silk

Meniscus replacement

Cartilage

Lubricin

ABSTRACT

The menisci protect the articular cartilage by reducing contact pressure in the knee. To restore their function after injury, a new silk fibroin replacement scaffold was developed. To elucidate its tribological properties, friction of the implant was tested against cartilage and glass, where the latter is typically used in tribological cartilage studies. The silk scaffold exhibited a friction coefficient against cartilage of 0.056, which is higher than meniscus against cartilage but in range of the requirements for meniscal replacements. Further, meniscus friction against glass was lower than cartilage against glass, which correlated with the surface lubricin content. Concluding, the tribological properties of the new material suggest a possible long-term chondroprotective function. In contrast, glass always produced high, non-physiological friction coefficients.

1. Introduction

The semilunar menisci are located between the femoral condyles and the tibial plateau of the knee joint [1–4]. They play a decisive role in load distribution by increasing the contact area between the incongruent femoral and tibial articular surfaces. Additionally, they are involved in secondary joint stabilisation, nutrient distribution and providing joint motion at low friction [3–5]. Loads of up to 3.5 times body weight are transferred through the knee joint during activities of daily life, whereby in general 45–70% of the total load is transmitted through the menisci [6,7]. In experiencing such high mechanical stress, the menisci are prone to injuries requiring surgical intervention in approximately 85% of cases [8]. The most frequent surgical therapy for meniscus injuries is a partial meniscectomy. However, various studies have shown that a partial meniscectomy determines the onset of cartilage degeneration, leading to osteoarthritis (OA) in the long term [9–11].

Removing meniscal tissue leads to a reduced contact area associated not only with an increased contact pressure but also with greater friction [3–5,10–12]. McCann et al. additionally identified fibrillation of the cartilage surfaces immediately after removal of meniscal tissue and wear of the articular cartilage [12]. Therefore, concepts for the restoration of meniscal function by implantable devices should comprise not only the ability to transmit loads but should also consider how

to mimic the low friction provided by the native meniscus. Various biomaterials with different biomechanical properties have been developed to replace the injured meniscal tissue and restore its function [13,14]. Two resorbable scaffolds (CMI® by Ivy Sports Medicine GmbH, Actifit® by Orteq Ltd.) are currently available and in clinical practice. However, Sandmann et al. showed their lack of biomechanical stability in comparison to the native meniscus within an *in vitro* study [15]. Another non-resorbable scaffold for partial meniscal replacement based on silk fibroin (FibroFix™ Meniscus, Orthox Ltd., Abingdon, UK) was recently investigated in a sheep model, showing promising results regarding biocompatibility and the prevention of OA after 6 months [16]. However, no results are currently available predicting its long-term chondroprotective function. To maintain the chondroprotective properties of a meniscal scaffold over an extended period of time, its frictional behaviour is of major importance as a high friction coefficient leads to wear, which is associated with cartilage fibrillation.

In general, friction is defined as the resistance of motion between two surfaces that are in contact. According to Coulomb, the friction force F_R is equal to the product of the friction coefficient μ and normal force F_N . Therefore, the friction coefficient is a material property and could be calculated from the quotient of friction and normal force. However, within synovial joints, friction is much more complex. This is due to the biphasic viscoelastic nature of the opposing surfaces of the meniscus and articular cartilage lubricated by synovial fluid [17].

* Corresponding author.

E-mail address: daniela.warnecke@uni-ulm.de (D. Warnecke).

<http://dx.doi.org/10.1016/j.triboint.2017.01.038>

Received 24 November 2016; Received in revised form 26 January 2017; Accepted 29 January 2017

Available online 31 January 2017

0301-679X/ © 2017 The Authors. Published by Elsevier Ltd.

This is an open access article under the CC BY license (<http://creativecommons.org/licenses/by/4.0/>).

Various studies investigated the frictional behaviour of articular cartilage [18–26]. Regarding the three lubrication modes transferred from mechanical friction analysis (i.e., fluid, boundary and mixed lubrication), numerous tribology theories were postulated to describe the remarkable frictional behaviour of articular cartilage [17,26–31]. Within these studies, it has been shown that the friction in synovial joints is multifactorial and several parameters, including applied normal load and strain, sliding speed, time and lubricant, influence the friction mode [23–26,31]. Furthermore, the opposing surface used to test friction characteristics naturally has a major effect on the friction coefficient. Glass, which was typically used in most cartilage friction studies [19,22,25,28,32], provides a smooth counter surface, but its use appears at least debatable in terms of its lack of physiological properties. Testing articular cartilage against glass leads to an increase in friction over time until an equilibrium is reached due to the biphasic, viscoelastic nature of cartilage [33]. This phenomenon is most likely attributable to interstitial fluid pressurisation within the articular cartilage [19,20,22,25,34]. It has been shown that the applied load is initially supported by the fluid phase of the biphasic cartilage, resulting in a very low friction coefficient. Under a persisting load, the load support is continuously transferred to the solid matrix, resulting in an increasing friction coefficient [22,34]. This phenomenon is typically observed in highly hydrated and biphasic tissue.

The above mentioned silk fibroin based scaffold for permanent meniscal replacement is processed into a porous matrix with a smooth surface [16]. Although its ultrastructure differs considerably from the native meniscus it showed promising results in a first *in vivo* trial in sheep [16]. Additionally, Parkes et al. demonstrated a cartilage-like friction response of silk protein hydrogels in articular cartilage repair [35]. Based on these findings, we hypothesised that the friction coefficient of the silk fibroin scaffold for meniscal replacement is comparable to physiologically articulating surfaces. We further hypothesised that glass as an opposing surface leads to higher friction coefficients not only for articular cartilage but also for meniscus and scaffold in comparison to those achieved when tested against cartilage.

2. Method

2.1. Study design

The frictional properties of the silk fibroin scaffold for meniscal replacement were determined in comparison to the physiologically articulating surfaces of meniscus and articular cartilage. Therefore, cylindrical samples were prepared from the silk fibroin scaffold as well as being retrieved from the meniscus and tibial cartilage of seven intact bovine knee joints (age: 3 months) (Fig. 1). Each cylindrical sample was first tested against a flat cartilage sample, which was also harvested



Fig. 2. Macroscopic image of the meniscal silk fibroin scaffold (FibroFix™, Orthox Ltd., Abindon, UK).

from the bovine knee joints, using a *pin-on-plate* friction-testing device. During testing, the flat opposing surface slid cyclically against the cylindrical samples, while a constant normal load of 14.6 N was applied to them, resulting in a detectable friction force. All samples were stored overnight in phosphate-buffered saline (PBS) at 4 °C for recovery and tested against glass the next day to test the second hypothesis.

2.2. Detailed procedure

2.2.1. Sample preparation

The scaffold samples used in this study were manufactured by Orthox Ltd. and consisted of a biomaterial based on the protein, fibroin, extracted from silk fibres of the mulberry silk moth *Bombyx mori*, which was subsequently processed into a porous matrix (Fig. 2). Seven scaffold samples were retrieved from 6 flat sheets (height $h_0 = 3.4 \text{ mm} \pm 0.6 \text{ mm}$) using a biopsy punch ($\phi = 6 \text{ mm}$). Seven fresh intact bovine knee joints were ordered from a local butcher and stored at -20°C . The day before testing, the joints were kept at 4°C to thaw. Cylindrical meniscus samples ($\phi = 6 \text{ mm}$) were punched out from the medial meniscus at the transition of the posterior horn and the *pars intermedia* perpendicular to the surface that was physiologically in contact with the femoral condyle. For later fixation in the friction testing apparatus, the cylindrical samples required parallel surfaces.

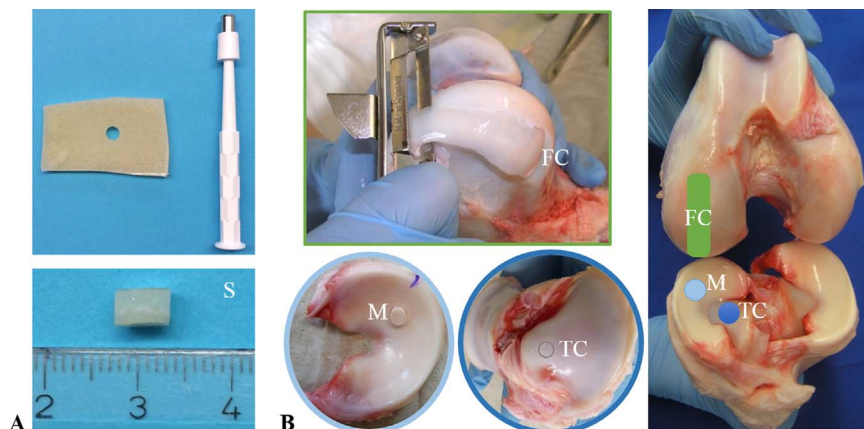


Fig. 1. Cylindrical samples were prepared from flat sheets of the silk fibroin scaffold (S) (a), as well as being retrieved from the meniscus (M) and tibial cartilage (TC) of bovine knee joints (b). Flat cartilage samples were taken from the femoral condyle (FC) serving as the opposing surface during friction testing (b).

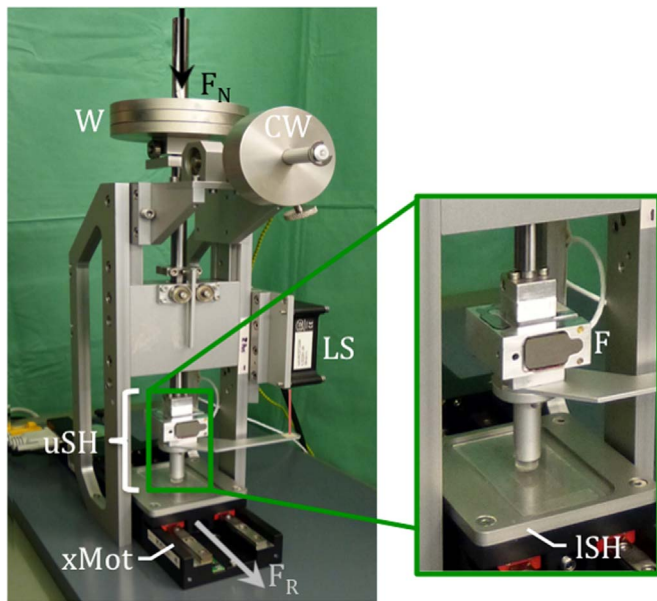


Fig. 3. Pin-on-plate friction-testing device. A constant normal load ($F_N=14.6$ N) was applied by placing weights (W) to the upper sample holder (uSH), on the end of which the cylindrical samples (meniscus M, silk fibroin scaffold S, tibial cartilage TC) were mounted. During testing, the lower sample holder (ISH) with the femoral cartilage (FC) or glass (G) sample was sliding against it, driven by a linear motor (xMot). A force sensor (F) recorded the resulting friction force F_R , while a contactless laser distance sensor (LS) additionally measured the displacement signal of the cylindrical samples. Counter-weights (CW) served as prevention for unintentional load application due to the tare weight of the testing apparatus to the cylindrical samples.

Therefore, the distal region of the meniscus, which articulates with the tibial plateau surface, was removed using a microtome, resulting in specimens 2 mm in height. In addition, cylindrical osteochondral specimens were harvested out of the medial tibial condyle at the *eminentia intercondylaris*, perpendicular to the surface, using a trephine drill ($\phi=6$ mm). The subchondral bone was removed and the cylindrical cartilage samples were cut, resulting in specimens approximately 2.5 mm in height. Flat cartilage samples were taken from each of the medial femoral condyle using a peeler ($n=7$). The flat cartilage samples served as an opposing surface during friction testing (approx. 40 mm length, 20 mm width and 2 mm height). To test the second hypothesis, an uncoated, smooth, glass microscope slide was used as the opposing surface (VWR* Plain Micro Slides, VWR International GmbH, Darmstadt, Germany). All specimens were maintained hydrated during preparation and were stored in PBS at 4 °C until testing.

2.2.2. Friction-testing apparatus

To determine the friction coefficient of the meniscal scaffold in comparison to meniscus and articular cartilage, a *pin-on-plate* friction-testing apparatus was designed (Fig. 3). It consisted of an aluminium frame with an upper specimen holder (uSH), including a custom 3 DOF load cell (F) ($F_{x,y}=\max 20$ N, $F_z=\max 50$ N; accuracy class: 0.5%; ME-Meßsysteme GmbH, Henningsdorf, Germany) and an adjustable counter-weight (CW) to prevent an unintentional load application to the small sample mounted on the uSH due to the tare weight of the testing apparatus. At the upper end of the uSH, weights (W) were placed to apply a constant axial load F_N . A computer-controlled linear motor (xMot) (M-404.4PD, Physik Instrumente PI GmbH & Co. KG, Karlsruhe, Germany) was mounted underneath the uSH carrying the sliding counter surface of femoral cartilage or glass, representing the lower sample holder (ISH).

Additionally, a contactless laser distance sensor (LS) (ILD 2220-20, MicroEpsilon, Ortenburg, Germany) was mounted on the aluminium frame, continuously recording the specimen deformation.

A custom-made LabVIEW program (LabVIEW, National Instruments, Austin, USA) was used to control the motor and for data acquisition.

2.2.3. Testing protocol

Before each test, the cylindrical samples (FibroFix™ Meniscus scaffold: S, meniscus: M, tibial cartilage: TC) were fixed in the uSH of the friction-testing apparatus in randomised order. On the first experimental day, each sample was tested against the flat femoral cartilage sample as the opposing surface.

After starting the testing software, weights of approx. 1.5 kg were placed on the uSH, inducing a constant load F_N of 14.6 N. This load corresponds to a contact pressure of 0.5 MPa, which is representative of light physiological loading conditions in quadrupeds during walking [36,37]. The lower sample was slid against the uSH for 250 cycles at a velocity of 1 mm/s with a stroke length of ± 15 mm until the equilibrium was reached, resulting in a total testing time of 125 min. During testing, the friction force F_R and normal force F_N were continuously recorded from the 3 DOF load cell at a sample rate of 100 Hz.

On day two and after a recovery time of > 12 h in PBS at 4 °C without any load application, the friction tests were repeated against glass, which was typically used as a counter surface in friction studies. The tests on both days were performed at a room temperature of approximately 20 °C and a humidity of approximately 34% using bovine synovial fluid as a lubricant. Here, special attention was paid that the samples were fully covered with lubricant throughout the entire testing period to prevent sample dehydration. Consequently, additional lubricant was provided when deemed necessary. All samples and biological materials were brought to room temperature before testing.

To evaluate the frictional behaviour, the friction coefficient at the beginning of the experiment (μ_0) and after reaching the equilibrium (μ_{eq}) as well as the strains (ϵ_0 and ϵ_{eq}) at the respective times was determined. The friction coefficients μ_0 and μ_{eq} were calculated using the quotient of the friction force F_R and normal force F_N recorded during the first and the last three cycles of the experiment, respectively. The strains were determined by dividing the deformation recorded by the LS by the initial sample height h_0 .

2.3. Lubricin analysis

After reviewing the initial friction experiments, the results indicated that the friction coefficient at equilibrium was higher for articular cartilage than for meniscus when tested against glass. We speculated that a difference in the surface structure of the two tissues may be responsible for this. Because surface lubricin has been attributed an important role in low friction of joints [26,38,39], we decided to investigate the lubricin content on the surface of the meniscus and articular cartilage of additional bovine knee joints. Cylindrical meniscal samples ($\phi=6$ mm) were taken from the anterior horn of the medial meniscus ($n=10$) while cylindrical tibial cartilage samples were obtained from both the *eminentia intercondylaris* ($n=6$) and the tibial plateau ($n=6$).

To detect the native form of bovine lubricin, 6.8 μ m cryosections of the samples were cut and stained immunohistologically using a monoclonal mouse anti-bovine lubricin antibody (clone 3A4, MD Bioproducts, Zurich, Switzerland). As a secondary antibody, biotin-conjugated anti-mouse immunoglobulin was used as well as the detection kit LSAB-universal kit (K0690, DAKO, Hamburg, Germany) with horseradish peroxidase-conjugated streptavidin, as described by the manufacturer's protocol.

To quantify the amount of lubricin, the length of the positively stained tissue surface was determined using the image analysis software AxioVision 4.8.2 (Zeiss, Oberkochen, Germany) and related to the total length of the tissue in one histological slide for each specimen.

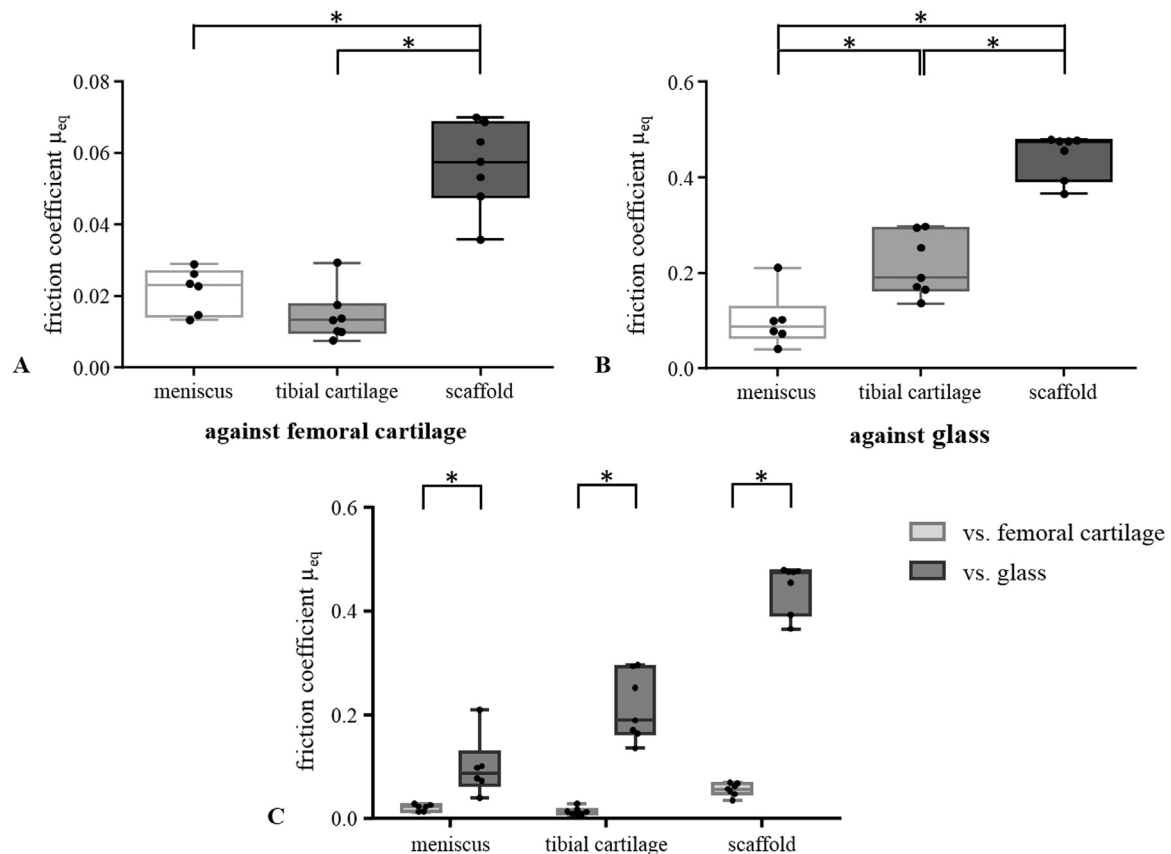


Fig. 4. Box plot with median, minimum and maximum values of the equilibrium friction coefficient μ_{eq} of all cylindrical samples (meniscus, tibial cartilage and the meniscal scaffold) obtained during testing against the femoral cartilage sample (A) and glass (B) and their comparison (C). * $p < 0.05$ $n=7$.

2.4. Statistics

All recorded and calculated friction data were classified into six groups (each $n=7$) depending on the material pairings: meniscal scaffold vs. femoral cartilage; meniscal scaffold vs. glass; native meniscus vs. femoral cartilage; native meniscus vs. glass; tibial cartilage vs. femoral cartilage; tibial cartilage vs. glass. As the friction coefficients for each group at the onset of the test (μ_0) and after reaching the equilibrium (μ_{eq}) as well as the strains at these two different time points (ε_0 and ε_{eq} , respectively) were normally distributed (normal probability plot, Shapiro-Wilk test [40]), the data were averaged. All further statistical analyses were performed using GraphPad Prism® software (GraphPad Software, Inc., La Jolla, USA).

To compare the frictional behaviour of all cylindrical samples depending on the opposing surface, one-factor analysis of variance

(ANOVA) with uncorrected Post-Hoc Fisher's LSD tests with a single pooled variance were performed. To detect differences according to the opposing surfaces as well as to obtain information on the time-dependent changes in friction coefficients, two-factor ANOVA with repeated measures were conducted. Due to the testing procedure, there were two strain values per cylindrical sample, one measured when tested against femoral cartilage and one when tested against glass. To exclude any influence of the opposing surface on the strain, the difference between each cylindrical sample according to the opposing surface was determined by performing paired t -tests.

The amounts of lubricin determined from the evaluation of the lubricin analysis were classified into three groups according to each sample's localisation: meniscus, *eminentia intercondylaris*, and tibial plateau. Because these values were normally distributed (Shapiro-Wilk test [40]) for each group, the data were averaged and the differences

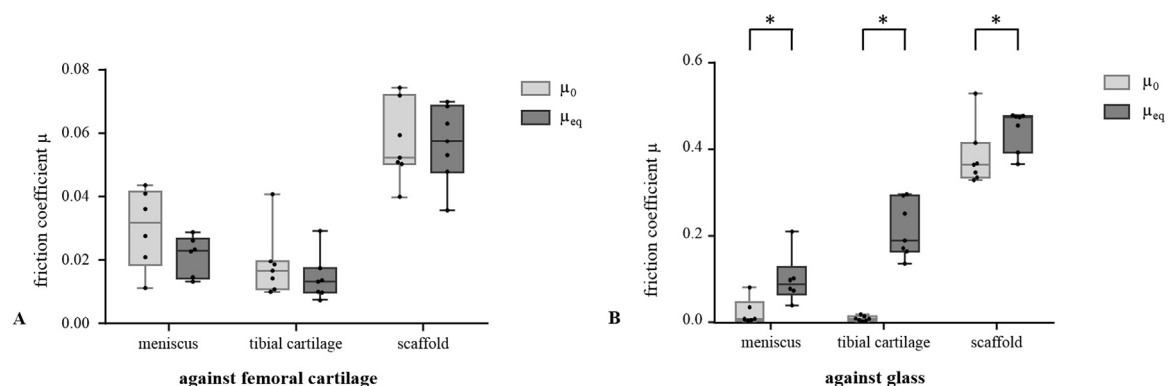


Fig. 5. Box plot with median, minimum and maximum values of the friction coefficient determined at the onset of the test μ_0 in comparison to that obtained after reaching the equilibrium μ_{eq} with femoral cartilage (A) and glass (B) as the counter surfaces. * $p < 0.05$, $n=7$.

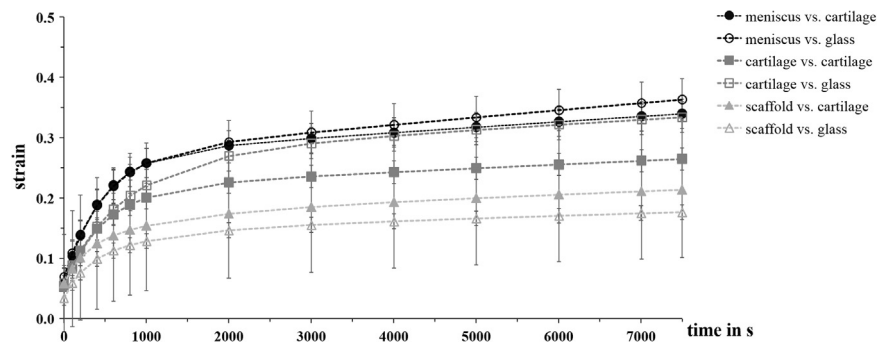


Fig. 6. Strains of all cylindrical samples (mean \pm standard deviation) tested against the flat femoral cartilage samples (filled data points) and glass (empty data points). All strain values displayed an increase with time until an equilibrium was reached, which was typical for an unconfined creep configuration.

between the three localisations were determined by an ordinary one-way ANOVA with an additional uncorrected Fisher's LSD test.

In all cases, a significance level was set at $p < 0.05$.

3. Results

3.1. Friction study

The silk fibroin scaffold reached an equilibrium friction coefficient μ_{eq} when sliding against femoral cartilage of 0.056 ± 0.012 , which was significantly higher in comparison to the physiologically articulating surfaces of both the meniscus against cartilage ($\mu_{eq} = 0.021 \pm 0.006$, $p < 0.0001$) and the cartilage against cartilage ($\mu_{eq} = 0.014 \pm 0.007$, $p < 0.0001$) (Fig. 4, A). Using glass as the opposing surface, the μ_{eq} of all material pairings were significantly higher compared to the friction coefficients obtained with the physiological counter surface (meniscus vs. glass: 0.100 ± 0.058 , $p = 0.0032$; tibial cartilage vs. glass: 0.215 ± 0.065 , $p < 0.0001$; silk fibroin scaffold vs. glass: 0.446 ± 0.047 , $p < 0.0001$) (Fig. 4, C). Additionally, with the glass as opposing surface, there was a significant difference between the pairings, with the μ_{eq} of tibial cartilage being higher compared to meniscus ($p = 0.0022$). In contrast, when using cartilage as the opposing surface, no significant difference was observed between meniscus and tibial cartilage ($p = 0.1815$) (Fig. 4, B).

For the tibial cartilage samples, the μ_{eq} increased most by almost 15 times when using glass as the opposing surface in comparison with cartilage, while for the meniscus and the replacement scaffold this increase with glass was approximately 4.5 and 8 fold higher, respectively.

The three cylindrical samples revealed no significant changes with time in comparison with the friction coefficient μ_0 determined at the experimental onset when tested against femoral cartilage (meniscus: $\mu_0 = 0.030 \pm 0.012$, $\mu_{eq} = 0.021 \pm 0.006$, $p = 0.060$; tibial cartilage: $\mu_0 = 0.019 \pm 0.010$, $\mu_{eq} = 0.014 \pm 0.007$, $p = 0.293$; silk fibroin scaffold: $\mu_0 = 0.057 \pm 0.012$, $\mu_{eq} = 0.056 \pm 0.012$, $p = 0.906$) (Fig. 5, A). In contrast, their equilibrium friction coefficient μ_{eq} was significantly increased in comparison to the initial friction coefficient μ_0 when tested against glass (meniscus: $\mu_0 = 0.023 \pm 0.030$, $p = 0.0056$; tibial cartilage: $\mu_0 = 0.009 \pm 0.006$, $p < 0.0001$, silk fibroin scaffold $\mu_0 = 0.384 \pm 0.070$, $p = 0.0131$) (Fig. 5, B).

The strains of all the cylindrical samples displayed an increase over time until an equilibrium was reached, which is a typical behaviour for biphasic materials in an unconfined creep configuration (Fig. 6). With regard to the three types of cylindrical sample, the equilibrium strain value ϵ_{eq} was lowest of the scaffold at 0.269 ± 0.178 and 0.219 ± 0.133 when tested against femoral cartilage and glass, respectively. The highest strain level at equilibrium (ϵ_{eq}) was attained by the meniscus samples at 0.339 ± 0.042 and 0.363 ± 0.034 when tested against femoral cartilage and glass, respectively. Furthermore, the strain values obtained when testing against femoral cartilage on day 1 and against

glass on day 2 did not differ significantly (meniscus: $p = 0.247$, tibial cartilage: $p = 0.200$, scaffold: $p = 0.121$).

3.2. Lubricin analysis

Approximately 80% of the meniscus surface was covered with lubricin (Fig. 7, A). Therefore, the superficial lubricin deposition on meniscus was significantly higher than on the cartilage samples from the medial tibial plateau ($p = 0.0266$) and the *eminencia intercondylaris* ($p < 0.0001$). The least lubricin was found at the tibial eminence, where $< 20\%$ of the surface was positively stained (Fig. 7, B).

4. Discussion

The silk fibroin scaffold tested in the current study exhibited equilibrium friction coefficients that were significantly different to that of physiologically articulating surfaces when tested against articular cartilage. This refutes the first hypothesis. However, the resultant friction coefficient after > 2 h testing ($\mu_{eq} = 0.056$) was still within the range of the basic requirements of tribological properties for meniscal substitutes, further elaborated by Rongen et al. [13]. Within these requirements, the friction coefficient is proposed to be as similar as possible to those of the meniscus and to be ≤ 0.05 . However, testing against glass, which was typically performed in most previous friction studies [19,22,25,28,32], led to a significant increase in the friction coefficient of meniscus ($\mu_{eq} = 0.100$), articular cartilage ($\mu_{eq} = 0.215$) and silk fibroin scaffold ($\mu_{eq} = 0.446$). Similar high friction coefficients were also demonstrated by Galley et al. for a polyurethane scaffold as a meniscal replacement when tested against glass ($\mu_{eq} \approx 0.5$) [32].

The large differences between the friction coefficients when testing against femoral cartilage and glass demonstrated in the current study are most likely attributable to the lack of pressurisation of the interstitial fluid in both non-biological tissues (i.e. the silk fibroin scaffold and the opposing glass surface) [22]. Previous studies have shown that the friction coefficient of cartilage increases with time when tested against a non-biologic material like glass from a mean of $\mu_0 = 0.01$ to $\mu_{eq} = 0.25$ [19,22–25,32]. This phenomenon results from the fluid load support, which decreases with time from almost 100% at the test onset to almost 0% once equilibrium is reached [19,20,22,34]. Assuming the tissue that bears the load is responsible for the friction, it becomes clear that the fully pressurised fluid creates the observed low friction coefficient at the time of load application. During the creep process, a continuous transfer of the load from the fluid to the solid matrix occurs with full support provided by the solid matrix after reaching equilibrium. Hence, in this state, the solid matrix is mainly responsible for the increased friction coefficient. Therefore, provided at least one of the opposing surfaces is of cartilaginous tissue, a low initial friction coefficient is achieved, which is not the case for scaffold against glass.

Nevertheless, the friction coefficient of tibial cartilage determined

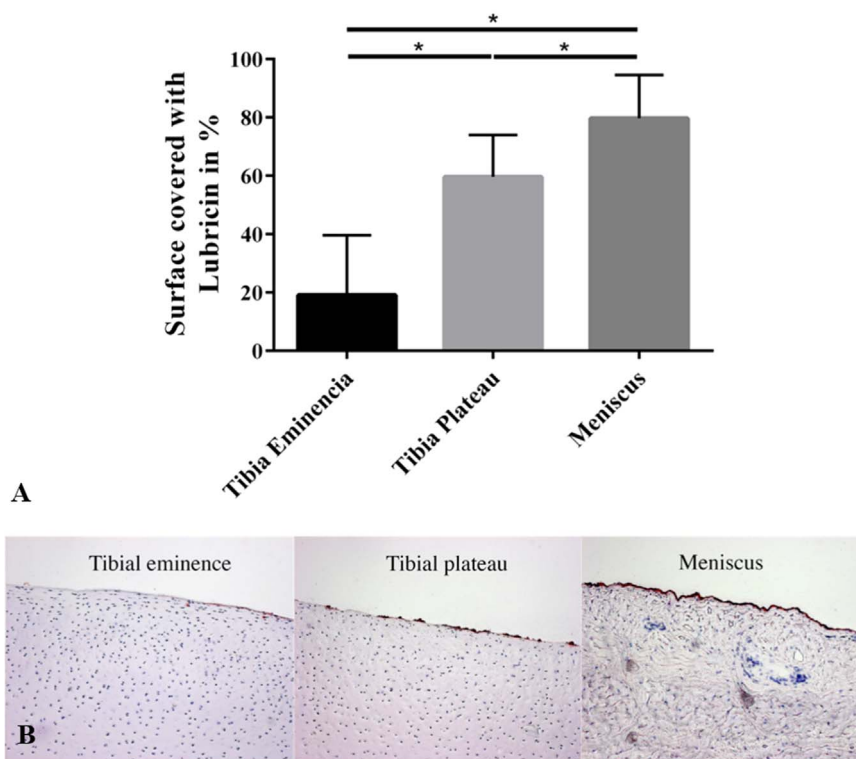


Fig. 7. Mean percentage and standard deviation of the lubricin coverage of the tissue surface of the meniscus (n=10), tibial plateau (n=6) and tibial eminence (n=5) covered with lubricin; *p < 0.05 (A) and a representative histological slide of each surface (B). Lubricin is stained in red. (For interpretation of the references to color in this figure legend, the reader is referred to the web version of this article).

in the current study against glass ($\mu_{eq}=0.215 \pm 0.065$) fits well to previously published value ranges [19,22]. This in turn emphasises the validity of the friction-testing apparatus and therefore of the results in the present study.

Interestingly, the friction coefficient resulting when cartilage was the opposing surface was always significantly less in comparison with glass as the opposing surface, which confirmed the second hypothesis. In addition, it emphasises the importance of choosing appropriate articulating surfaces to obtain relevant friction coefficients for joints. This in particular applies to the characterisation of the frictional behaviour of materials for meniscal replacement to assess whether future implants also ensure a long-term chondroprotective function.

In contrast to the friction coefficient determined when glass was the opposing surface, no increase in friction with time could be detected when the tests were performed against cartilage. This was true for both the biological tissues, cartilage and meniscus, and also for the silk fibroin scaffold. The main reason for the constant low friction was the choice of the opposing surface. The testing configuration of a flat opposing cartilage surface sliding against a constantly loaded pin allows a cyclic loading of the flat cartilage sample. While the tissue in the uSH was permanently loaded, the contact area on the opposing flat cartilage sample moved along the sample and was, therefore, loaded only for the time the upper cylindrical sample needed to pass one sample diameter. This enabled the different regions of the flat cartilage samples to recover before the pin loaded that region again and consequently no creep occurred. Due to the biphasic ultrastructure of the biological samples, the fluid phase supported the applied load during the entire experiment. Shi et al. and Caligaris et al. both demonstrated a similar constant, low friction coefficient with time for a cartilage-on-cartilage testing configuration [19,21]. Shi et al. tested an aluminium pin against a cartilage disc (AC configuration) and no increase in friction with time was detectable, as well. This AC configuration is comparable to the scaffold against cartilage configuration we tested in the present study, whereby no increase in the friction

was similarly observed. In addition, Shi et al. estimated the corresponding fluid load support, which remained >80% during the experiment. This result supports the evidence of the fluid pressurisation theory and specifically its important role in friction studies.

The meniscus samples also displayed an increase in friction with time when tested against glass, but reached a significantly reduced equilibrium friction value compared to articular cartilage. The meniscus and articular cartilage vary considerably in their extracellular matrix composition, in particular, the type of collagen and the amount of proteoglycans. While the articular cartilage is composed of collagen type II, the meniscus mainly consists of collagen type I and has only 10% of the proteoglycan content of articular cartilage [1–4]. However, when considering the friction properties, it is logical to pay closer attention to the tissue's surface properties. Therefore, we additionally assessed the lubricin content on the surface of the bovine meniscus, the articular cartilage from the *eminencia intercondylaris* and from the tibia plateau. We found that 80% of the meniscus surface was covered with lubricin. In contrast, only 60% of the tibia plateau and 20% of the *eminencia intercondylaris* were covered with lubricin. These results correlate with the lower friction coefficient of the meniscus compared to articular cartilage observed in the current study (Fig. 5, B).

4.1. Limitations

The test setup was designed according to a *pin-on-plate* configuration. Therefore, flat cartilage samples had to be harvested from the three-dimensionally convex shaped femoral condyles. Consequently, any small unevenness in the surface of the flat cartilage may have affected not only the friction force but also the strain measurements. However, the displacement signal of each cylindrical sample determined by the contactless laser distance sensor LS and the resultant strain values displayed no statistical difference when tested against cartilage or the smooth glass surface ($p \geq 0.15$).

4.2. Conclusion

The current study presents for the first time a characterisation of the frictional properties of a meniscal replacement material. The friction coefficient of a scaffold based on silk fibroin was higher compared to the physiologically articulating surfaces, but still within the range of the basic requirements for meniscal substitutes [13]. Whether this enables silk fibroin scaffold to provide a long-term chondroprotective function has to be confirmed *in vivo*. Interestingly, it could also be shown that glass as the opposing surface is not appropriate for friction testing of implants, as it produces significantly higher friction coefficients than occurring in the physiological environment. Glass may be useful to perform comparative studies on different biomaterials. However, investigating physiologically relevant friction coefficients occurring in a synovial joint requires the use of cartilage as the opposing surface.

Acknowledgements

This research was supported by the German Research Foundation [DFG DU254/7-1] and the German Armed Forces [E/U2AD/ED001/EF551].

The authors thank the Wellcome Trust [100917/Z/13/Z] and Innovate UK [101604], [102162] for supporting the scaffold development and Brunhilde Amann for her technical assistance.

References

- [1] Mow VC, Huiskes R. Structure and function of articular cartilage and meniscus. In: Mow VC, Huiskes R, editors. *Basic Orthopaedic Biomechanics & Mechano-Biology*. Third edition. Philadelphia: Lippincott Williams & Wilkins; 2005. p. 182–257.
- [2] McDermott ID, Masouros SD, Bull AM, Amis AA. Anatomy. In: Beaufils P, Verdonk R, editors. *The Meniscus*. Heidelberg, New York: Springer-Verlag; 2010. p. 11–8.
- [3] Brindle T, Nyland J, Johnson DL. The meniscus: review of basic principles with application to surgery and rehabilitation. *J Athl Train* 2001;36:160–9.
- [4] Masouros SD, McDermott ID, Amis AA, Bull AM. Biomechanics of the meniscus-meniscal ligament construct of the knee. *Knee Surg Sports Trauma Arthrosc* 2008;16:1121–32.
- [5] Masouros SD, McDermott ID, Bull AM, Amis AA. Biomechanics. In: Beaufils P, Verdonk R, editors. *The Meniscus*. Heidelberg, New York: Springer-Verlag; 2010. p. 29–37.
- [6] Lee SJ, Aadalen KJ, Malaviya P, Lorenz EP, Hayden JK, Farr J, et al. Tibiofemoral contact mechanics after serial medial meniscectomies in the human cadaveric knee. *Am J Sports Med* 2006;34:1334–44.
- [7] Kutzner I, Heinlein B, Graichen F, Bender A, Rohlmann A, Halder A, et al. Loading of the knee joint during activities of daily living measured *in vivo* in five subjects. *J Biomech* 2010;43:2164–73.
- [8] Majewski M, Susanne H, Klaus S. Epidemiology of athletic knee injuries: a 10-year study. *Knee* 2006;13:184–8.
- [9] Fairbank TJ. Knee joint changes after meniscectomy. *J Bone Jt Surg Br* 1948;30B:664–70.
- [10] Seitz AM, Lubomierski A, Friemert B, Ignatius A, Dürselen L. Effect of partial meniscectomy at the medial posterior horn on tibiofemoral contact mechanics and meniscal hoop strains in human knees. *J Orthop Res* 2012;30:934–42.
- [11] Baratz ME, Fu FH, Mengato R. Meniscal tears: the effect of meniscectomy and of repair on intraarticular contact areas and stress in the human knee. A preliminary report. *Am J Sports Med* 1986;14:270–5.
- [12] McCann L, Ingham E, Jin Z, Fisher J. Influence of the meniscus on friction and degradation of cartilage in the natural knee joint. *Osteoarthritis Cartil* 2009;17:995–1000.
- [13] Rongen JJ, van Tienen TG, van Bochove B, Grijpma DW, Buma P. Biomaterials in search of a meniscus substitute. *Biomaterials* 2014;35:3527–40.
- [14] Warth RJ, Rodkey WG. Resorbable collagen scaffolds for the treatment of meniscus defects: a systematic review. *Arthroscopy* 2015;31:927–41.
- [15] Sandmann GH, Adamczyk C, Grande Garcia E, Doebele S, Buettner A, Milz S, et al. Biomechanical comparison of menisci from different species and artificial constructs. *BMC Musculoskelet Disord* 2013;14:324.
- [16] Gruchenberg K, Ignatius A, Friemert B, von Lubken F, Skaer N, Gellynck K, et al. *In vivo* performance of a novel silk fibroin scaffold for partial meniscal replacement in a sheep model. *Knee Surg Sports Trauma Arthrosc* 2015;23:2218–29.
- [17] Ateshian GA, Mow VC. Friction, lubrication, and wear of articular cartilage and diarthrodial joints. In: Mow VC, Huiskes R, editors. *Basic Orthopaedic Biomechanics & Mechano-Biology*. Third edition. Philadelphia: Lippincott Williams & Wilkins; 2005. p. 447–93.
- [18] McCann L, Udofia I, Graindorge S, Ingham E, Jin Z, Fisher J. Tribological testing of articular cartilage of the medial compartment of the knee using a friction simulator. *Tribol. Int* 2008;41:1126–33.
- [19] Caligaris M, Ateshian GA. Effects of sustained interstitial fluid pressurization under migrating contact area, and boundary lubrication by synovial fluid, on cartilage friction. *Osteoarthritis Cartil* 2008;16:1220–7.
- [20] Soltz MA, Ateshian GA. Experimental verification and theoretical prediction of cartilage interstitial fluid pressurization at an impermeable contact interface in confined compression. *J Biomech* 1998;31:927–34.
- [21] Shi L, Sikavitsas VI, Striolo A. Experimental friction coefficients for bovine cartilage measured with a pin-on-disk tribometer: testing configuration and lubricant effects. *Ann Biomed Eng* 2011;39:132–46.
- [22] Krishnan R, Kopacz M, Ateshian GA. Experimental verification of the role of interstitial fluid pressurization in cartilage lubrication. *J Orthop Res* 2004;22:565–70.
- [23] Forster H, Fisher J. The influence of loading time and lubricant on the friction of articular cartilage. *Proc Inst Mech Eng H* 1996;210:109–19.
- [24] Forster H, Fisher J. The influence of continuous sliding and subsequent surface wear on the friction of articular cartilage. *Proc Inst Mech Eng H* 1999;213:329–45.
- [25] Gleghorn JP, Bonassar LJ. Lubrication mode analysis of articular cartilage using Stribeck surfaces. *J Biomech* 2008;41:1910–8.
- [26] Jahn S, Seror J, Klein J. Lubrication of articular cartilage. *Annu Rev Biomed Eng* 2016;18:235–58.
- [27] McCutchen CW. The frictional properties of animal joints. *Wear* 1962;5:1–17.
- [28] Walker PS, Dowson D, Longfield MD, Wright V. "Boosted lubrication" in synovial joints by fluid entrapment and enrichment. *Ann Rheum Dis* 1968;27:512–20.
- [29] Medley JB, Dowson D, Wright V. Transient elastohydrodynamic lubrication models for the human ankle joint. *Eng Med* 1984;13:137–51.
- [30] Hou JS, Mow VC, Lai WM, Holmes MH. An analysis of the squeeze-film lubrication mechanism for articular cartilage. *J Biomech* 1992;25:247–59.
- [31] Neu CP, Komvopoulos K, Reddi AH. The interface of functional biotribology and regenerative medicine in synovial joints. *Tissue Eng Part B Rev* 2008;14:235–47.
- [32] Galley NK, Gleghorn JP, Rodeo S, Warren RF, Maher SA, Bonassar LJ. Frictional properties of the meniscus improve after scaffold-augmented repair of partial meniscectomy: a pilot study. *Clin Orthop Relat Res* 2011;469:2817–23.
- [33] Mow VC, Kuei SC, Lai WM, Armstrong CG. Biphasic creep and stress relaxation of articular cartilage in compression? Theory and experiments. *J Biomech Eng* 1980;102:73–84.
- [34] Ateshian GA. The role of interstitial fluid pressurization in articular cartilage lubrication. *J Biomech* 2009;42:1163–76.
- [35] Parkes M, Myanr C, Dini D, Cann P. Tribology-optimised silk protein hydrogels for articular cartilage repair. *Tribol. Int* 2015;89:9–18.
- [36] Pickard J, Ingham E, Egan J, Fisher J. Investigation into the effect of proteoglycan molecules on the tribological properties of cartilage joint tissues. *Proc Inst Mech Eng H* 1998;212:177–82.
- [37] Taylor WR, Ehrig RM, Heller MO, Schell H, Seebeck P, Duda GN. Tibio-femoral joint contact forces in sheep. *J Biomech* 2006;39:791–8.
- [38] Jay GD, Torres JR, Rhee DK, Helminen HJ, Hyttinen MM, Cha CJ, et al. Association between friction and wear in diarthrodial joints lacking lubricin. *Arthritis Rheum* 2007;56:3662–9.
- [39] Peng G, McNary SM, Athanasiou KA, Reddi AH. The distribution of superficial zone protein (SZP)/lubricin/PRG4 and boundary mode frictional properties of the bovine diarthrodial joint. *J Biomech* 2015;48:3406–12.
- [40] Shapiro SS, Wilk MB. An Analysis of Variance Test for Normality (Complete Samples). 52; 1965. p. 591–611.

8.3. Manuscript 3

WARNECKE D, MEßEMER M, DE ROY L, STEIN S, GENTELINI C, WALKER R, SKAER N, IGNATIUS A, DÜRSELEN L. Articular cartilage and meniscus reveal higher friction in swing phase than in stance phase under dynamic gait conditions. Sci Rep 2019; 9: 5785. DOI: 10.1038/s41598-019-42254-2.

Open access



Creative Commons Attribution License 4.0 International (CC BY 4.0,
<http://creativecommons.org/licenses/by/4.0/>)

DW carried out all mechanical tests and evaluations as well as the statistical analyses. Additionally, DW drafted the manuscript.

SCIENTIFIC REPORTS

OPEN

Articular cartilage and meniscus reveal higher friction in swing phase than in stance phase under dynamic gait conditions

Daniela Warnecke¹ , Maxi Meßmer¹, Luisa de Roy¹, Svenja Stein¹, Cristina Gentilini², Robert Walker², Nick Skaer², Anita Ignatius¹ & Lutz Dürselen¹ 

Most previous studies investigated the remarkably low and complex friction properties of meniscus and cartilage under constant loading and motion conditions. However, both load and relative velocity within the knee joint vary considerably during physiological activities. Hence, the question arises how friction of both tissues is affected by physiological testing conditions occurring during gait. As friction properties are of major importance for meniscal replacement devices, the influence of these simulated physiological testing conditions was additionally tested for a potential meniscal implant biomaterial. Using a dynamic friction testing device, three different friction tests were conducted to investigate the influence of either just varying the motion conditions or the normal load and also to replicate the physiological gait conditions. It could be shown for the first time that the friction coefficient during swing phase was statistically higher than during stance phase when varying both loading and motion conditions according to the physiological gait pattern. Further, the friction properties of the exemplary biomaterial were also higher, when tested under dynamic gait parameters compared to static conditions, which may suggest that static conditions can underestimate the friction coefficient rather than reflecting the *in vivo* performance.

The fibro-cartilaginous menisci play a decisive role within the knee joint. Due to its semi-lunar shape and wedge-shape cross section, it increases the contact area between the incongruent articulating surfaces of femur and tibia, thereby homogenising the load distribution within the joint^{1–4}. Additionally, it is involved in joint stabilisation, nutrient distribution and lubrication^{1–3,5,6}. Due to the high loads up to 3 times bodyweight (BW)^{7,8}, which are transmitted through the menisci, it is prone to injuries. Here, the gold standard therapy is still a (partial) meniscectomy, although it has been shown that this can lead to cartilage degeneration in the long-term due to both an increase in contact pressure and a greater friction^{9–13}. Consequently, there is an increased need for treatment strategies to restore and/or replace the meniscus. Among different research approaches, it is not yet possible to replace meniscal tissue by a material that exhibits both satisfying mechanical and tribological performance^{14–16}. Here, it is stated in the literature that the tribological properties should mimic that of the native tissue as close as possible, thereby friction coefficients less than 0.05 are desirable for a well-functioning replacement material¹⁷. We recently reported friction coefficients of around 0.056 of a silk fibroin scaffold for partial meniscal replacement, which is in the range of the requirements for meniscal replacements postulated by Rongen *et al.*^{17,18}.

The knee as a synovial/diarthrodial joint is a complex biological and mechanical system, which allows articulation and movement over millions of load cycles during a lifespan of more than 80 years¹⁹. This is granted by unique lubrication mechanisms provided by articular cartilage, menisci and synovial fluid and their special biphasic ultrastructure^{1,3,4,20–23}. In general, meniscus and cartilage consist of a fluid (water; 70–85%) and a solid phase, which is composed of a highly specialized extracellular matrix in each of these tissues¹. Both native forms of the tissues exhibit remarkably low friction coefficients of partly less than 0.01^{12,18,23,24}, which are, however, complex as they depend on a variety of parameters, like a variation over time, lubricant, sliding velocity, applied normal load and opposing surface^{19,25–27}. Nevertheless, most previous studies investigated cartilage and

¹Institute of Orthopaedic Research and Biomechanics, Centre for Trauma Research Ulm, Ulm University Medical Centre, Ulm, Germany. ²Orthox Ltd., Abingdon, UK. Correspondence and requests for materials should be addressed to D.W. (email: daniela.warnecke@uni-ulm.de)

meniscus friction under constant normal loading conditions and sliding velocities ranging from 0.02–4 MPa and 0.1–50 mm/s, respectively^{18,23,25,26,28,29}. Based on these static testing conditions and on the three lubrication modes (boundary-, mixed- and fluid lubrication), tribological theories were postulated to describe the low friction properties^{19,28–33}. But taking into account that during gait the tibiofemoral contact loads acting parallel to the tibial axis (axial load)³⁴ as well as the velocity of femoral and tibial surfaces relative to each other vary considerably^{35–37}, it is obvious that the testing conditions used so far do not reflect the conditions typically occurring *in vivo*^{18,19,28–33}. In general, a gait cycle of one leg can be divided into a stance phase (60%) initiated by heel strike and terminated by toe-off and a swing phase (40%), respectively. The tibiofemoral contact forces differ considerably between both phases. While a double-peak loading characteristic of 2–3 times BW occur within stance phase, the loads during swing phase are much lower^{34,38,39}. Simultaneously, the surfaces of femur, meniscus and tibia move relative to each other. During stance phase the knee flexion angle increases from 0° at heel strike to a maximum of 15°, while during swing phase the flexion angle rises to approximately 60°^{34–38}. This results in relative velocities between the articulating surfaces of 150 mm/s in average during stance- and up to 300 mm/s during swing phase^{19,35}, which is far beyond the velocities that were typically used in previous friction studies. To the best of our knowledge, there are only two studies assessing the friction of the physiologically articulating surfaces and a meniscal replacement material under sinusoidal²⁷ or simulated physiological loading conditions of the knee joint, respectively¹⁶. However, both used constant sliding velocities of 1 mm/s²⁷ and 4 mm/s¹⁶, which were not in the range of physiological velocities in the knee joint^{35,36}. Consequently, there is a lack of information in literature regarding the influence of both continuously varying the sliding velocity and simultaneously varying loading and motion conditions according to a gait cycle on friction coefficient of articular surfaces. Thus, the aim of this study was first to investigate the friction properties of the articulating surfaces within the knee joint – meniscus and articular cartilage – under testing conditions characteristically occurring within the joint during walking and second, to examine the influence of these simulated physiological testing conditions also on a potential biomaterial for meniscal replacement and therefore making possible predictions regarding its chondroprotective effect *in vivo*. Therefore, a dynamic friction testing device was developed in a *pin-on-plate* testing configuration applying normal, gait-related loading and motion conditions derived from stance- and swing phase to material pairings of articular cartilage, meniscus and a silk fibroin based hydrogel scaffold. To quantify the friction properties, the friction coefficient μ was identified throughout the tests.

Material and Methods

Sample preparation. Ten fresh bovine knee joints were ordered from a local butcher and frozen at -20°C until the day before testing. After thawing for 1 day at 4°C , the knees joints were examined in terms of integrity and dissected according to our standard protocol. Cylindrical meniscus and cartilage as well as the flat cartilage samples were harvested out of each knee joint as previously described within the static friction study of the silk fibroin scaffold using a trephine drill or a biopsy punch ($\varnothing = 6\text{ mm}$) and a peeler, respectively¹⁸. As an additional testing material, ten cylindrical samples were punched out of flat sheets (initial height: $4.9 \pm 0.2\text{ mm}$) of material for meniscal replacement (FibroFix Meniscus, Orthox Ltd.) using a 6 mm biopsy punch, as well.

Dynamic friction testing device. To investigate the frictional behaviour of the different material pairings under physiological testing conditions, a dynamic materials testing machine (ElectroForce 5500, including a 1 DOF load cell, 200 N, accuracy class $\leq 1\%$, WMC-50-456, both BOSE/TA Instruments, New Castle, USA) was equipped with a linear motor (linear stage VT-75, PI miCos GmbH, Eschbach, Germany) mounted on a customized aluminium frame (Fig. 1). The aluminium frame comprised four linear guidances, an intermediate plate, a ball cushion, a *pin* sample holder and a second load cell for measuring the resultant friction force F_f (3 DOF, maximum $F_{x,y} = 20\text{ N}$, maximum $F_z = 50\text{ N}$; accuracy class: 0.5%; ME-Meßsysteme GmbH, Henningsdorf, Germany). Additional counter weights were installed to prevent any load application to the *pin* due to the tare weight of the frame. The linear motor, carrying the flat cartilage sample within a sample well, moved the *plate* sample holder in reciprocating manner.

Next to quasi-static testing conditions, the dynamic materials testing machine provided dynamic, freely configurable load application profiles to the *pin*. Using this feature, it was possible to generate loading conditions acting in the knee joint during normal level walking at a physiological walking speed of 5 km/h. Hence, a double-peak loading regime was applied representing the stance phase ($p_{\max,1} \cong 0.9\text{ MPa}$, $p_{\max,2} \cong 0.8\text{ MPa}$) followed by a low load plateau ($p \cong 0.2\text{ MPa}$) simulating the swing phase in the knee joint³⁴. Simultaneously, the stage motor, driven in a position controlled mode, followed up the distances that were ran over during both phases of a gait cycle in a defined period of time of 1.1 s. The input data were defined by assuming a constant radius of the femoral condyles of $r = 25\text{ mm}$ as well as 15° and 60° as the maximum flexion angles during stance and swing phase, respectively. The resultant stroke lengths of 6 mm for stance- and 25 mm for swing phase were calculated using the radian measure (1).

$$b = \pi r \frac{\alpha}{180} \quad (1)$$

To ensure that both actuators, the linear motor and dynamic materials testing machine, were moving synchronously, every simulated gait cycle a trigger signal was sent by the dynamic materials testing machine to a custom-made LabVIEW program (LabVIEW, National Instruments, Austin, USA). This software was developed to control the linear motor and processes these signals for data acquisition, whereby the applied normal force F_N and the resultant friction force F_f were continuously recorded (sample rate: 100 Hz) to determine the friction coefficient μ (2).

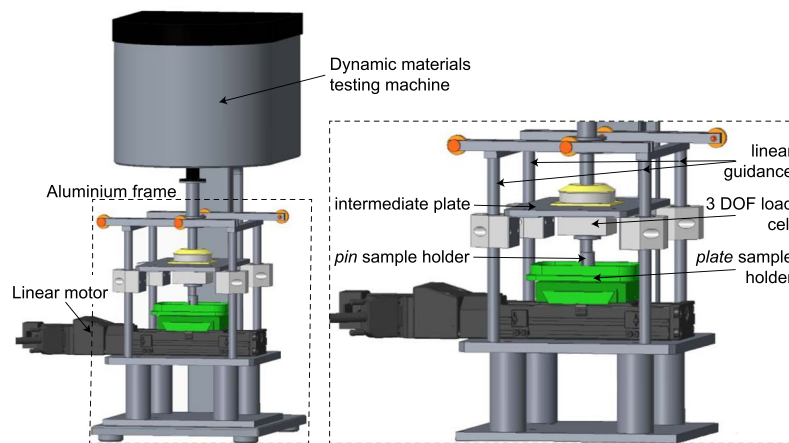


Figure 1. Dynamic friction testing device consisting of a dynamic materials testing machine (ElectroForce 5500, including a 1 DOF load cell, 200 N, accuracy class $\leq 1\%$, WMC-50-456, both BOSE/TA Instruments, New Castle, USA) equipped with a linear motor (linear stage VT-75, PI miCos GmbH, Eschbach, Germany), which was mounted on an additional aluminium frame (left). This frame was designed out of four linear guidance, an intermediate plate, a ball cushion (not shown in detail), the pin sample holder, a second load cell for measuring the resultant friction force F_F (3 DOF, maximum $F_{x,y} = 20$ N, maximum $F_z = 50$ N; accuracy class: 0.5%; ME Meßsysteme GmbH, Henningsdorf, Germany) (right) and additional counter weights (not shown).

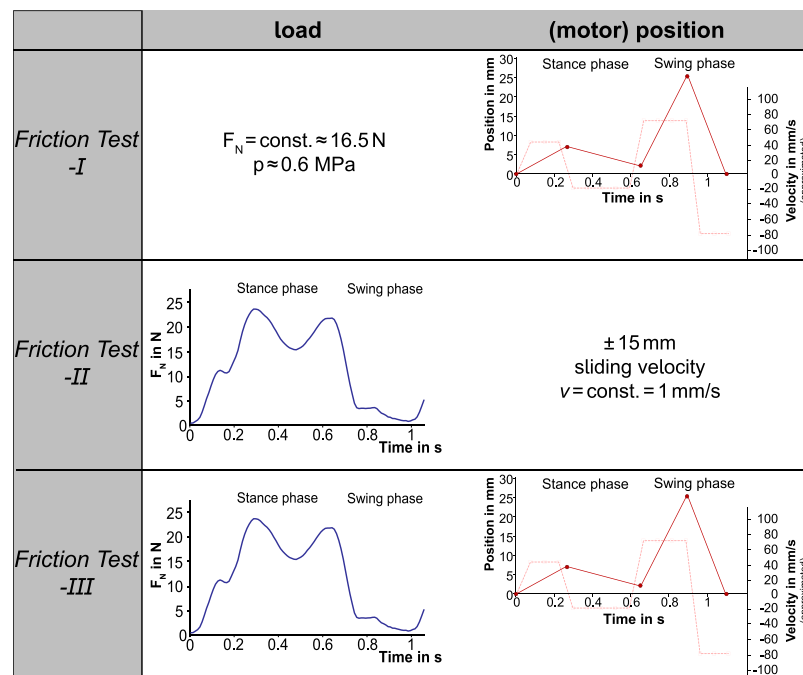


Figure 2. Overview of the three friction test scenarios and the resultant applications of load (F_N) and motion: (motor) position and the approximated velocity in mm/s.

$$\mu = \frac{F_F}{F_N} \quad (2)$$

Testing protocol. As the current study is the first synchronously applying loading and motion conditions typically occurring in the knee joint during stance- and swing phase to the mentioned friction pairings, the influence of just varying normal load F_N or velocity v on their friction properties should be additionally addressed. Therefore, the testing protocol was divided into three test scenarios (FT-I, -II, -III) conducted on three consecutive days (Fig. 2).

Based on the literature showing a decrease in the friction coefficient of articular cartilage when the testing velocity exceeds 50 mm/s^{14,26}, on the first experimental day, each cylindrical sample (meniscus M, tibial cartilage TC and FibroFix Meniscus scaffold S) was tested against the corresponding flat femoral cartilage sample (FC) under constant axial loading conditions ($p = 0.5\text{--}0.6$ MPa, acc. to¹⁸) and varying velocities according to stance- and swing phase of a human gait cycle with a physiological walking speed of 5 km/h (Fig. 2: FT-I).

To validate the dynamic friction testing device with the literature especially with the two studies investigating cartilage and/or meniscus friction as well as the friction properties of a potential material for meniscal replacement^{16,27}, a second friction test (FT-II) was added to the testing protocol. Here, the sliding velocity of the *plate* was kept constant (1 mm/s) as previously done¹⁸ and the load application to the *pin* (F_N) varied cyclically according to the double-peak loading regime acting during stance phase followed by a low plateau simulating the swing phase of a gait cycle (Fig. 2: FT-II).

The third friction test (FT-III) combined both dynamic load and motion application to test the material pairings under conditions best resembling normal gait (Fig. 2: FT-III).

This resulted in a total of three tests per friction pairing (e.g. TC1/M1/S1 vs. FC1) each with a testing duration set to 20 minutes. Throughout the whole testing period, special attention was paid that all samples had the same recovery time without any load application once between each test within a test scenario (FT-I, -II, -III) but also between the test scenarios themselves (>12 h in PBS at 4 °C). The tests were performed at room temperature of approximately 24 °C and a humidity of approximately 21%. Ovine synovial fluid aspirated from skeletally healthy knee joints directly after slaughtering, served as a lubricant. Throughout the testing period, care was taken that the samples were fully covered with lubricant.

Statistics. The friction coefficient μ ($\mu = F_f/F_N$) was determined at the onset (μ_0) and at the end of the testing duration of 20 minutes (μ_{end}) using a customized MATLAB script. (MATLAB R2013b, The MathWorks Inc., Natick, USA.). Therefore, μ of the first and last three simulated gait cycles were averaged for μ_0 and μ_{end} , respectively, each additionally separated for stance- and swing phase.

Based on the previous static friction study¹⁸, a power analysis was performed to detect differences in the friction coefficient between the friction pairings (M, TC, S vs. FC) using G*Power⁴⁰. A total sample size of 5 was calculated to get an actual power of 0.99. Due to the complexity of the defined testing protocol, the maximum calculated samples size was doubled leading to a final total samples size of $n = 10$.

All further statistical analyses were performed using GraphPad Prism[®] software (GraphPad Software Inc., La Jolla, USA).

1. The effect of the testing duration on the friction coefficient (here the comparison of μ_0 and μ_{end}) of the different friction pairings (M, TC, S vs. FC) within each specific test scenario (FT-I, -II, -III), were evaluated using repeated measures one-way Analyses of Variances (ANOVA) with Sidak's post hoc test for multiple comparison, if the data were normally distributed. Otherwise, the nonparametric Friedman test with Dunn's post hoc test for multiple comparison were conducted.
2. To determine differences in the friction coefficient of stance- and swing phase due to the different load patterns in the test scenarios (FT-I vs. FT-II vs. FT-III) for each friction pairing (M, TC, S vs. FC), one-way ANOVAs with Sidak's post hoc test for multiple comparison were performed, if the data were normally distributed. Otherwise, the nonparametric Friedman test with Dunn's post hoc test for multiple comparison were conducted.
3. To compare the friction coefficients of stance- and swing phase between the friction pairings (M, TC, S vs. FC) for each test scenario (FT-I, -II, -III), mixed-effects analysis (REML) with Tukey's post hoc test for multiple comparison were accomplished.

The statistical significance level was set to $p < 0.05$.

Results

A summary of all friction coefficients (μ_0 and μ_{end}) obtained during the three test scenarios (FT-I, -II, -III) separated for both phases of a gait cycle, stance- and swing phase as well as for the friction pairings: tibial cartilage (TC), meniscus (M) and the silk fibroin scaffold (S) each against a flat, femoral cartilage sample (FC) are given in Table 1 as mean \pm standard deviation (SD). Here, the three different test scenarios were established to determine the influence of only varying the sliding velocity (FT-I) or normal force F_N (FT-II) according to the motion and loading conditions during gait, and finally the combination of both as the most physiological friction test (FT-III).

The evaluation of the friction coefficient revealed no time-dependent differences (μ_0 vs. μ_{end}) for each material pairing (M, TC or S vs. FC). This was also true for each of the three test scenarios (FT-I, -II, -III; Fig. 3). Consequently, all other analyses and comparisons were performed using the friction coefficient determined after 20 minutes testing (μ_{end}).

No differences between the friction coefficients obtained during simulated stance- and swing phase could be found for both cartilaginous tissues, meniscus and tibial cartilage, each tested against flat cartilage samples when varying only the velocity (FT-I) or normal load (FT-II). Interestingly, this changed as soon as both testing parameters synchronously varied as it occurs during a physiological gait cycle (FT-III). Here, the simulated low-loaded swing phase revealed significantly higher friction coefficients than the stance phase (Fig. 3, left and central column). Additionally, the friction coefficient of meniscus against cartilage (M vs. FC) was highest for FT-III (0.030 ± 0.008) during swing phase in comparison to the other two load scenarios (FT-I and -II, 0.017 ± 0.006 and 0.017 ± 0.012 , respectively), while during stance phase no differences in friction could be found for each of the three different test scenarios ($p \leq 0.05$; Fig. 4b). However, the cartilage against cartilage pairing remained in general uninfluenced by the different load scenarios for both, stance- and swing phase (Fig. 4a). The silk fibroin

FT-I	TC vs. FC		M vs. FC		S vs. FC	
	Stance- &	swing phase	Stance- &	swing phase	Stance- &	swing phase
μ_0	0.022 ± 0.012	0.025 ± 0.010	0.019 ± 0.008	0.017 ± 0.005	0.034 ± 0.013	0.036 ± 0.014
μ_{end}	0.018 ± 0.005	0.024 ± 0.009	0.020 ± 0.006	0.017 ± 0.006	0.036 ± 0.011	0.038 ± 0.009
FT-II						
μ_0	0.021 ± 0.013	0.027 ± 0.018	0.026 ± 0.024	0.030 ± 0.028	0.077 ± 0.041	0.122 ± 0.058
μ_{end}	0.013 ± 0.010	0.019 ± 0.021	0.015 ± 0.010	0.017 ± 0.012	0.061 ± 0.034	0.092 ± 0.046
FT-III						
μ_0	0.018 ± 0.005	0.032 ± 0.013	0.015 ± 0.009	0.033 ± 0.007	0.042 ± 0.017	0.043 ± 0.021
μ_{end}	0.019 ± 0.005	0.029 ± 0.009	0.016 ± 0.007	0.030 ± 0.008	0.057 ± 0.019	0.047 ± 0.020

Table 1. Summary of all friction coefficients (mean \pm standard deviation) obtained during the three different test scenarios: FT-I ($F_N = \text{const.}$, v acc. to gait cycle), -II (F_N acc. to gait cycle, $v = \text{const.}$) and -III (F_N and v acc. to gait cycle) for the friction pairings: tibial cartilage (TC), meniscus (M) and the silk fibroin scaffold (S) each against a flat, femoral cartilage sample (FC).

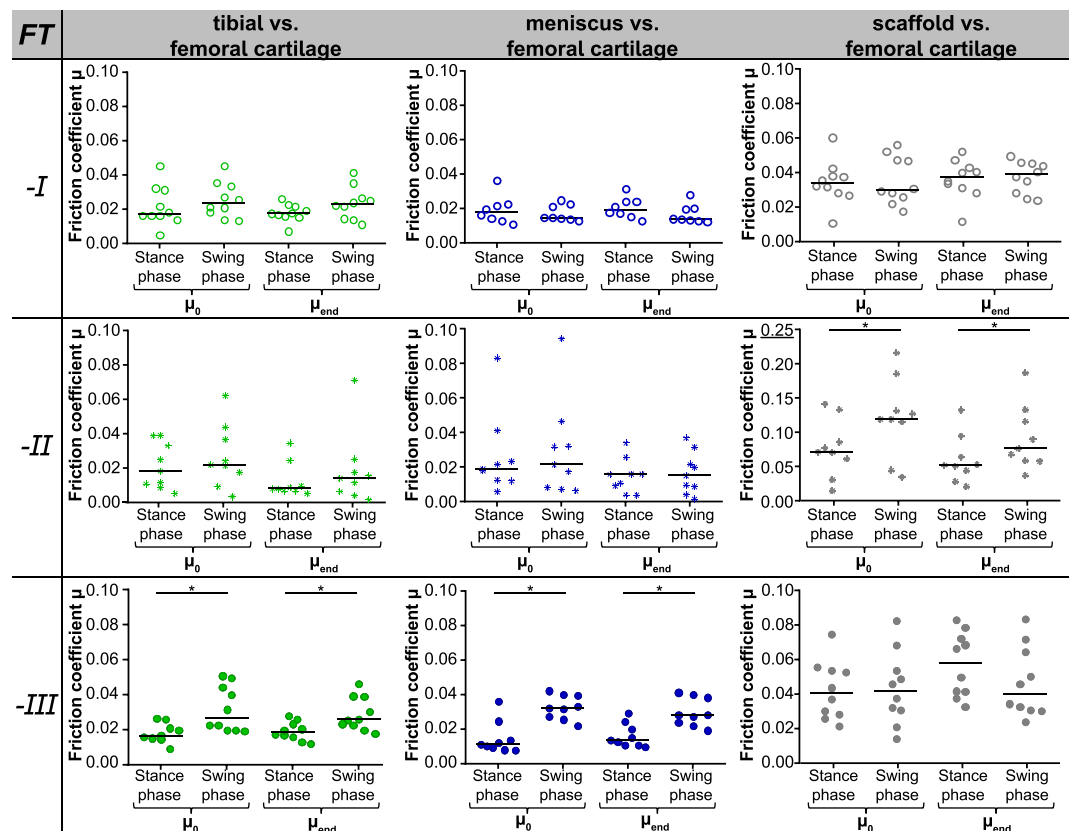


Figure 3. Comparison of the friction coefficients (median with raw data) for each material pairing (M, TC, S vs. FC, divided by column) obtained in the three different friction test scenarios (FT-I: $F_N = \text{const.}$, v acc. to gait cycle, FT-II: F_N acc. to gait cycle, $v = \text{const.}$, FT-III: F_N and v acc. to gait cycle, divided by rows). * $p \leq 0.05$ with a minimum actual power of 70.1% (FT-II scaffold vs. femoral cartilage).

scaffold tested against cartilage showed in general higher friction coefficients under FT-II conditions (averaged stance phase: $\mu = 0.069 \pm 0.011$ and swing phase: $\mu = 0.107 \pm 0.021$; Fig. 3, right column), which was additionally statistically significant in comparison to FT-I and FT-III (0.038 ± 0.009 and 0.047 ± 0.020 , respectively) during swing phase (Fig. 4c).

Testing the material pairings either under constant loads but varying velocities (FT-I) or inversely varying the normal forces F_N according to the loading conditions during normal walking at 5 km/h but maintaining a constant velocity (1 mm/s, FT-II), the silk fibroin scaffold revealed the highest friction coefficients in comparison to tibial cartilage- and meniscus samples, for both, stance- and swing phase, respectively (Fig. 5a,b). This was also true during stance phase when testing under simulated physiological loading and motion conditions (FT-III, Fig. 5c). Even though, the scaffold showed a higher friction coefficient by tendency also during swing phase, no

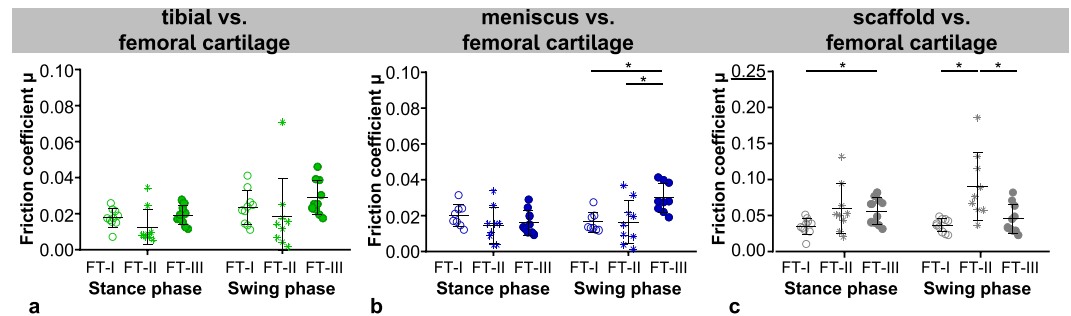


Figure 4. Comparison of the friction coefficients (μ_{end}) obtained for each material pairing: tibial cartilage (a), meniscus (b) and scaffold (c) each against femoral cartilage within the three different friction test scenarios ($n = 8-10$, mean \pm standard deviation and raw data; \circ FT-I, \ast FT-II, \bullet FT-III), $\ast p \leq 0.05$ with a minimum actual power of 96.1% and 73.1% for the comparisons the meniscus and scaffold friction coefficient, respectively.

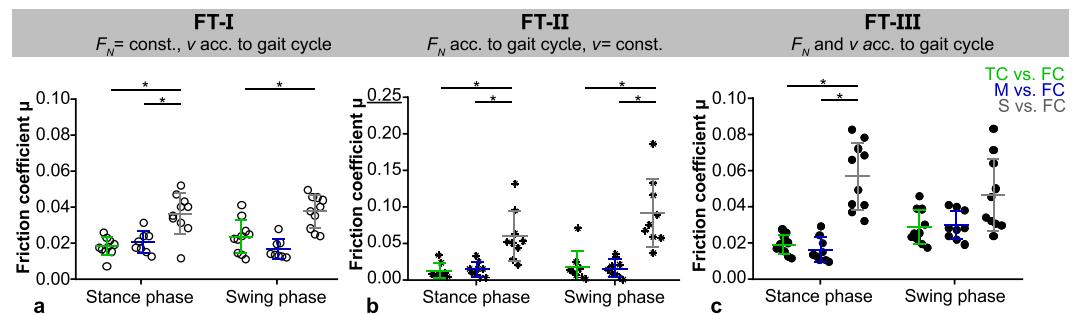


Figure 5. Comparison of the friction coefficients (μ_{end}) obtained within each friction test scenarios (\circ FT-I: A, \ast FT-II: B, \bullet FT-III: C) for the different material pairings (TC, M, S vs. FC; $n = 8-10$, mean \pm standard deviation and raw data) $\ast p \leq 0.05$ with an actual power of approximately 99%.

statistical differences were detected. The friction coefficient of meniscus and tibial cartilage each against femoral cartilage did not differ statistically during all three test scenarios.

Discussion

For the first time we were able to assess friction coefficients of the articulating surfaces of the knee joint, meniscus and articular cartilage, under simulated physiological loading and motion conditions occurring during normal walking. Additionally, a silk fibroin scaffold was used for testing to investigate the influence of these new testing conditions on a potential material for meniscal replacement.

When tested under physiological testing conditions (FT-III), the friction coefficients for both cartilaginous tissues, tibial cartilage and meniscus, each tested against cartilage (TC/M vs. FC) were higher during the low-loaded swing phase (TC vs. FC: 0.029 ± 0.009 , M vs. FC: 0.030 ± 0.008) than during the high-loaded stance phase (TC vs. FC: 0.019 ± 0.005 , M vs. FC: 0.016 ± 0.007). Although this phenomenon appears contradictory, Majd *et al.* and Krishnan *et al.* showed an increase in friction within low-loaded phases, as well^{16,27}. Krishnan *et al.* simultaneously detected negative values of the fluid load support W^p/W of less than -1.75^{27} and consequently made the assumption that suction might occur between the cartilage and the counter glass platens^{16,27}. This additionally led to an increased solid-to-solid contact force, resulting in higher friction coefficient, although the applied normal force is smallest²⁷. Thus, once the load is rapidly decreased, the contact between the loaded cartilage-pin and glass after a long load application might lead to a sticking of the cartilage to the glass plate. Even if in both studies (inter alia) an impermeable opposing surface (e.g. glass) was used^{16,27}, this phenomenon could also be observed with flat cartilage samples as counterpart during the current study especially in FT-III (and FT-II for S vs. FC), when dynamically varying the axial load. Despite the fact that Krishnan *et al.* and Majd *et al.* applied a constant velocity of 1 mm/s and 4 mm/s^{16,27}, respectively, which is far below the surface velocities in the knee joint of 50–300 mm/s³⁵, their testing conditions compared well with our second friction test (FT-II) also carried out at 1 mm/s. Here, the silk fibroin scaffold generally showed the highest friction coefficients, which were again significantly increased within the low-loaded swing phase (0.092 ± 0.046 ; stance phase: 0.061 ± 0.034). This is again in line with the study of Majd *et al.* evaluating the friction properties of another potential material for meniscal repair under similar conditions. These authors found a more than 15-fold higher friction coefficient of the replacement material during swing phase than during stance phase (approximately 0.7 vs 0.04), while during swing phase μ of the silk fibroin based hydrogel scaffold tested in the current study was only 50% higher¹⁶. In consideration of the different lubricants used of Majd *et al.* and the current study (solution of PBS and different lubrication molecules vs. synovial fluid, respectively), the obtained results fit nevertheless quite well to the results of the referenced study (stance phase: 0.06 vs 0.04), which showed the validity of the testing device.

Next to the soaking effect and the resultant rise in the friction coefficient when the applied force rapidly decreases at the transition of stance- and swing phase, it is also known that a quite thick fluid film of approximately 1.6 μm can be formed during swing phase^{19,35} that is much larger than the average surface roughness of articular cartilage ($R_a = 200\text{ nm}$). Transferring these to the simulated gait conditions (FT-III) of the current study, it can be concluded that together with the assumed high Hersey number (low normal load and high velocity), hydrodynamic lubrication occurs in the swing phase^{19,26}. This fluid film is subsequently squeezed out due to the rapid increase in load at 'heel strike' with beginning of the stance phase. Since, this load application has an impact characteristic ($<0.1\text{ s}$), the fluid film is pressurised but can be preserved between the deformable bearing material of meniscus and/or cartilage. Taking the identified low friction coefficient in the upcoming stance phase of <0.02 into account, elasto-hydrodynamic lubrication can be assumed as this is the lubrication mode of least friction coefficient in the Stribeck curve¹⁹. Throughout a stance phase of low velocity-to-load ratio, the synovial fluid still separates the articulating surfaces until 'toe off' and the initiation of the next swing phase. The distinct lubrication mechanisms of elasto-hydrodynamic- and hydrodynamic lubrication within the simulated stance- and swing phase can consequently be an explanation for the obtained differences in the friction coefficients between these gait phases when testing under physiological loading and motion conditions (FT-III). However, tibial cartilage samples were rather uninfluenced by the three different loading scenarios. The cartilage – cartilage friction pairing indeed showed by tendency the lowest friction coefficient of approx. $\mu = 0.013$ during stance- and $\mu = 0.019$ during swing phase and when testing under varying loading (FT-II) conditions, while μ was nearly identical during FT-I and FT-III (stance phase: $p = 0.6415$, swing phase: $p = 0.3163$). This indicates that additionally varying the velocity in a physiological range affect cartilage friction. The authors speculate that a reason might be the differences in the extracellular matrix (ECM) compositions of articular cartilage and meniscal tissue. Since with progressive duration of friction testing, the interstitial fluid of the loaded cylindrical samples (*pin*) of both tissues is squeezed out, the applied load is carried by their ECM and is therefore responsible for the friction coefficient. While the ECM of articular cartilage is composed of 5–10% wet wt. of proteoglycans (PG), meniscal tissue contains only a fifth of this¹. Additionally, their main collagen type differ, as well: articular cartilage: 10–20% wet wt. collagen type II vs. meniscal tissue: 15–25% wet wt. collagen type I, which may alter the resistance to high velocities and consequently shear forces of the tissue^{1–4}.

It was already shown that the friction coefficients of meniscus and cartilage are multifactorial depending on several parameters and operating conditions²⁶ rather than being just a material constant as described within Coulomb's friction law. Consequently, the mechanisms of the mentioned lubrication modes will significantly differ depending on the testing parameters, as well^{26,41}. Although, it is important to perform friction tests under clearly defined static testing and lubrication regimes²⁶, one should be aware that such data do not perfectly reflect the friction coefficients occurring *in vivo*, e.g. during gait. This is supported by the literature as there is a general consent that (elasto-)hydrodynamic- but also mixed lubrication mechanisms can synergistically contribute to the remarkably low friction properties of the joint^{19,42} as the loading and motion conditions vary considerably within a normal gait cycle.

As a potential material for meniscal replacement, a silk fibroin based hydrogel scaffold was additionally tested under the three different testing conditions (FT-I, -II and -III). In a previous study, the scaffold already showed friction coefficients of 0.056, which was higher than friction of native meniscus ($\mu = 0.021$) but in the range of the requirements for meniscal replacement postulated by Rongen *et al.*¹⁷. Within the current study the material met these requirements again also under simulated gait conditions (FT-III: 0.057 ± 0.019 and 0.047 ± 0.020 for stance and swing phase, respectively).

Since the physiological testing conditions revealed higher friction coefficients for meniscal tissue especially within the simulated swing phase of almost 0.030, this suggests that static testing methods as reported in the literature with friction coefficients of less than 0.01 can underestimate friction coefficients rather than reflecting the complex *in vivo* performance. This might especially be important for potential replacement materials and their prediction regarding their chondroprotective effect *in vivo*.

For all three tests (FT-I, -II, -III) in general, no time-dependent differences in the friction coefficient (μ_0 vs. μ_{end}) could be observed for each material pairing (M, TC or S vs. FC) either during stance- or during swing phase. However, this was not surprising as previous studies already showed that if the moving opposing surface (*plate*) is cartilaginous, no increase in friction will develop^{18,23,43}. Consequently, the interstitial fluid pressurization was maintained in all three test scenarios as well as for all material pairings. While the *pin* was loaded throughout the whole test, the moving contact area of the flat cartilage surface (*plate*) was able to recover during the time of unloading before it was loaded again. Therefore its fluid phase supported the load during the whole testing duration and thus, the friction coefficient remained at the observed low level.

Limitations. The friction testing device developed in the current study was designed according to a *pin-on-plate* configuration. Using this test setup, it was possible to apply loads and velocities occurring in the knee joint during normal walking. However, it is a simplification of the complex joint kinematics as the combined rolling and sliding motion coexisting during flexion and extension of the knee joint is not considered. Nevertheless, using a "rolling-gliding wear simulator" it was already shown that during rolling, and rolling with slip motion, the signs of wear were least when testing different artificial material pairings⁴⁴. Consequently, the main part of friction occurs during sliding, which was considered within the dynamic friction testing device investigated in the current study. Nevertheless, to further take the rolling and sliding within the knee joint into account during friction analysis, a pendulum friction simulator would be an alternative test setup. The advantage of this test setup is that the entire knee joint is tested and therefore considered as one biomechanical and tribological system, preserving the physiological geometries and joint kinematics^{45–47}. However, this also represents a disadvantage, since no distinction can be made between friction properties of cartilage and/or meniscus.

Conclusion. The current study presents new insights in joint friction mechanics as it showed significantly lower friction coefficients during simulated stance- than during the low-loaded swing phase. This phenomenon was observed for meniscus and articular cartilage only when testing under conditions with varying both normal load and velocity as it appears during gait. The high velocities occurring in the swing phase may cause a transition from elasto-hydrodynamic to hydrodynamic lubrication and therefore, increased friction coefficient. Consequently, due to the multifactorial characteristics of cartilage and meniscus friction, the current study emphasizes the need of adding friction tests under physiological testing conditions to the tribological characterisation of materials relevant for joints and especially for potential meniscal or cartilage replacement materials. Thereby, the tested silk fibroin based hydrogel scaffold matched the friction coefficient as demanded in the basic requirements for meniscal replacement materials.

References

1. Mow, V. C. & Huiskes, R. Structure and function of articular cartilage and meniscus, Third Edition. In: *Basic Orthopaedic Biomechanics & Mechano-Biology* (eds Mow, V. C. & Huiskes, R.), 182–257 (Lippincott Williams & Wilkins, 2005).
2. Masouros, S. D., McDermott, I. D., Amis, A. A. & Bull, A. M. Biomechanics of the meniscus-meniscal ligament construct of the knee. *Knee Surg Sports Traumatol Arthrosc.* **16**(12), 1121–32 (2008).
3. Masouros, S. D., McDermott, I. D., Bull, A. M. & Amis, A. A. Biomechanics, In: *The Meniscus* (eds Beaufils, P. & Verdonk, P.), 29–37 (Springer, 2010).
4. McDermott, I. D., Masouros, S. D., Bull, A. M. & Amis, A. A. Anatomy, In: *The Meniscus* (eds Beaufils, P. & Verdonk, R.), 11–18 (Springer, 2010).
5. Bullough, P. G., Munuera, L., Murphy, J. & Weinstein, A. M. The strength of the menisci of the knee as it relates to their fine structure. *J Bone Joint Surg Br.* **52**(3), 564–7 (1970).
6. Brindle, T., Nyland, J. & Johnson, D. L. The meniscus: review of basic principles with application to surgery and rehabilitation. *J Athl Train.* **36**(2), 160–9 (2001).
7. Kutzner, I. *et al.* Loading of the knee joint during activities of daily living measured *in vivo* in five subjects. *J Biomech.* **43**(11), 2164–73 (2010).
8. Pena, E., Calvo, B., Martinez, M. A., Palanca, D. & Doblare, M. Finite element analysis of the effect of meniscal tears and meniscectomies on human knee biomechanics. *Clin Biomech.* **20**(5), 498–507 (2005).
9. Fairbank, T. J. Knee joint changes after meniscectomy. *J Bone Joint Surg Br.* **30B**(4), 664–70 (1948).
10. Fukubayashi, T. & Kurosawa, H. The contact area and pressure distribution pattern of the knee. A study of normal and osteoarthrotic knee joints. *Acta Orthop Scand.* **51**(6), 871–9 (1980).
11. Baratz, M. E., Fu, F. H. & Mengato, R. Meniscal tears: The effect of meniscectomy and of repair on intraarticular contact areas and stress in the human knee. A preliminary report. *Am J Sports Med.* **14**(4), 270–5 (1986).
12. McCann, L., Ingham, E., Jin, Z. & Fisher, J. Influence of the meniscus on friction and degradation of cartilage in the natural knee joint. *Osteoarthr Cartil.* **17**(8), 995–1000 (2009).
13. Seitz, A. M., Lubomierski, A., Friemert, B., Ignatius, A. & Dürselen, L. Effect of partial meniscectomy at the medial posterior horn on tibiofemoral contact mechanics and meniscal hoop strains in human knees. *J Orthop Res.* **30**(6), 934–42 (2012).
14. Gleghorn, J. P. *et al.* Analysis of frictional behavior and changes in morphology resulting from cartilage articulation with porous polyurethane foams. *J Orthop Res.* **28**(10), 1292–9 (2010).
15. Maher, S. A. *et al.* A pre-clinical test platform for the functional evaluation of scaffolds for musculoskeletal defects: the meniscus. *HSS J.* **7**(2), 157–63 (2011).
16. Majd, S. E. *et al.* An *in vitro* study of cartilage-meniscus tribology to understand the changes caused by a meniscus implant. *Colloids Surf B Biointerfaces.* **155**, 294–303 (2017).
17. Rongen, J. J., van Tienen, T. G., van Bockhove, B., Grijpma, D. W. & Buma, P. Biomaterials in search of a meniscus substitute. *Biomaterials.* **35**(11), 3527–3540 (2014).
18. Warnecke, D. *et al.* Friction properties of a new silk fibroin scaffold for meniscal replacement. *Tribol Int.* **109**, 586–592 (2017).
19. Neu, C. P., Komvopoulos, K. & Reddi, A. H. The interface of functional biotribology and regenerative medicine in synovial joints. *Tissue Eng Part B Rev.* **14**(3), 235–47 (2008).
20. Mow, V. C., Kuei, S. C., Lai, W. M. & Armstrong, C. G. Biphasic creep and stress relaxation of articular cartilage in compression? Theory and experiments. *J Biomech Eng.* **102**(1), 73–84 (1980).
21. Ateshian, G. A. & Wang, H. A theoretical solution for the frictionless rolling contact of cylindrical biphasic articular cartilage layers. *J Biomech.* **28**(11), 1341–55 (1995).
22. Soltz, M. A. & Ateshian, G. A. Experimental verification and theoretical prediction of cartilage interstitial fluid pressurization at an impermeable contact interface in confined compression. *J Biomech.* **31**(10), 927–34 (1998).
23. Calligaris, M. & Ateshian, G. A. Effects of sustained interstitial fluid pressurization under migrating contact area, and boundary lubrication by synovial fluid, on cartilage friction. *Osteoarthr Cartil.* **16**(10), 1220–7 (2008).
24. McCann, L. *et al.* Tribological testing of articular cartilage of the medial compartment of the knee using a friction simulator. *Tribol Int.* **41**(11), 1126–1133 (2008).
25. Forster, H. & Fisher, J. The influence of loading time and lubricant on the friction of articular cartilage. *Proc Inst Mech Eng H.* **210**(2), 109–19 (1996).
26. Gleghorn, J. P. & Bonassar, L. J. Lubrication mode analysis of articular cartilage using Stribeck surfaces. *J Biomech.* **41**(9), 1910–8 (2008).
27. Krishnan, R., Mariner, E. N. & Ateshian, G. A. Effect of dynamic loading on the frictional response of bovine articular cartilage. *J Biomech.* **38**(8), 1665–73 (2005).
28. McCutchen, C. W. The frictional properties of animal joints. *Wear.* **5**, 1–17 (1962).
29. Walker, P. S., Dowson, D., Longfield, M. D. & Wright, V. “Boosted lubrication” in synovial joints by fluid entrapment and enrichment. *Ann Rheum Dis.* **27**(6), 512–20 (1968).
30. Ateshian, G. A. & Mow, V. C. Friction, lubrication, and wear of articular cartilage and diarthrodial joints, Third Edition. In: *Basic Orthopaedic Biomechanics & Mechano-Biology* (eds Mow, V. C. & Huiskes, R.), 447–493 (Lippincott Williams & Wilkins, 2005).
31. Jahn, S., Seror, J. & Klein, J. Lubrication of Articular Cartilage. *Annu Rev Biomed Eng.* **18**, 235–58 (2016).
32. Medley, J. B., Dowson, D. & Wright, V. Transient elastohydrodynamic lubrication models for the human ankle joint. *Eng Med.* **13**(3), 137–51 (1984).
33. Hou, J. S., Mow, V. C., Lai, W. M. & Holmes, M. H. An analysis of the squeeze-film lubrication mechanism for articular cartilage. *J Biomech.* **25**(3), 247–59 (1992).
34. ISO, B., 14243-1, Implants for surgery–Wear of total knee joint prostheses– Part 1: Loading and displacement parameters for wear-testing machines with load control and corresponding environmental conditions for test (2009).
35. Unsworth, A. Tribology of human and artificial joints. *Proc Inst Mech Eng H.* **205**(3), 163–72 (1991).
36. Andriacchi, T. P., Dyrby, C. O. & Johnson, T. S. The use of functional analysis in evaluating knee kinematics. *Clin Orthop Relat Res.* **410**, 44–53 (2003).

37. Andriacchi, T. P., Johnson, T. S., Hurwitz, D. E. & Natarajan, R. N. Musculoskeletal Dynamics, Locomotion, and Clinical Applications, Third Edition. In: *Basic Orthopaedic Biomechanics & Mechano-Biology* (eds Mow, V. C. & Huiskes, R.), 91–121 (Lippincott Williams & Wilkins, 2005).
38. Taylor, W. R., Heller, M. O., Bergmann, G. & Duda, G. N. Tibio-femoral loading during human gait and stair climbing. *J Orthop Res.* **22**(3), 625–32 (2004).
39. Heinlein, B. *et al.* ESB Clinical Biomechanics Award 2008: Complete data of total knee replacement loading for level walking and stair climbing measured *in vivo* with a follow-up of 6–10 months. *Clin Biomech (Bristol, Avon)*. **24**(4), 315–26 (2009).
40. Faul, F., Erdfelder, E., Lang, A. G. & Buchner, A. G*Power 3: a flexible statistical power analysis program for the social, behavioral, and biomedical sciences. *Behav Res Methods*. **39**(2), 175–91 (2007).
41. Hersey, M. D. The laws of lubrication of horizontal journal bearings. *J Wash Acad Sci.* **4**(19), 542–552 (1914).
42. Thier, S. & Tonak, M. Influence of Synovial Fluid on Lubrication of Articular Cartilage *in Vitro*. *Z Orthop Unfallchir.* **156**(2), 205–213 (2018).
43. Shi, L., Sikavitsas, V. I. & Striolo, A. Experimental friction coefficients for bovine cartilage measured with a pin-on-disk tribometer: testing configuration and lubricant effects. *Ann Biomed Eng.* **39**(1), 132–46 (2011).
44. Richter, B. I., Ostermeier, S., Turger, A., Denkena, B. & Hurschler, C. A rolling-gliding wear simulator for the investigation of tribological material pairings for application in total knee arthroplasty. *Biomedical engineering online*. **9**, 24 (2010).
45. Kawano, T. *et al.* Mechanical effects of the intraarticular administration of high molecular weight hyaluronic acid plus phospholipid on synovial joint lubrication and prevention of articular cartilage degeneration in experimental osteoarthritis. *Arthritis Rheum.* **48**(7), 1923–9 (2003).
46. Crisco, J. J., Blume, J., Teeple, E., Fleming, B. C. & Jay, G. D. Assuming exponential decay by incorporating viscous damping improves the prediction of the coefficient of friction in pendulum tests of whole articular joints. **221**(3), 325–33 (2007).
47. Liu, A., Jennings, L. M., Ingham, E. & Fisher, J. Tribology studies of the natural knee using an animal model in a new whole joint natural knee simulator. *J Biomech.* **48**(12), 3004–11 (2015).

Acknowledgements

This work is independent research funded by the National Institute for Health Research (Invention for Innovation (i4i), Development of manufacturing capability and pilot clinical evaluation of FibroFix: A mechanically advanced, tissue regenerative, meniscal cartilage repair device, II-LB-0417-20005). The views expressed in this publication are those of the author(s) and not necessarily those of the NHS, the National Institute for Health Research or the Department of Health and Social Care.

Author Contributions

D.W. carried out the experimental study as well as all analyses and drafted the manuscript. M.M. developed the test setup. L.d.R. and S.S. helped performing the experimental study and writing the manuscript. C.G., R.W. and N.S. supplied the scaffold material and proof read the manuscript. L.D. and D.W. conceived the study and L.D. and A.I. participated in its design and coordination. All authors read and approved the final manuscript.

Additional Information

Competing Interests: Authors Cristina Gentilini, Robert Walker and Nick Skaer are employees of Orthox Ltd. (Abingdon, UK). Oliver Kessler is a consultant to Orthox Ltd. (Abingdon, UK). All other authors declare no competing interest.

Publisher's note: Springer Nature remains neutral with regard to jurisdictional claims in published maps and institutional affiliations.



Open Access This article is licensed under a Creative Commons Attribution 4.0 International License, which permits use, sharing, adaptation, distribution and reproduction in any medium or format, as long as you give appropriate credit to the original author(s) and the source, provide a link to the Creative Commons license, and indicate if changes were made. The images or other third party material in this article are included in the article's Creative Commons license, unless indicated otherwise in a credit line to the material. If material is not included in the article's Creative Commons license and your intended use is not permitted by statutory regulation or exceeds the permitted use, you will need to obtain permission directly from the copyright holder. To view a copy of this license, visit <http://creativecommons.org/licenses/by/4.0/>.

© The Author(s) 2019

Acknowledgements

...removed due to reasons of data protection.

Curriculum vitae

Personal data

Daniela Warnecke

born in Nienburg/Weser, Germany in 1987

German

Academic career

02/2014 – today Research associate and PhD student,
Institute of Orthopaedic Research and Biomechanics,
Centre for Trauma Research Ulm, Ulm University Medical
Centre, Germany

04/2011 – 09/2013 Master course (M. Sc.) in Biomedical Engineering,
Leibniz University Hannover, Germany

09/2007 – 03/2013 Bachelor course (B. Eng.) Medical Engineering,
Jade Hochschule, Wilhelmshaven, Germany

School education

08/2000 – 06/2007 German university entrance level (Abitur),
Marion-Dönhoff-Gymnasium Nienburg/Weser, Germany

08/1994 – 07/2000 Basic education (Grundschule und Orientierungsstufe),
Nienburg/Weser, Germany

List of publications

- 2019 SUTER C, VON ROHR M, MAJEWSKI M, DÜRSELEN L, **WARNECKE D**, SCHILD N, NOWAKOWSKI AM. A biomechanical comparison of two plating techniques in lateral clavicle fractures. *Clin Biomech* 2019; 67: 78 - 84.
- 2019 **WARNECKE D**, MEßEMER M, DE ROY L, STEIN S, GENTELINI C, WALKER R, SKAER N, IGNATIUS A, DÜRSELEN L. Articular cartilage and meniscus reveal higher friction in swing phase than in stance phase under dynamic gait conditions. *Sci Rep* 2019; 9: 5785.
- 2018 STEIN SEC, VON LÜBKEN F, **WARNECKE D**, GENTILINI C, SKAER N, WALKER R, KESSLER O, IGNATIUS A, DÜRSELEN L. The challenge of implant integration in partial meniscal replacement: an experimental study on a silk fibroin scaffold in sheep. *Knee Surg Sports Traumatol Arthrosc* 2018; 27: 369 - 80.
- 2018 **WARNECKE D**, STEIN S, HAFFNER-LUNTZER M, DE ROY L, SKAER N, WALKER R, KESSLER O, IGNATIUS A, DÜRSELEN L. Biomechanical, structural and biological characterisation of a new silk fibroin scaffold for meniscal repair. *J Mech Behav Biomed Mater* 2018; 86: 314 - 24.
- 2018 XU P, WERNER J, MILERSKI S, HAMP C, KUZENKO T, JÄHNERT M, GOTTMANN P, DE ROY, L, **WARNECKE D**, ABAEI A, PALMER A, HUBER-LANG M, DÜRSELEN L, RASCHE V, SCHÜRMANN A, WABITSCH M, KNIPPSCHILD U. Diet-induced obesity affects muscle regeneration after murine blunt muscle trauma – a broad spectrum analysis. *Front Physiol* 2018; 9: 674.

- 2017 WANNER R, GEY M, ABAEI A, **WARNECKE D**, DE ROY L, DÜRSELEN L, RASCHE V, KNÖLL B. Functional and Molecular Characterization of a Novel Traumatic Peripheral Nerve-Muscle Injury Model. *Neuromolecular Med* 2017; 19: 357 - 74.
- 2017 **WARNECKE D**, SCHILD NB, KLOSE S, JOOS H, BRENNER RE, KESSLER O, SKAER N, WALKER R, FREUTEL M, IGNATIUS A, DÜRSELEN L. Friction properties of a new silk fibroin scaffold for meniscal replacement. *Tribol Int* 2017; 109: 586 - 92.